Kinetics of Lime Dissolution and Iron Oxide Reduction in Oxygen Steelmaking

By

Pramod Kumar Gupta

DEPARTMENT OF MATERIALS AND METALLURGICAL ENGINEERING
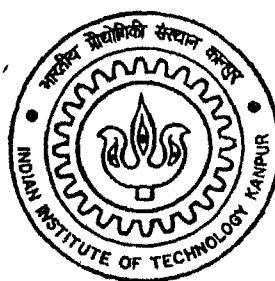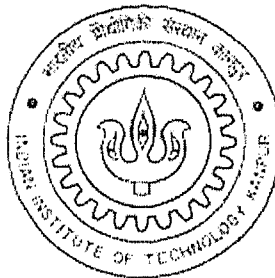
INDIAN INSTITUTE OF TECHNOLOGY KANPUR

DECEMBER, 2003

Kinetics of Lime Dissolution and Iron Oxide Reduction in Oxygen Steelmaking

By

Pramod Kumar Gupta

DEPARTMENT OF MATERIALS AND METALLURGICAL ENGINEERING

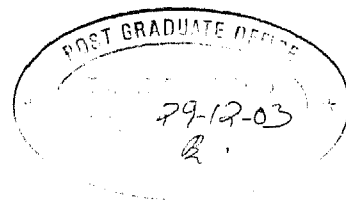**INDIAN INSTITUTE OF TECHNOLOGY, KANPUR**

December, 2003

CERTIFICATE

It is certified that the work contained in the thesis entitled "**Kinetics of Lime Dissolution and Iron Oxide Reduction in Oxygen Steelmaking**" by Pramod Kumar Gupta has been carried out under my supervision and this work has not been submitted elsewhere for a degree.

(Dr. Brahma Deo)

(Professor)

Department of Materials and Metallurgical Engineering

Indian Institute of Technology, Kanpur

December, 2003

ACKNOWLEDGEMENT

DEDICATED

TO

MY BELOVED PARENTS

Contents

List of Figure Captions

List of Tables

Page

ABSTRACT

Slag formation behaviour in BOF vessels is very closely related to the kinetics of lime dissolution and iron oxide reduction. Theoretical and practical aspects of lime dissolution are investigated. Analysis of the results of laboratory investigations reveal that liquid slag penetrates into the pores of lime and CaO-FeO solution is formed within the lime and also next to the lime surface. Through this layer the mass transfer of CaO takes place toward the bulk slag resulting in dissolution of lime. The dicalcium silicate also forms but at distance slightly away from lime. Under the turbulent conditions of BOF this layer may not be a continuous one, break away, or may have large slits channels to allow the outward diffusion of CaO. A kinetic model is developed on the basis of these assumptions and then applied to data collected for a 300 ton BOF by taking slag samples during the blow. The value of mass transfer coefficient is calculated and it is found that the value varies during the blow due to rapid changes in slag viscosity caused by precipitation or dissolution of dicalcium silicate and entrainment of gas bubbles in the slag. Average value of mass transfer coefficient of CaO in slag is found to be 2×10^{-4} cm/s. Two different slag viscosity models are used to compute the slag-gas-solid viscosity. In the middle of the blow the solid fraction may be as high as 60%. The kinetics of lime dissolution is discussed in chapter 1.

Reduction of FeO in slag occurs primarily by the carbon rich metal droplets which are thrown into the slag due to the impact of the jet. Thus nozzle design parameters and lance height also affect the kinetics of iron oxide reduction because they decide the amount of droplets thrown into slag per minute, defined as iron conversion. The residence time of metal droplets in slag however depends upon the composition, temperature and hence viscosity of slag. A kinetic model of reduction of FeO is developed and then applied to 300 ton BOF. The kinetic models of FeO reduction reported in literature are critically reviewed. It is found that mass transfer coefficient of FeO in slag is the rate controlling step and for 300 ton BOF the average value of the mass transfer coefficient is 3.5×10^{-3} cm/s.

As in the case if lime dissolution, the mass transfer coefficient of FeO in slag also changes during the blow due to variations in slag viscosity. This is the main cause of variability of the BOF process. At times the slag may become nearly solid due large amount of solids present in slag while in other instances it may become very foamy due to fast reduction rate of FeO in slag. The kinetic models of lime dissolution and iron oxide reduction developed in this work provide a basis for the manipulation of lance height and changes in the oxygen flow rate in such manner so as to avoid the extreme situations of solid slag formation or intensive foaming (popularly known as slopping).

The kinetics of reduction of FeO in BOF slags is discussed in chapter 2 followed by the suggestion for future work.

CHAPTER 1

Kinetics of Lime Dissolution in Oxygen Steelmaking

1.1 Introduction

The composition and temperature of slag as well as its amount and physical nature (foamy, viscous, fluid, heterogeneous, or a liquid slag with varying proportions of solid) play an important role in the operation of basic oxygen steel making process (BOF).The physico-chemical nature of slag controls the kinetics of refining reactions, refractory lining wear, and the phenomenon of lance skulling and post combustion within the vessel. A typical slag path is shown in Figure 1.1 [1]. The choice of slag path is dictated by the composition of hot metal and the desired end point composition and temperature of steel at tap. The dissolution rate of lime into slag determines the slag path as the blow progresses.

A variety of studies on dissolution of lime have been reported in literature [1-9] for blast furnace type slags (CaO-Al$_2$O$_3$-SiO$_2$ slags [4,5]), BOF slags (CaO-FeO-SiO$_2$ [2-4,6,7], FeO-SiO$_2$ [7] and CaO-FeO-SiO$_2$-MgO [6] type slags), both in static and stirred baths, in laboratory experiments and in pilot plant and full-scale experiments. In this work, we shall focus on the theoretical and practical aspects of dissolution of lime in BOF slags only. It is well understood that the phenomenon of lime dissolution into slags depends upon the operating parameters of BOF (oxygen blow rate, lance height, flux addition sequence and amount, etc.) and also the accompanying processes simultaneously going on in the BOF vessel (post combustion, foaming, droplet ejection, etc.). As soon as the lime at ambient temperature comes into contact with liquid slag, the process of lime dissolution proceeds through a sequence of steps [2, 4, 10-12]:

    a. Heating up of lime, while a slag layer is solidified around the lime particles (due to quenching effect) [10]

    b. Re-liquefaction of the frozen slag layer and further penetration of slag into the pores of lime [2,4,11,12]

1

c. Diffusion of slag components through the diffusion (boundary) layer around the lime [6,10,11,13,14]

d. Breakdown of crystal lattice of lime into separate crystallites [8,14]

e. Dissolution of separate crystallites into slag [8,14]

In the early part of the blow in BOF, the bulk slag composition is essentially iron silicate $(2FeO.SiO_2)$ and the chemical reaction can be represented as

$$4\ CaO_{solid} + \{2FeO.SiO_2\} \rightarrow 2\ (CaO\text{-}FeO)\ _{solid\ solution} + (2CaO.SiO_2)\ _{solid} \qquad (1.1)$$
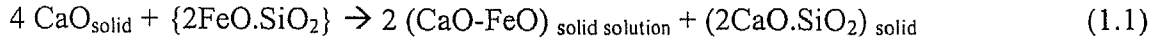
As the blow progresses, the concentration of CaO in the liquid slag increases and the overall chemical reaction is

$$n\ CaO_{solid} + \{n_1 CaO,\ n_2\ FeO,\ n_3\ SiO_2\} = (n\text{-}x)\ (2\ CaO.SiO_2)_{solid} +$$
$$\{(n+2(n_1\text{-}x))\ CaO,\ n_2\ FeO,\ (n_3\text{-}n+x)\ SiO_2\} \qquad (1.2)$$
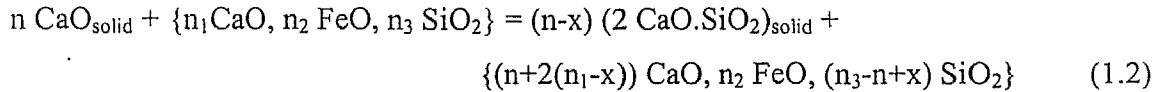
The slag path in Figure 1.1 [1] implies that the slag composition moves progressively with the precipitation/dissolution of dicalcium silicate in the middle part of the blow, until the end point is reached. At the end of the blow the slag is heterogonous and contains fine metal droplets, small un-dissolved lime particles and entrained gas bubbles. Dissolution of lime into MgO saturated slags $(CaO\text{-}FeO\text{-}MgO\text{-}SiO_2)$ proceeds in a slightly different way:

$$(2\ FeO.SiO_2)\ _{liquid} + 2(CaO.MgO)\ _{solid} = (2\ CaO.SiO_2)\ _{solid} + 2(CaO.FeO)_{solid\ solution} \qquad (1.3)$$
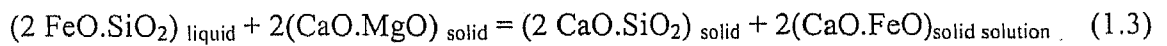
The process of dissolution of lime into a slag containing MgO becomes complicated due to formation of MgO-FeO solid solution around the dolomite particles. In this work we shall focus on BOF slags containing little or no MgO.

A satisfactory test of the rate of dissolution of lime into steel making slag should be carried out in a setup wherein the experimental conditions, including slag dynamics, are

2

representative of the conditions in BOF. The slag should, at least, be well agitated so as to render a comparison with the turbulent conditions in the BOF worthwhile. A full-scale or a pilot–scale experiment suffers from the lack of reproducibility of operating variables from one test to another, and, similarly, the difficulty faced with laboratory investigations, in general, is that they do not correspond to the turbulent and multiphase conditions existing in an actual basic oxygen furnace (BOF).

In this chapter, we will be concerned with the analysis of physico-chemical factors (size and reactivity of lime) which affect the dissolution rate of lime in BOF slags. Actual plant data are analyzed (300 ton combined blown BOF) and a kinetic model of dissolution of lime is developed on the basis of slag samples collected at different stages of the blow.

It is reported in literature that the dicalcium silicate layer, formed close to the surface of lime, plays an important role in the dissolution rate of lime. In the present work, complementary experiments have been carried out in the laboratory to understand the effect of physico-chemical factors on the dissolution rate of lime .The role played by the dicalcium silicate layer is also analysed.
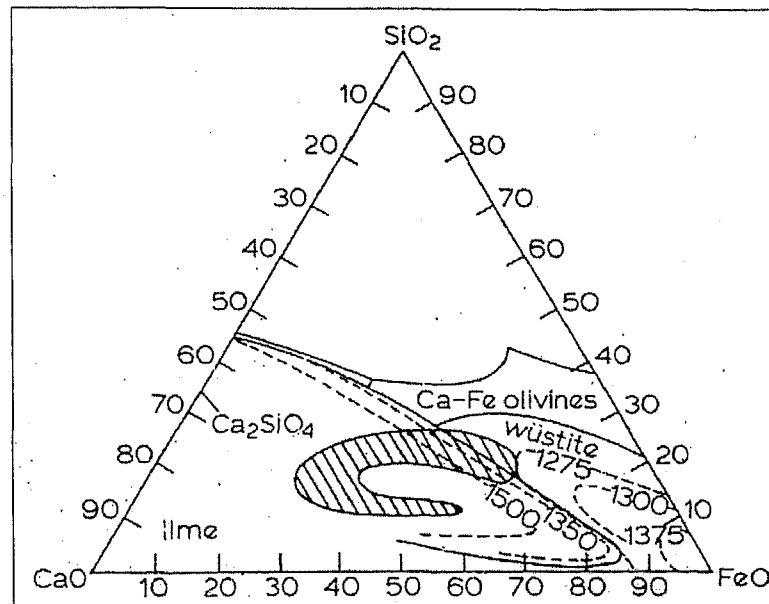
Figure 1.1: Simplified ternary diagram for CaO-SiO_2-FeO slags showing a slag path within shaded region [1]

1.2 Size versus reactivity of lime

Two important physico-chemical factors which affect the dissolution of lime are the size and the reactivity of lime. The method adopted for limestone crushing, selection of size fraction to be charged into the kiln, kiln temperature together with residence time (duration of heating) decide the microscopic properties (internal surface, porosity and apparent density) as well as macroscopic properties (heat penetration, loss on ignition, particle size distribution after calcination and friability) [14]. The standard ASTM C110 test (slaking test) is generally used to determine the reactivity of lime. Once the size range is fixed, reactivity can be taken as a rough measure of the microscopic properties of lime [8, 16-18]. Since weathering of lime is an external influence and not a direct property of the calcined lime itself, it is recommended [8] to use, in order to obtain an accurate value of reactivity, a re-calcination treatment at 910 °C before performing the reactivity test; the re-calcination process restores the original property of lime obtained immediately after the burning in kiln.

The BOF operator desires that lime should dissolve rapidly into the slag so as to attain a required basicity and therefore prefers a lime of high reactivity. There are, however, conflicting views on the relevance of reactivity of lime to actual lime dissolution rates observed in the BOF process. For example it is possible that a lime which reacts rapidly with water may or may not react rapidly with a molten steelmaking slag. Natalie et al [6] did reactivity test for seven commercially available lime samples out of which four lime samples were produced in the rotary kilns while the remainder three were produced in vertical or shaft kilns. The laboratory experiments provided strong evidence that lime classified as more reactive by water tests did dissolve more rapidly in slag (when there is relative motion between the slag and lime), as shown in Figure 1.2 [6]. However, according to the same authors [6], the sintering of a reactive lime at elevated temperatures changed the expected behaviour considerably. For example, it was found that the lime samples lost the advantage of higher reactivity when they were held at a moderate temperature for a long time, or at a high temperature for a short time. In BOF at least a part of the lime charged may take some time to come in direct contact with liquid

slag and during this time it can get heated by radiation leading to sintering. Thus reactivity alone is not the only important parameter for the dissolutions of lime.

Both the porosity of lime and calcination temperature are important factors in determining the reactivity of lime. Pores may exert only a short time influence because as soon as the pores of lime get filled up with liquid slag, further dissolution is controlled by diffusion of FeO (or diffusion of CaO) through the boundary layer. It is observed [8] that the effect degree of calcination on dissolution rate of lime is more pronounced in the case of $FeO-SiO_2-CaO$ slag than in the case of $FeO-SiO_2$ slag; the lime calcined for 95 percent dissolves about 60 percent faster than fully calcined lime in $FeO-SiO_2$ slag, irrespective of calcination temperature. On the other hand, lime calcined for 95 percent dissolves about 150 percent faster than fully calcined lime in $FeO-SiO_2-CaO$ slag, irrespective of the calcination temperature.

1.2.1 Laboratory experiments with synthetic BOF slag to study the effects of size and reactivity [9]

Synthetic slag (160-170 gm) of composition   40 % SiO_2- 45 % FeO and 15 % CaO (expressed as mass percent) was added on top of 21 kg of metal (2.0% C, 0.04% Mn, 0.025% P -0.01% S, 0.25% Si and rest iron) at 1550 ^oC kept inside a 25 kg induction furnace. The selected compositions of both metal and slag correspond roughly to the situation in BOF during middle blow period.

Factorial design of 2 ×2 ×5 was chosen to study the effects of reactivity, size, and time, respectively, on dissolution rate of lime. Two levels of lime reactivity chosen were (R=31, 45 ^oC/min) and (R=10, 15 ^oC/min) and the size of lime samples (in the shape of a bar) were (10mm ×10mm ×40mm) and (20mm ×20mm ×40mm). All the samples (typical composition given in Table 1.1 [9]) were transported in under dry conditions to avoid the weathering. At a time four different samples (small and large of high reactivity, small and large of low reactivity) were mounted on the sample holder and submerged in the molten slag simultaneously. The induction power was reduced to minimum so as to maintain a

layer of constant slag thickness. The first set of samples was submerged for 10 s, and the second for 30 s. The samples of third, fourth and fifth set were first preheated in an oven for 60 seconds at 1500 °C and then submerged for 60,120 and 180 s, respectively. During each experiment a fresh sample of slag was taken. After submerging for the required time, the lime samples were cooled down, cut into half and embedded into inert resin, and photographed to determine the reduction in size; Figure 1.3 [9] shows the typical profile of lime samples after the experiment and Figure 1.4 [9] shows the outline of the lime-slag interface (manner of penetration of slag into the pores of lime). Each sample was analysed using X ray microanalysis (for Ca, Fe, Si, Mg, O) by moving the probe in a straight line along the cross-section of the sample. The typical concentration profile is shown in Figure 1.5 [9]; the dashed vertical lines in Figure 1.5 [9] correspond to the boundaries between slag layer, penetration layer and the pure lime core. The average composition of the three distinct layers is given in Table 1.2 [9].
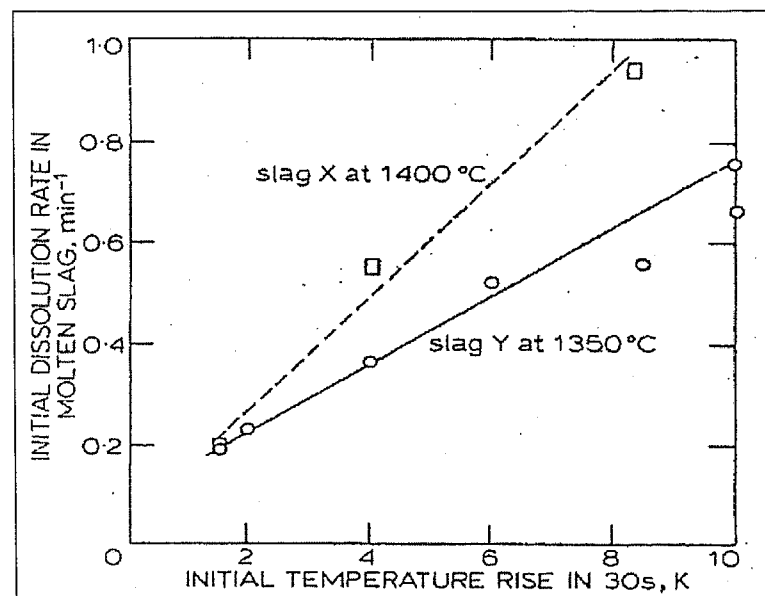
Figure 1.2: Results of laboratory experiments [6] showing good correlation between initial dissolution rate in molten slag and initial temperature rise (i.e. reactivity) during 30 second of ASTM water test [6]

6

Table 1.1: Chemical analysis of the lime [9]

	small size, low react.	large size, low react.	small size, high react.	large size, high react.
CaO w-%	96.8	96.8	99.0	99.0
MgO	0.72	0.72	0.38	0.38
S	0.151	0.151	0.009	0.009
SiO_2	1.51	1.51	0.06	0.06
Al_2O_3	0.35	0.35	0.03	0.03
Fe_2O_3	0.19	0.19	0.08	0.08
CO_2	0.20	0.20	0.30	0.30
reactivity °C/min	10	15	31	45

Table 1.2: X-ray analysis by microprobe line scans [9]

composition weight-%	hard burned		soft burned	
	small	large	small	large
slag layer				
SiO_2	29,3	45,5	50,0	49,9
CaO	63,9	35,4	23,4	29,4
FeO	2,9	15,1	23,9	13,2
O (excess)	3,9	4,0	2,7	7,4
penetration layer				
SiO_2	0,3	0,5	0,2	0,2
CaO	86,1	78,0	91,5	89,6
FeO	2,8	5,1	4,7	3,7
O (excess)	10,8	16,4	3,5	6,5
lime core				
CaO	87,5	72,4	80	88
O (excess)	12,5	27,6	20	12
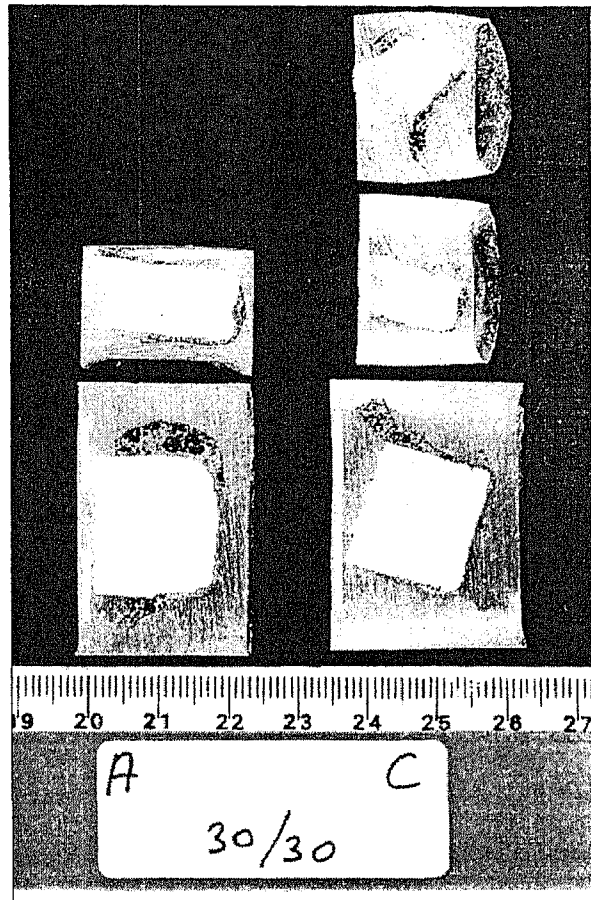
Figure 1.3: A set of lime samples dipped in slag [9]
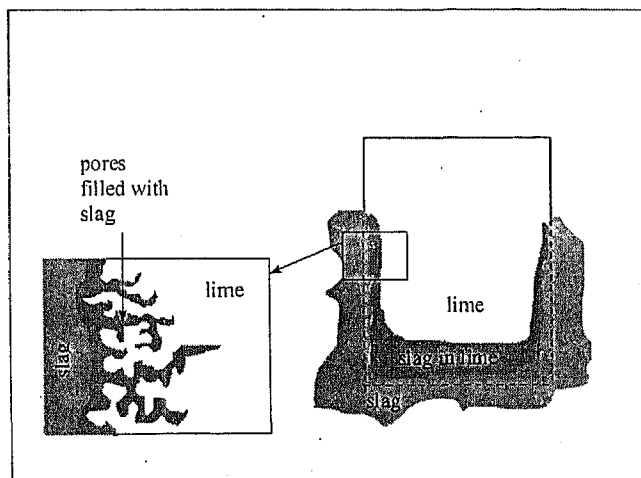
Figure 1.4: Outline of the lime sample when dipped in slag [9]
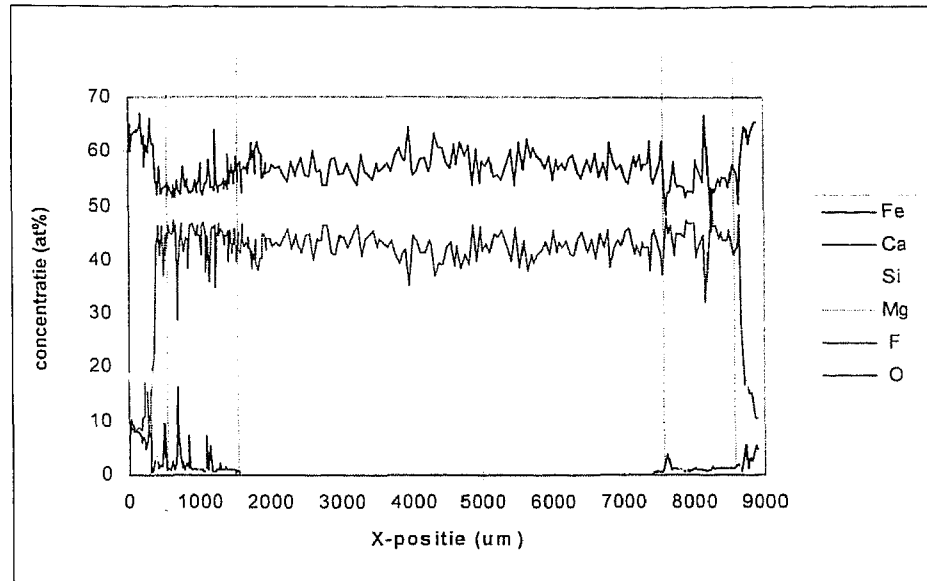
Figure 1.5: A typical plot of the micro-probe line scan over the slag dipped lime sample [9]

1.2.1.1 Results and discussion of the laboratory experiments

The lime samples gradually dissolved into slag with time and the average decrease in thickness as well as the thickness of the penetration zone was estimated from the micrographs (plotted in Figure 1.6). The analysis of variance, carried out on the basis of results in Figure 1.6, shows that the size of the samples has a strong influence on dissolution and the effect of reactivity is not significant (at 95 % confidence level). In this work, a wide variation in reactivity was not allowed, keeping in mind that in a actual plant situation also the reactivity of lime charged in BOF varies in a small range. Perhaps only at very high rates of stirring (than used in the present work) the contribution of reactivity may become more significant than the size of lime.

It was observed that the lime samples which were not preheated had a frozen slag layer to start with. The comparison of results in Figure 1.6 (a, b) with Figure 1.6 (c, d) [9] confirms that dissolution of lime took place only after the penetration of molten slag into the pores. The X-ray analysis shows that in the penetration layer only FeO and CaO are present. It is not certain whether FeO forms calcium ferrite or CaO-FeO solid solution;

9

present. It is not certain whether FeO forms calcium ferrite or CaO-FeO solid solution; perhaps CaO-FeO solid solution is formed because excess of lime is already present. Preferential attack of FeO along the grain boundaries of crystallites in lime can help in breaking down of the solid lime structure and also the subsequent dissolution of the grains. In smaller pieces of lime the penetration of heat will be faster and this will enhance FeO penetration into lime along the grains and thereby promote the breakdown of lime particles. Thus, it appears that under actual operating conditions in BOF the size of lime plays a dominant role and should be controlled for ensuring predictable dissolution rates.

The practical observations [9] for a 300 ton BOF (blowing oxygen at the rate of 900 m^3/min) have shown that the lime particles below 7 mm in size can be ejected out of (or carried away) from mouth along with the off gas; it is therefore preferred (for economical reasons) that 80% of the lime charged is in the range of 10 mm to 20 mm. Shop floor experience has shown that consistency in the size of lime is required for good process control.

a
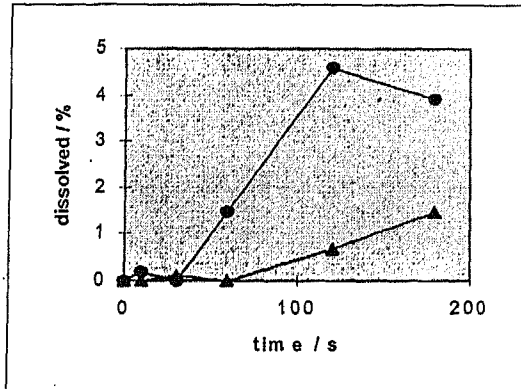
b
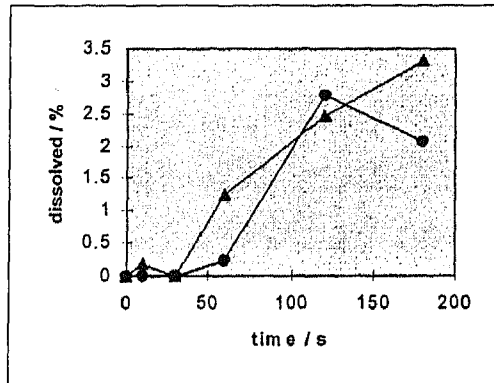
c
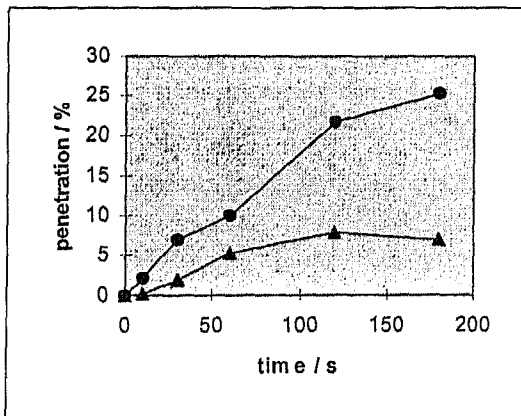
d
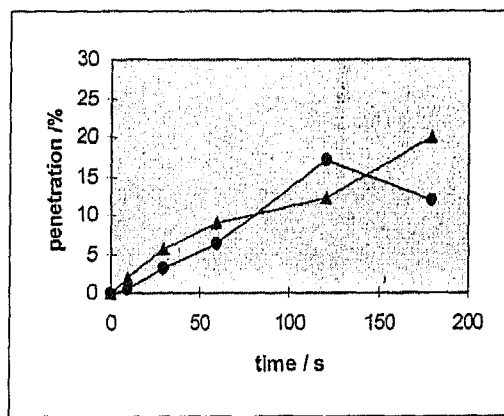
Figure 1.6a (left hand, top) dissolution of the lime sample, the x-axis shows the time of dipping in the slag; ▲ results for the large samples; • results for the small samples.

Figure 1.6b (right hand, top) dissolution of the lime sample, the x-axis shows the time of dipping in the slag: ▲ results of the hard burned samples; • results of the soft burned samples.

Figure 1.6c (left hand, bottom) slag penetration in the lime sample, the x-axis shows the time of dipping in the slag: ▲ the results of the large samples; • the results of the small samples.

Figure 1.6d (right hand, bottom) slag penetration in the lime sample, the x-axis shows the time of dipping in the slag: ▲ the results of the hard burned samples; • the results of the soft burned samples. [9]

11

1.3 Kinetic model of dissolution of lime in a 300 ton BOF vessel

According to equation (1.2), a continuous or discontinuous layer of dicalcium silicate may form slightly away from the lime surface, depending upon the bath condition (static or stirred). It is reported that in static bath condition, when lime comes in contact with slag containing FeO-SiO_2 or CaO-FeO-SiO_2 slag, a continuous layer of C_2S around the lime particles impedes the lime dissolution whereas in a stirred bath a discontinuous layer of forms with narrow channels (passages) through which mass transfer can easily occur, thus providing little or no barrier to the lime dissolution. It is interesting to see the results of some typical investigations with respect to the formation of C_2S layer as summarized in Table 1.3.

Hachtel et al. [2] and Oeters et al. [3] investigated the lime dissolution mechanism in a static bath. When solid lime was dipped into a static slag, solid lime-slag interface, as observed on SEM, contained FeO rich slag followed by a dicalcium silicate layer ($2CaO.SiO_2$) at some distance from the interface (Figure 1.7). The typical concentration profile of slag components is shown in Figure 1.8.They proposed the counter diffusion of CaO away from the interface and of SiO_2 from the bulk towards the interface as the rate controlling steps.

Matsushima et al. [4] investigated both BF and BOF type slags in static as well as in a stirred bath. It was proposed that the dissolution of solid lime was limited by diffusion of CaO through the FeO rich (or Al_2O_3 rich) slag layer adjacent to the lime specimen in the initial stages and later through the C_2S or C_3S films formed in the vicinity of the interface. In a in stirred slag bath some of $2CaO.SiO_2$ may disperse and dissolve into bulk slag by liquid flow. The formation and disappearance of C_2S or C_3S films could be repeated.
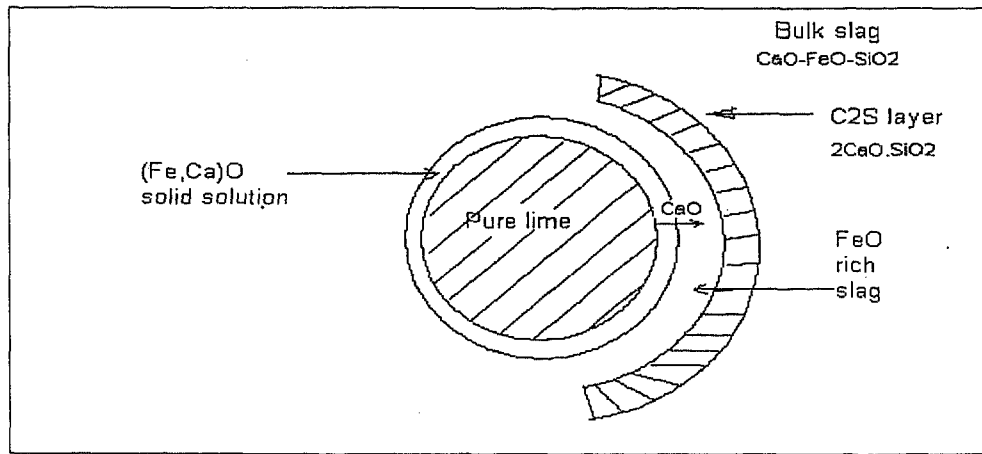
Figure 1.7: Lime dissolution in static slag proposed by Hachtel et al. and Oeters et al.
[2,3]
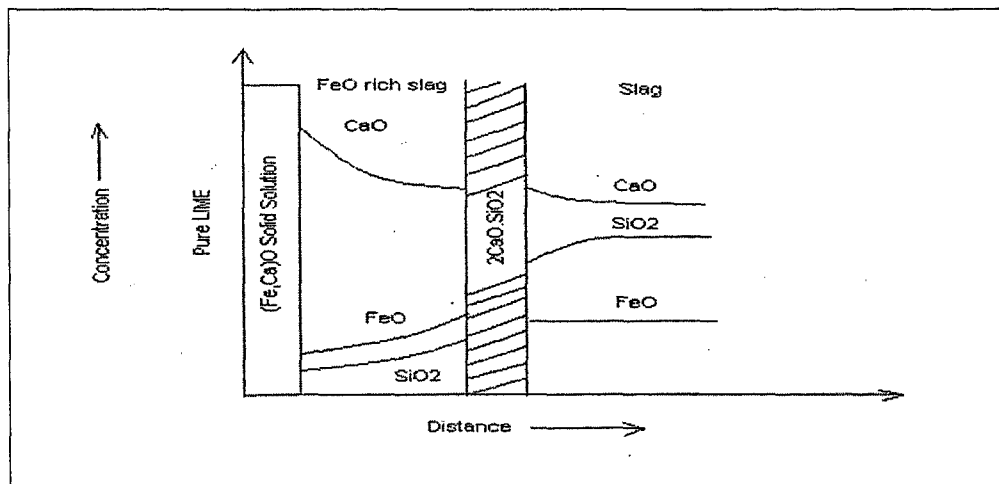
Figure 1.8: Schematic diagram of slag component near the surface

Natalie et al. [6] did experiments with BOF slag in a stirred bath condition and observed that a discontinuous C_2S (or C_3S) layer formed adjacent to the dissolving lime. The concentration of lime was high at the lime/slag interface and gradually decreased further away from the interface. Thus the difference in CaO concentration provided the driving force for diffusion of CaO away from the lime into the slag. Even though the C_2S layer was discontinuous it could offer a significant impediment to the diffusion of CaO away from the lime surface (and therefore retard the dissolution process) primarily due to the restriction of the area available for diffusion. Fresh dicalcium silicate could have been produced continuously within the boundary layer so as to maintain a steady state concentration of this species in the boundary layer.

Briggs et al. [7] did experiments with hard and soft burnt lime in static as well as in stirred bath condition with $FeO-SiO_2$ slag system. The phases observed by them in hard burnt lime were FeO rich liquid region next to lime surface and a zone of C_2S layer next to FeO rich layer. In the case of soft burnt lime the calico-wustite layer also formed next to lime. The mechanism proposed for lime dissolution was the diffusion of CaO away from the lime/slag interface into the bulk slag.

Kor et al. [8] did experiments with slag containing $FeO-CaO-SiO_2$ (BOF slag) using calcined lime in stirred bath condition. The phases observed were (Ca, Fe) O solid solution next to the lime surface with FeO rich layer next to (Ca, Fe) O solid solution layer and C_2S (or C_3S) layer slightly away from the lime surface.

Noguchi et al. [15] studied the mechanisms involved in the dissolution of calcium oxide crystals in silicate melts. Their procedure consisted of melting a silicate sample on a hot filament. Once the silicate had melted, a crystal of CaO was placed in the melt and then observed directly through a microscope. Analysis was carried out for each element using an X ray micro-analyzer. The authors observed that with binary slag ($CaO-SiO_2$) a solid layer of dicalcium silicate was formed on the surface of CaO. The layer of C_2S was observed to grow with time at a decreasing rate, which was accelerated by disruption of the film. Thickness of the film was less than 100 micrometer after 160 sec exposure to

slag. Careful examination of the C_2S layers revealed the presence of cracks through which the melt had penetrated and presence of a layer, similar in composition to the bulk of the slag and presumably liquid, between the C_2S layer and the CaO crystal. A C_2S layer was also observed in slag system that consisted of $CaO\text{-}FeO\text{-}SiO_2$. It was found that this layer appeared only after a prolonged exposure. When a slag contained more than 10% FeO, the C_2S layer had many cracks which perhaps allowed CaO dissolution. Distributed C_3S silicate layers were also observed.

On the basis of results summarized in Table 1.3 and also the laboratory experiments in section 1.2.1.1, the following assumptions can be made a priori in the kinetic model:

- A layer of FeO-CaO solid solution forms next to lime surface followed by a discontinuous layer of $2CaO.SiO_2$ (having narrow canals or slits) slightly away from lime (Figure 1.9).

- Owing to the turbulent nature of BOF process, the C_2S layer has canals or slits present in it).

- The dissolution of lime proceeds by diffusion of CaO present in the FeO-CaO solid solution layer through the bulk slag, as shown in Figure 1.9; presence or absence of C_2S layer with canals or slits may slowdown the mass transfer rate of the lime in the bulk slag

The mass transfer rate of CaO through the boundary layer in the bulk slag will be affected by the physical nature of slag. The viscosity of slag can be calculated [19] from the knowledge of gas void fraction, solid slag (C_2S) content, and the amount and size of liquid metal droplets circulating through slag. It should however be noted that by analysing industrial data only a representative/functional kinetic model can be developed and this model will be suitable for a specific set of operating conditions in BOF (vessel size, oxygen flow rate, nozzle design, slag chemistry, lance height etc.).The same functional model, however, can be easily tuned to a different set of operating conditions in another vessel.

The expression for mass transfer usually employed in literature, when concentration difference is the only driving force, is

$$J = -DC\frac{dX}{dy} = -k(C_b - C_i) \tag{1.4}$$

where X is mole fraction of the diffusing component and C molar density (mol/m^3). In convective mass transfer the term $D/\Delta y$ is replaced by mass transfer coefficient k and concentration gradient is written as $(C_b - C_i)$ where subscript b and i refer to bulk and interface, respectively. The above expression should be used with care as it will not be applicable and does not explain up-hill diffusion. The approximations made in using the above expression must be kept in mind, specially in the case of two phase slag-metal reactions where large differences in chemical potential of diffusing components can arise due to reactions taking place at the interface. The argument applies equally well to reactions in which the precipitating phase has a different structure altogether, for example precipitation of Al_2O_3 or other non-metallic compounds in liquid or solid metal.

A more fundamental expression for mass transfer, based on the difference in chemical potential at the interface and bulk, is

$$J^{''} = -\frac{n_A}{N_o}B_A\frac{d\mu}{dy} = -\frac{n_A}{N_o}\frac{D}{k_bT}\frac{d\mu}{dy} \tag{1.5}$$

n_A is the number of atoms of A per unit volume, N_o is Avagadro's number, B_A is the mobility of A in the presence of energy gradient and is equal to $\dfrac{D}{k_bT}$ (from Nernst-Einstein Equation, where k_b is Boltzman constant and T is temperature), μ is chemical potential, y is the distance coordinate, and $J^{''}$ is the flux of atoms passing through unit area. The term $\dfrac{n_A}{N_o}$ is molar concentration C_m and molar flux J can be equated to $J^{''}/N_o$.

On substituting these we get,

$$J = -D.C_m \cdot \left(\frac{\partial \mu}{\partial y} \right) \cdot \frac{1}{RT} \qquad (1.6)$$

By definition

$$\mu = \mu_0 + RT \ln(a) \qquad (1.7)$$

Where 'a' is the Raoultian activity

Now differentiating μ w.r.t a, we get

$$\frac{\partial \mu}{\partial a} = RT \cdot \frac{1}{a} \qquad (1.8)$$

$$\partial \mu = RT \cdot \frac{\partial a}{a} \qquad (1.9)$$

On substituting $d\mu$ in Eq. (1.6) we get

$$J = -D.C_m \cdot \left(\frac{\partial a}{a} \right) \cdot \frac{1}{\partial y} \qquad (1.10)$$

As a first approximation it can be assumed that $dy = \Delta y$ and $\frac{D}{\Delta y} = k''$ where k" is similar to mass transfer coefficient in a non-ideal solution. Further, on approximating $da \approx \Delta a = (a_b - a_i)$, $a_b = \gamma_b X_b$ and $a_i = \gamma_i X_i$ where γ is the Raoultian activity coefficient, subscript b and i represent the bulk and interface, respectively, and X is the mole fraction. Concentration is related to mole fraction as follows:

$C_m = \frac{X_b . n_{tot}}{V_m}$ where n_{tot} is the total number of moles and V_m is the volume, on

substitution into (1.9) we get

$$J = -k'' . n_{tot} \frac{(a_b - a_i)}{V_m \gamma_b} \qquad (1.11)$$

17

It can be seen that in an ideal solution when $\gamma_b = \gamma_i = 1$ Eq. (3) reduces to

$$ J = -k''.(C_b - C_i) \tag{1.12} $$

It is thus proved that Eq. (1.12) is a special case of Eq. (1.6). As stated earlier, Eq. (1.12) is used when concentration difference is the only driving force for mass transfer. As a precaution it is recommended to use Eq. (1.11) and not Eq. (1.12) because most of the cases of slag-metal systems encountered in steelmaking the equality $\gamma_b = \gamma_i = 1$ is usually not true, either for the components in the slag phase or in the metal phase. In oxygen steel making (BOF), the FeO content of slag increases to as high as 32 % in the early part of the blow, even though metal is nearly saturated with carbon. This is a situation far away from equilibrium. Only when the system is very close to equilibrium, viz. towards the end of the refining process, the equality $\gamma_b = \gamma_i = 1$ is approached. A similar phenomenon is encountered in the beginning of blow in the AOD process or during oxygen injection in the EAF, when carbon content of metal is high (say ≈ 0.8-2%).

On rearranging Eq (1.11) for mass transfer rate (flux) of CaO in slag

$$ -\frac{\partial n_{CaO}}{A.\partial t} = -k_{CaO}.n_{tot}.\left(\frac{a_b - a_i}{V_m.\gamma_b} \right) \tag{1.13} $$

$$ A.k_{CaO} = \frac{\partial n_{CaO}}{n_{tot}.\partial t}.\left(\frac{V_m.\gamma_b}{a_b - a_i} \right) \tag{1.14} $$

Where n_{tot} is the total numbers of moles and V_m is the volume of slag

$$ V_m = Ws / \rho_s $$

$$ A.k_{CaO} = \frac{\Delta n_{CaO}.\gamma^b_{CaO}.W_s}{\Delta t.n_{tot}.\rho_s} \cdot \frac{1}{\left[\gamma^b_{CaO} X^b_{CaO} - a^i_{CaO} \right]} \tag{1.15} $$

18

The activity of CaO in the binary FeO-CaO system as shown in Figure 1.10 is nearly constant at 0.95 when X_{CaO} changes from 0.5-0.9 [20]. The value of γ^b_{CaO}, the activity coefficient of CaO in bulk phase, can be calculated for a given composition of liquid slag by using quasi-regular solution model [21]; for the slag compositions given in Table 1.4 It is found that the activity γ^b_{CaO} is almost constant at 0.2 as shown in Figure 1.11. It may be noted that X^b_{CaO} is mole fraction of CaO corresponding to composition of bulk liquid slag, which changes with time along the liquidus line in the CaO-FeO-SiO$_2$ ternary diagram. As shown in Figure 1.12, the liquidus composition is determined by connecting CaO centre i.e. point of the pure lime (or, alternatively to C$_2$S point on the CaO- SiO$_2$ line) to the point of slag composition. If the slag composition lies in the liquid phase then it is not necessary to calculate the point of intersection with liquidus line.

Table 1.3: Summary of work done by various investigators

Investigators	Bath conditions	Lime Type	Slag Type	Phases observed	Rate controlling mechanism proposed
Matsushima et al. [3]	Static	40 % porosity	(i) FeO-CaO-SiO$_2$ (BOF slag) (ii) CaO-SiO$_2$-Al$_2$O$_3$ (BF slag)	(i) CaO-FeO solid solution next to the lime surface (ii) FeO rich layer next to (Ca, Fe) O solid solution layer (iii) C$_2$S (or C$_3$S) layer slightly away from the lime surface	Diffusion of CaO through the FeO (or Al$_2$O$_3$) rich slag layer adjacent to the lime specimen and through the C$_2$S (or C$_3$S) layer
	Stirred				
Hachtel et al. [1]	Static	Porous	FeO-CaO-SiO$_2$ (BOF slag)	(i) CaO-FeO solid solution next to the lime surface (ii) FeO rich layer next to (Ca, Fe) O solid solution layer (iii) C$_2$S (or C$_3$S) layer slightly away from the lime	Counter diffusion of CaO from the interface and SiO$_2$ from the bulk leads to the formation of C$_2$S

20

				surface	
Oeters et al. [2]	Static	Porous	FeO-CaO-SiO$_2$ (BOF slag)	(i) (Ca, Fe) O solid solution next to the lime surface (ii) FeO rich layer next to (Ca, Fe) O solid solution layer (iii) C$_2$S (or C$_3$S) layer slightly away from the lime surface	Counter diffusion of CaO from the interface and SiO$_2$ from the bulk leads to the formation of C$_2$S
Kimura et al.[5]	Static	Porous	CaO-SiO$_2$-Al$_2$O$_3$ (BF slag)	(i) (Ca, Al) O solid solution next to the lime surface (ii) Al$_2$O$_3$ rich layer next to lime surface (ii) C$_2$S (or C$_3$S) layer slightly away from the lime surface	Counter diffusion of CaO from the interface and SiO$_2$ from the bulk leads to the formation of C$_2$S
Natalie et al. [4]	Stirred	Porous	FeO-CaO-SiO$_2$ (BOF slag)	(i) Discontinuous C$_2$S (or C$_3$S) layer adjacent to the dissolving lime (ii) CaO in the liquid phase will be high at the	Diffusion of CaO from · the lime/slag interface to the bulk slag

				lime/slag interface and will be lower further away from the interface	
Briggs et al. [5]	Static Stirred	Lime (Hard 25% porosity and soft 43% porosity)	FeO-SiO$_2$	(a) Hard burnt lime (i) Iron oxide rich liquid region (ii) Zone of C$_2$S layer next to FeO rich layer (b)Soft burnt lime (i) Calciowustite layer next to lime (ii) FeO rich layer next to Calciowustite layer (iii) C$_2$S layer	Diffusion of CaO from the lime/slag interface to the bulk slag
Martonic et al.[6]	Stirred	Calcined lime	FeO-CaO-SiO$_2$ (BOF slag)	(i) (Ca, Fe) O solid solution next to the lime surface (ii) FeO rich layer next to (Ca, Fe) O solid solution layer (iii) C$_2$S (or C$_3$S) layer slightly away	Diffusion of CaO through the lime/slag interface

				from the lime	
Present work	Stirred	Pure lime	FeO-CaO-SiO$_2$ (BOF slag)	(i) (Ca, Fe) O solid solution next to the lime surface (ii) Discontinuous C$_2$S layer having narrow canals in it.	Diffusion of CaO from FeO-CaO solid solution layer to the bulk slag
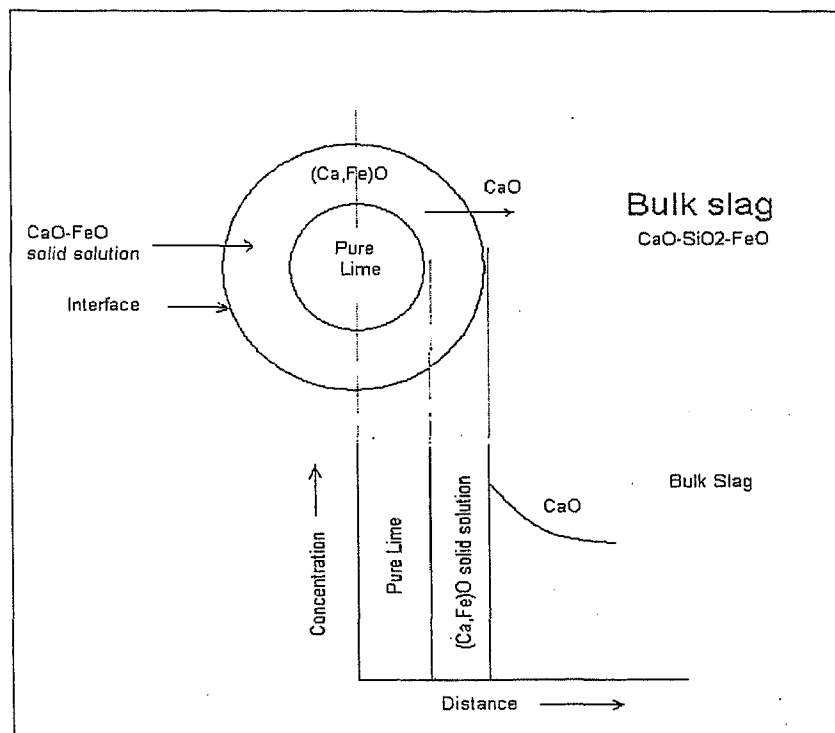
Figure1.9: Proposed model of lime dissolution in a BOF (stirred bath)
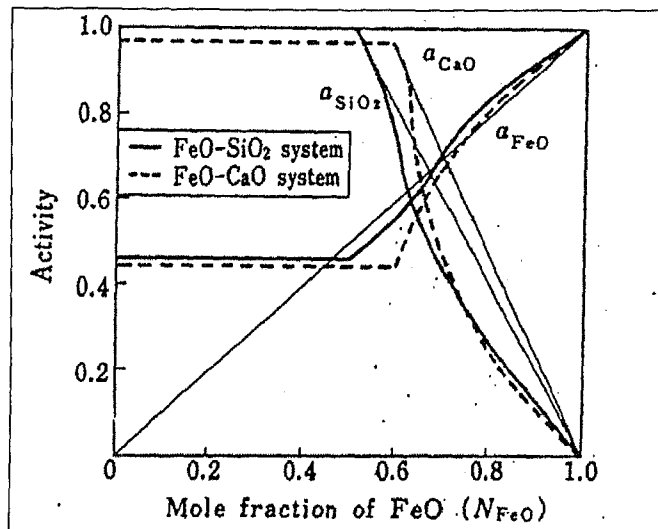
Figure 1.10: Activity curve for FeO-CaO and FeO-SiO$_2$ slag in equilibrium with solid iron at 1560 °C [34]
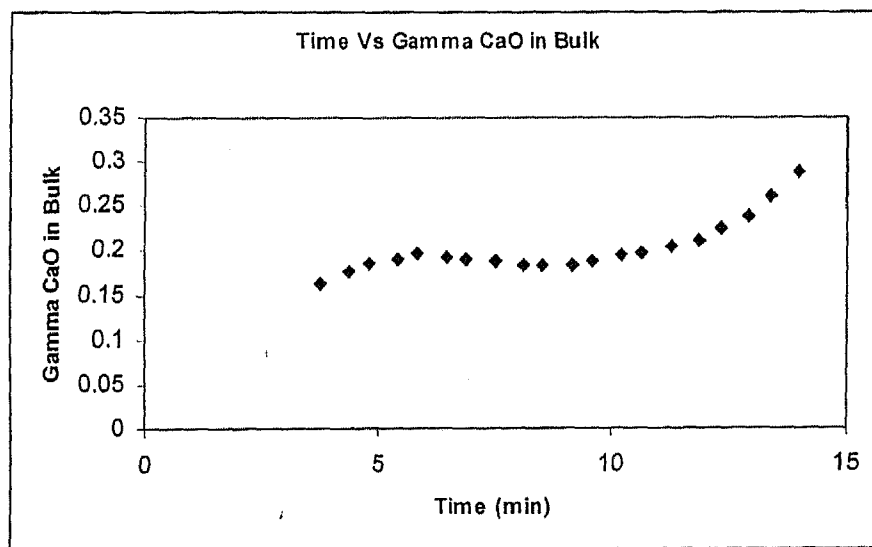
Figure 1.11: γ_{CaO}^{b} variation with time

24

Figure 1.12: Ternary diagram for the calculation of bulk concentration

1.3.1 Plant data on lime dissolution studies for a 300 ton BOF

The plant data for lime dissolution in 300 ton BOF was obtained (Table 1.4) by taking slag samples during the middle period of the blow (between 3.75 min. to 13.95 min of blow period). After converting to quasi ternary composition the data are plotted in Figure 1.13. The details of the procedure adopted for collection of slag samples are provided elsewhere [1]. Each set of values in Table 1.4 represents an average value for approximately 20 heats made under approximately similar conditions of hot metal composition and temperature, scrap amount, oxygen blow rate, lance height and blowing regime, addition sequence and amount of flux and ore, etc.

Figure 1.13: Slag path for slag composition given in Table 1.4; liquidus lines of different temperature are also shown

Table 1.4: Industrial data used to calculate mass transfer coefficient of CaO k_{CaO} for 300 ton BOF

Time, min	Liquidus Temp, °C	CaO Wt %	SiO$_2$ Wt %	FeO Wt %	Weight of slag, kg
3.75	1429	37.8	28.7	33.5	17353
4.35	1460	39.0	29	32	17647
4.8	1481	40	29.3	30.7	17647
5.4	1491	41.6	29.5	28.9	17941
5.85	1499	43.2	30	26.8	17941
6.45	1496	45	30.4	24.6	17941
6.9	1491	47.2	30	22.8	18088
7.5	1486	49	29.5	21.5	17941
8.1	1481	50.2	29.6	20.2	17941
8.55	1481	52	28.5	19.5	17941
9.15	1481	53.6	27.7	18.7	17647
9.6	1486	54.6	27.2	18.2	17941
10.2	1499	55.8	24.9	19.3	17941
10.65	1502	56.2	23.7	20.1	17941
11.25	1522	56.3	22.3	21.4	18235
11.85	1538	55.3	21.5	23.2	18823
12.3	1558	55	20.8	24.2	19412
12.9	1584	54	19.7	26.3	20000
13.35	1620	52.7	18.7	28.6	20882
13.95	1656	51.3	18.1	30.6	21765

1.4 Procedure of calculating mass transfer coefficient of CaO (k_{CaO}) in slag

The procedure involves calculations of

- Composition of liquid part of slag
- Number of moles of CaO dissolved in slag in between consecutive sampling periods
- Activity Coefficient of CaO in Bulk slag
- Total area of lime particles
- Viscosity of slag, solid content of slag, droplet content of slag etc for a given gas void fraction

(a) Calculation of liquidus composition of slag at each time step

For a given temperature and overall composition of slag the solid fraction (of C_2S) is calculated from quasi ternary diagram shown in Figure 1.12 by applying the lever rule. Suppose the overall composition of slag is 37 mass pct CaO, 33.5 mass pct FeO and 28.7 mass pct SiO_2 at 1429 °C which lies at point B in Figure 1.12. From the CaO corner, a straight line is drawn passing through composition point B, which cuts the liquidus line at 1429 °C represented by point D (Figure 1.12).Liquidus composition of slag at point D is - 36.3 mass % CaO, 35.1 mass % FeO and 28.6mass % SiO_2 at 1429 °C .All calculated values are summarised in Table 1.5.

Alternatively, by following a similar procedure the liquidus composition and solid fraction (of C_2S) can be calculated with respect to C_2S point. The calculated values are shown in Table 1.6

Table 1.5: Liquidus composition obtained by program from CaO corner

Time (min)	Slag Temp	Liquidus composition			Δn_{CaO}
		(CaO)b	(FeO)b	(SiO2)b	
3.75	1429	36.3	35.1	28.6	---------
4.35	1460	38.4	31.9	29.6	8686.0
4.8	1481	39.1	31.3	29.5	2121.6
5.4	1491	39.5	30.8	29.7	3331.7
5.85	1499	41.5	27.5	31.0	6359.0
6.45	1496	42.2	25.8	32.0	2239.0
6.9	1491	42.7	24.7	32.6	2873.7
7.5	1486	43.1	23.7	33.3	124.6
8.1	1481	43.1	23.4	33.5	126.4
8.55	1481	43.1	23.4	33.5	0.0
9.15	1481	43.1	23.4	33.5	2262.7
9.6	1486	44.0	22.0	34.1	5032.9
10.2	1499	42.9	24.6	32.4	3363.0
10.65	1502	41.6	27.5	30.9	4236.7
11.25	1522	41.0	28.8	30.2	296.2
11.85	1538	40.6	30.3	29.1	2792.0
12.3	1558	39.5	33.2	27.2	704.5
12.9	1584	39.2	35.0	25.8	3113.6
13.35	1620	39.2	36.8	24.1	5846.2
13.95	1656	39.7	37.8	22.5	8259.7

Table 1.6: Liquidus composition and solid fraction obtained when tie line is drawn starting from C_2S point lying on $CaO-SiO_2$ line

		Liquidus composition			Δn_{CaO}
Time (min)	Slag Temp	(CaO)b	(FeO)b	(SiO2)b	
3.75	1429	35.6	36.4	28.0	-----------
4.35	1460	37.4	33.9	28.7	7550.6
4.8	1481	38.0	33.7	28.3	1844.6
5.4	1491	38.5	33.1	28.4	3606.1
5.85	1499	39.7	30.9	29.5	3780.0
6.45	1496	39.5	31.1	29.4	559.0
6.9	1491	37.7	35.0	27.3	4899.5
7.5	1486	34.5	40.8	24.7	11191.7
8.1	1481	33.6	42.6	23.8	2790.4
8.55	1481	27.3	56.2	16.5	20262.6
9.15	1481	22.8	68.8	8.5	15594.9
9.6	1486	26.2	67.6	6.2	12005.8
10.2	1499	39.4	54.3	6.4	42278.3
10.65	1502	42.4	51.1	6.5	9802.5
11.25	1522	43.6	49.2	7.2	6204.7
11.85	1538	43.7	48.5	7.8	4969.2
12.3	1558	45.8	45.8	8.4	11552.8
12.9	1584	45.5	45.1	9.4	3743.8
13.35	1620	46.9	42.2	10.9	12523.4
13.95	1656	46.3	41.2	12.5	4924.1

(b) Calculation of change in the numbers of moles of CaO (Δn_{CaO}) developed between two consecutive slag samples

Suppose at t = 3.75 min, mass pct CaO in liquid slag is 36.3 mass % and slag weight is 17353 kg. Then moles of CaO in liquid slag at this time can be calculated as

$$n_{3.75} = \frac{36.29 \times 17353 \times 1000}{56 \times 100} moles$$

Similarly at t = 4.35 min

$$n_{4.35} = \frac{38.444862 \times 17647 \times 1000}{56 \times 100} moles$$

Hence, number of moles of CaO dissolved in slag in the time interval 3.75 and 4.35 minutes is

$$\Delta n_{CaO} = n_{4.35} - n_{3.75} = 8686.04 moles$$

During each time interval change in number of moles of CaO in liquid slag is thus calculated and the values are included in Table 1.5.

(c) Calculation of activity coefficient of CaO, γ_{CaO}, in liquid slag using regular solution model [21]:

According to the regular solution model [21] the activity coefficient of component, $i.e$ in a multi-component regular solution is expressed by following equation:

$$\bar{G}_i^E = \Delta \bar{H}_i = RT \ln \gamma_i \qquad (1.16)$$

$$RT \ln \gamma_i = \sum a_{ij} X_j^2 + \sum \sum (a_{ij} + a_{ik} - a_{jk}) X_j X_k \qquad (1.17)$$

Where $\bar{G}_i^E$ is the excess partial molar free energy, $\Delta \bar{H}_i$ is the relative partial molar enthalpy, X_i and X_k are the respective mole fractions of the cation species j and k and a_{ij} is the interaction energy between cations i.e ,(i cations)-O-(j cations). The values of

interaction energy parameters (a_{ij}) for CaO-FeO-SiO$_2$ slag are given in Table 1.7. From equation (1.17) the value of γ_{CaO} for the CaO-FeO-SiO$_2$ slag can be calculated by using the following equation

$$RT \ln \gamma_{CaO} = -133890 X^2_{SiO_2} - 31380 X^2_{FeO} - 123430 X_{FeO} X_{SiO_2} \qquad (1.18)$$

$$\ln \gamma_{CaO} = -133890(0.30)^2 - 31380(0.30)^2 - 123430(0.30 \times 0.30)/(8.31 \times 1702)$$

$$\gamma_{CaO} = 0.16$$

Thus by knowing the respective mole fractions CaO, SiO$_2$ and FeO and temperature the value γ_{CaO} can be calculated for all compositions, the calculated values are plotted in (Figure 1.11).

Table 1.7: Interaction energy parameters (a_{ij}) for CaO-FeO-SiO$_2$ slag

i \ j	Fe^{2+}	Ca^{2+}	Si^{2+}
Fe^{2+}	-	-31380	-41840
Ca^{2+}	-31380	-	-133890
Si^{2+}	-41840	-133890	-

(d) Calculation of surface area of lime particles

The following assumptions are made:

- Lime charged at the beginning is 10 tons =10000 kg
- Shape of the lime particle is spherical
- Density of the lime charged is ρ = 2691 kg/m^3
- Average radius of lime particles is assumed to be r =0.02 m ?

Volume of each lime particle, $V_p = \frac{4}{3} \times pi \times r^3 = 3.35 \times 10^{-5}$ m^3

Weight of one lime particle at t=0, $W_p = \rho V = 90$ g

Hence, number of lime particles charged at t = 0 , N = 10 ton/90 g = 110950

Total surface area of lime particles at the time of charging, $A_{t=0} = N \times 4 \times pi \times r^2 =$ 557.42 m^2

Mass of undissolved lime at t = 3.75 min = 10000-36.293129 % of 17343 = 3702.05 kg

Mass of each lime particle at t = 3.75 min = 3702.053325×1000/ N = 33.36 g

Volume of each lime particle at t= 3.75 min, $V_p = 30g / \rho$ = 1.23994 × 10^{-5} m^3

Corresponding radius of lime particle at t = 3.75 min = 1.50 cm

Total surface area of lime particles at the time t= 3.75 min, $A_{t=3.75} = N \times 4 \times pi \times r^2 =$ 557.4136 m^2

Thus total area of the lime particles can be calculated at each time step; the values are summarised in Table 1.8.

(e) Calculation of volumetric mass transfer coefficient, K_{CaO} (A k$_{FeO}$)

Knowing the values of all required parameters from sections (a)-(d) above the value of k_{CaO} can be calculated from equation (1.15) . The calculated values for both cases (CaO apex and C$_2$S point) are summarised in Table 1.9

Table 1.8: Calculated lime surface area at each time interval

Time,min	Undissolved lime,kg	Radius of each particles cm	Weight of each lime particles, g	Surface area, m2
3.75	3702.1	1.5	33.4	312.8
4.35	3215.6	1.4	29.0	285.1
4.8	3096.8	1.4	27.9	278.1
5.4	2910.2	1.4	26.2	266.9
5.85	2554.1	1.3	23.0	244.9
6.45	2428.8	1.3	21.9	236.9
6.9	2267.8	1.3	20.4	226.4
7.5	2274.8	1.3	20.5	226.9
8.1	2267.7	1.3	20.4	226.4
8.55	2267.7	1.3	20.4	226.4
9.15	2394.4	1.3	21.6	234.7
9.6	2112.6	1.2	19.0	216.0
10.2	2300.9	1.3	20.7	228.6
10.65	2538.2	1.3	22.9	243.9
11.25	2521.6	1.3	22.7	242.8
11.85	2365.2	1.3	21.3	232.8
12.3	2325.8	1.3	21.0	230.2
12.9	2151.4	1.3	19.4	218.7
13.35	1824.0	1.2	16.4	196.1
13.95	1361.5	1.1	12.3	161.7

Table 1.9: Calculated values of mass transfer coefficient (k_{CaO}, cm/s)

Time(min)	Ak_{CaO} (m³/s) CaO corner × 10⁻⁴	Ak_{CaO} (m³/s) C_2S point × 10⁻⁴	k_{CaO}(cm/s) CaO corner × 10⁻⁴	k_{CaO}(cm/s) C_2S point × 10⁻⁴
3.75	--------	-------	--------	--------
4.35	11.3	9.7	4.0	3.4
4.8	3.7	3.2	1.3	1.1
5.4	4.4	4.7	1.6	1.8
5.85	11.3	6.6	4.6	2.7
6.45	3.0	0.7	1.3	0.3
6.9	5.2	8.4	2.3	3.7
7.5	0.2	14.0	0.1	6.2
8.1	0.2	3.5	0.1	1.5
8.55	*	31.6	*	14.0
9.15	3.1	17.4	1.3	7.4
9.6	9.2	18.0	4.3	8.3
10.2	4.6	50.8	2.0	22.2
10.65	7.5	16.0	3.1	6.5
11.25	0.4	7.6	0.2	3.2
11.85	3.7	6.1	1.6	2.6
12.3	1.2	19.3	0.5	8.4
12.9	4.0	4.7	1.8	2.1
13.35	10.0	21.2	5.1	10.8
13.95	10.5	6.3	6.5	3.9

* value could not be calculated

1.5 Results and discussion

The value of k_{CaO} is plotted in Figure 1.14; the scatter in this the figure reveals the inherent fluctuation in the BOF process which in turn are manifested by dynamic changes in metal droplet content of slag, gas void fraction, solid content and hence their impact on slag viscosity and flow conditions. The fluid flow directly affects the magnitude of volumetric of the mass transfer coefficient. In the time period of 8-10 min, the value of k_{CaO} is not plotted in Figure 1.14 because of high solid fraction of slag.

The value of mass transfer coefficient, k_{CaO}, can be calculated by dividing K_{CaO}, $(A.k_{CaO})$ with average area of lime particles in contact with liquid slag. The calculated values of k_{CaO} assuming an average starting diameter of lime to be 20 mm, are listed in Table 1.10 and compared in Table 1.10 with other reported values in literature (along with the experimental conditions maintained in each case) in literature. Considering the wide variety of experimental conditions employed in each experimental setup, it is surprising that the order of magnitude of k_{CaO} values (of the order of 10^{-4}) is same for almost all cases. It implies that the models for BOF, in which dissolution rate of lime is to be calculated as a function of time (for example to compute foam height in a dynamic foaming model for BOF etc.), one can assume the mass transport of CaO to be rate controlling. This is partly in agreement with the results of laboratory experiments and observations on the shop floor that only "size of lime particle matters".

The slag samples taken at the end of blow, for almost all cases, show that the crystals of dicalcium silicate are uniformly distributed in slag; the size of crystals varies depending upon basicity and temperature [22]. Very small particles of calcium ferrite are also seen in the slag close to the dicalcium silicate particles (Figure 1.15). It only shows that dissolution of lime in BOF takes place in a complex environment which varies with time, right from the beginning to the end of process.

36

The magnitude of k_{CaO} increases marginally with blow time. The calculated viscosity of slag, slag-gas, and slag-gas-solid is plotted as a function of time in Figure. 1.16; the solid represents here the C_2S present in slag at different stages of the blow. While the viscosity of slag and slag-gas decrease with time, which of slag-gas-solid continuum increases with time. Slight increase in k_{CaO} value with time is in agreement with the decrease in viscosity of slag-gas-solid, in Figure 1.16.

It is assumed in the kinetic model that CaO-FeO solid solution layer forms next to lime. This is confirmed by the laboratory experiment done in the present work as well as in [8, 23]. The general conception is that FeO helps in the dissolution of lime. The main influence of FeO is transmitted through its impact on viscosity and melting point of slag. The content of FeO in slag in BOF increases and decreases through out the blow period where as lime continues to dissolve. Moreover the concentration of FeO is always high near the lime surface due to rejection of FeO at lime surface, when lime reacts with silica to form dicalcium silicate. The mass transfer of FeO may not be rate controlling as suggested in a recent work [24].

Table 1.10: Values of mass–transfer coefficient of CaO reported in literature and average value obtained in the present work.

Investigators	Static, k_{CaO} cm/s	Rotated, k_{CaO} cm/s	Speed of revolution Rev min^{-1}	Temp °C	Apparent porosity %
Green et al [25]	1.74×10^{-4}	3.5×10^{-4}	32	1300	25
Matsushima et al.[4]	....	9.7×10^{-4} 17.1×10^{-4}	200 400	1400 1400	40 40
Williams et al. [7]	2.8×10^{-4} (Hard lime) 9.8×10^{-4} (Soft lime) 12.3×10^{-4} 3.5×10^{-4} (Dolomitic lime)	13.1×10^{-4} 4.3×10^{-4}			25 45 50 50
Kor et al.[8]	Fully calcined lime	10.0×10^{-4}		1375	
Theoretical [26]	....	3.2×10^{-4}	50	1300	...
Present work (average value)	....	2.19×10^{-4} + 2 mw bar			
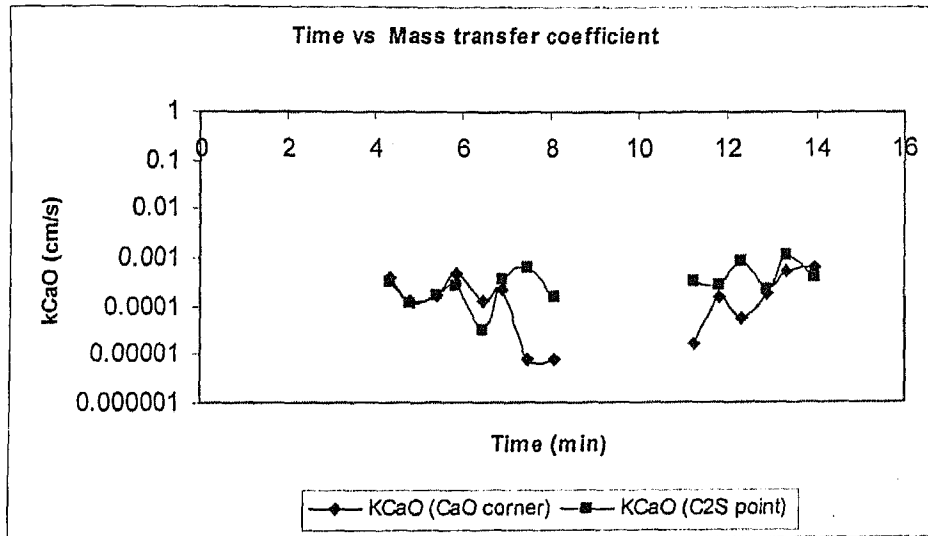
Figure 1.14: Variation of mass transfer coefficient (k_{CaO}, cm/s) with time.
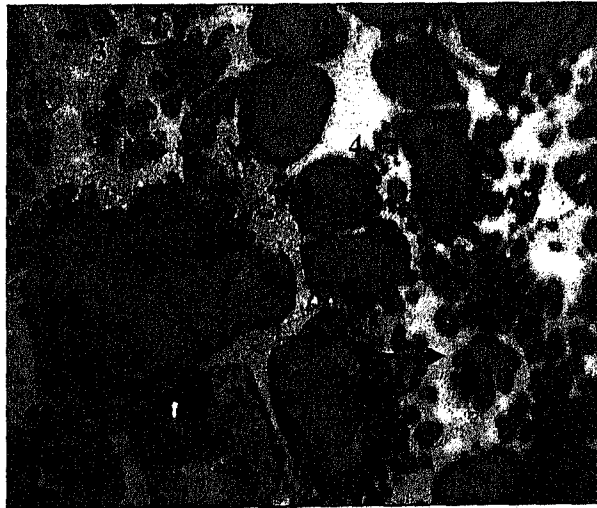
Figure 1.15: Optical micrograph of (high phosphorous (0.2%) hot metal) low (0.9 %) MgO slag. Basicity-3.9. Tapping temperature-1700^0C
Point-1 Dicalcium silicate (C_2S)
Point-2 Wustite solid solution
Point-3 Calcium aluminium ferrite
Point-4 Dicalcium silicate
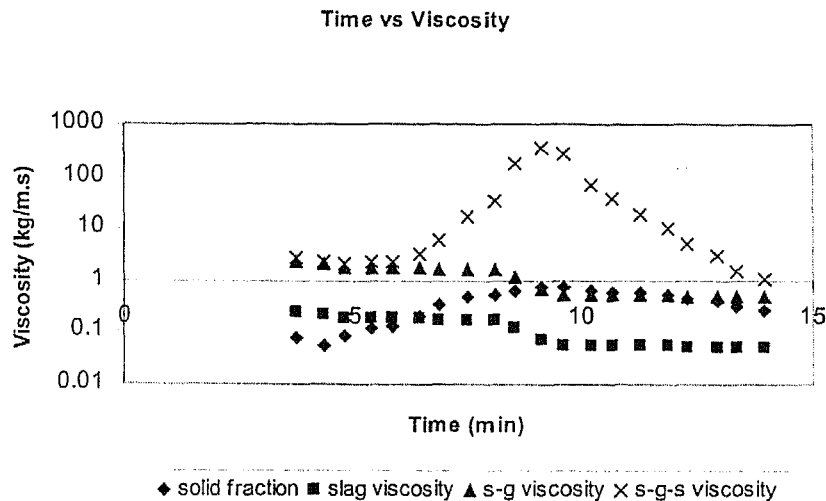
Figure 1.16: Calculated Viscosity of, slag, slag-gas, slag-gas-solid with blowing time

1.6 Conclusions

1. The laboratory experiment showed that:

- A frozen layer of slag forms on the surface of cold lime to start with. The layer melts and the pores of lime are penetrated by liquid slag. In the penetration layer only CaO and FeO are present.

- There is preferential attack of FeO on lime along the grain boundaries of lime.

- The size of lime has a strong influence on the dissolution rate.

2. A kinetic model is developed for lime dissolution by assuming mass transport of CaO in bulk slag to be rate controlling. Application of the model to industrial data for a 300 ton BOF shows that:

- Mass transfer coefficient of CaO in slag is approximately 2.19×10^{-5} m/s

- The dissolution rate of lime is greatly affected by the viscosity of slag.

- Even at the end of the blow the slag is heterogeneous and contains liquid metal droplets, un-dissolved lime, dicalcium silicate and CaO-FeO solid solution.

40

CHAPTER 2

Kinetics of Iron Oxide Reduction by Iron Carbon droplets in BOF Vessel

2.1 Introduction

There is a renewed interest in the study of kinetics of reaction between FeO in liquid slag and the carbon containing droplet with a view to develop control models for the foaming of slag in BOF process [27]. As soon as the metal droplet comes in contact with slag a gas film (or halo) is formed around the droplet and the direct contact between the slag and the carbon rich metal droplet is blocked. The overall reaction between carbon-containing liquid iron droplet and liquid slag containing FeO can be expressed as

$$(FeO) + C = CO + Fe \tag{2.1}$$

The reaction proceeds via two sequential reactions, with CO and CO_2 acting as gaseous intermediates, i.e.

$$CO + (FeO) = CO_2 + Fe \qquad \text{at gas/slag interface} \tag{2.2}$$
$$CO_2 + C = 2CO \qquad \text{at gas/metal interface} \tag{2.3}$$
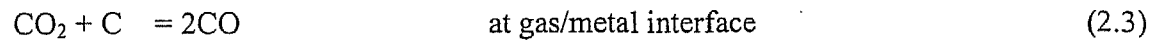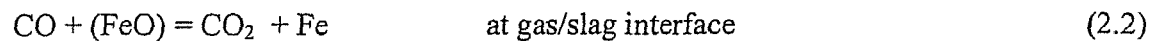
The existence of a gas film (or halo) between an iron oxide-containing slag and the solid carbon or liquid metal droplet, as shown in Figure 2.1 [30] has been confirmed by direct observations of the droplet using X-rays [29-30, 35-43].

The possible rate-controlling steps for the overall reaction (2.1) are:

1. Reduction of iron oxide in slag by CO gas at gas-slag interface, i.e., reaction (2.2)
2. Mass transfer of Fe^{2+} and O^{2-} ions from the bulk slag to slag-gas interface

3. Mass transfer of CO from the gas-metal interface to the gas-slag interface and mass transfer of CO_2 from the gas-slag interface to the gas-metal interface

4. Reaction of CO_2 with carbon in metal at gas/metal interface, i.e., reaction (2.3)

5. Mass transfer of carbon within the metal to gas metal interface

Although numerous studies have been reported in literature [27-34, 37-38, 44-45, 47, 52] on the kinetics of reduction of iron oxide in liquid slag by solid carbon or carbon dissolved in liquid metal, there exist large discrepancies concerning the magnitude of the rate constants and even the rate controlling steps. The values obtained by different workers for the assumed rate controlling steps are summarized in Table 2.1. The present study was undertaken to critically evaluate the rate constants and their dependence on the iron oxide content of slag, basicity of slag and reaction temperature. The role of interfacial reaction in the overall reduction process has been analyzed. A kinetic model of the iron oxide reduction in BOF slag is proposed and tested on the basis of data collected from the BOF by taking samples during the blow. The effect of slag foaming and emulsification in BOF on kinetics of FeO reduction has been incorporated by making use of earlier work [19,51] for calculating the residence time of the ascending gas bubbles and the settling time of the metal droplets in the slag at a given stage of the blow. The calculated rate constant and mass coefficient is then compared with the values reported in literature, as summarized in Table 2.1.

The experimental arrangements used by various investigators and their results are first briefly discussed in section 2.2. The kinetic model developed in this work and its application to BOF data is then described in section 2.3.

42
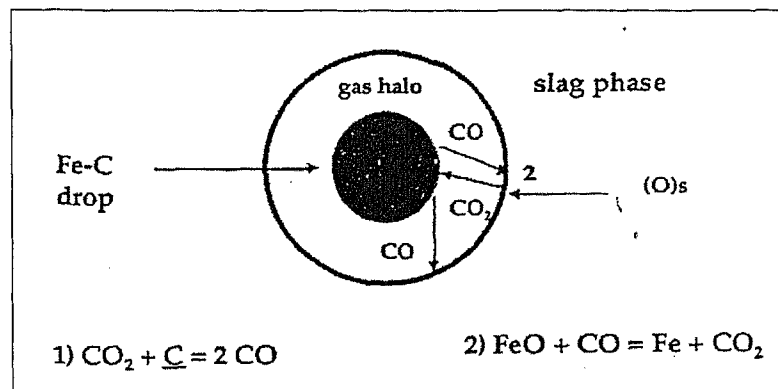
Figure 2.1: Gas halo around metal droplet [30]

Table 2.1: Reported rate constant and mass transfer coefficient values by various workers

Investigators (Gas-Metal reaction)	k_{g-m} rate constant (Mol cm^{-2} s^{-1} atm^{-1})	Temperature range
1. Kirkbride [57]	1.67×10^{-4} at 1430 °C	1430-1570 °C
2. Sugata et al [58]	$3.33- 8.3 \times 10^{-5}$ at 1400 °C	1350-1450 °C
3. Davis et al [59]	1.3×10^{-4} at 1400 °C	1400-1500 °C
4. Fay fun [60]	3.33×10^{-4}	1650 °C
5. Sain and Belton [28]	1.0 E-04 – 5.5×10^{-4} at 1400 °C (Depending upon Sulphur content)	1160-1600 °C
6. Lloyd et al [31]	3.16×10^{-3} at 1600 °C	1300-1600 °C
7. Grez et al [61]	3.5×10^{-4} at 1600 °C	
8. Sommerville et al [31]	3.33×10^{-4} at 1380 °C	1380 °C
9. Cramb and Belton [29]	3.9×10^{-4} at 1550 °C	1540-1740 °C
10. Present work	7.81×10^{-4} - 2.42×10^{-5}	**1429-1656 °C**
Investigators (Gas-Slag reaction)	k_{g-s} rate Constant (Mol cm^{-2} s^{-1} atm^{-1})	Temperature (K)
1. Min and Fruehan [37]	2.6×10^{-5}	
2. Li et al [32]	3.08×10^{-5}	1773 K
	1.84×10^{-5}	1673 K
3. T Sukihashi et al [45]	1.75×10^{-5}	1873 K
	1.25×10^{-5}	
4. Nagasaka et al [54]	1.46×10^{-5}	1723 K
	1.21×10^{-5}	
5. Schwerdtfeger et [30]	4.4×10^{-5}	
	7.0×10^{-5}	
6. Present work	1.39×10^{-3}– 1.958×10^{-5}	
Investigator (Mass Transfer of FeO in Slag)	k_{FeO} (cm/s)	
1. Min and Fruehan [37]	0.01 – 0.001	
2. Sain and Belton [28]	3.0 - 4.0×10^{-2}	
3. Molloseau et al [30]	1.3×10^{-3} (For 10 mass pct FeO) 3.8 E –	
4. Present work	**0.01838 - 0.004308**	**1702K-1929K**

44

2.2 Review of reduction of FeO in slags by iron-carbon melt

In the BOF process (Figure 2.2 [46]) pure oxygen is blown on to a molten iron bath for refining. In the hot spot region the oxygen reacts simultaneously with iron and the dissolved alloying elements. Due to the impact of the oxygen jet, iron droplets are ejected and then dispersed in the slag phase. The metal-slag dispersion is mixed further by the rising CO and CO_2 bubbles and serves as the main reaction zone. Droplets from the dispersion fall back into the bulk metal lying underneath the bulk slag.

Foaming of the slag is a characteristic feature of BOF steel making and the stability of the foam depends on rate of oxidation of carbon from the metal droplets as well as on the reduction of FeO from the slag. Several researchers have proposed that the rate of reduction of FeO from the slag depends mainly on the rate of decarburisation of the metal droplet present in the slag foam. The rate of the decarburisation of metal in the jet impact zone is determined by oxygen blowing conditions while intermediate formation of FeO in the hot spot serves as source for decarburisation in the slag. A brief review of the various experiments to understand and also to model the kinetics of the reduction of FeO in slag is provided below.

2.2.1 Gas-metal reaction as the rate controlling step

Many workers have suggested that the reaction of CO_2 in gas stream (gas halo) with Fe-C droplet can be rate controlling if sulphur content of metal droplet is greater than 0.001 pct. The reason for this is that sulphur acts as surface-active element and hence blocks the surface sites for the reaction.

(a) Sain and Belton [28] were the first researchers to measure the chemical rate of reaction of CO_2 with carbon dissolved in liquid iron. They used an innovative technique in which a gas jet impinged on the metal surface thereby avoiding gas phase mass transfer (GPMT) as a rate limiting step. The experiments were designed to avoid mass

transfer limitation by using an inductively stirred melt, high gas flow rate, and a geometrical arrangement to take further advantage of high mass transfer characteristics of the impinging gas jet which forced the system into a regime of interfacial reaction control. Carbon content of metal was either maintained at saturation or restricted to greater than about 1 mass pct. The rate of reaction was independent of carbon content and was first order with respect to the pressure of CO_2. The rate of chemisorption of CO_2 was thus a rate-controlling step.

a (i) Experimental technique used by Sain and Belton

- gas-metal system
- temperature range: 1160-1600 °C
- inductively stirred melt
- carbon saturated bath

The general experimental arrangement is illustrated in Figure 2.3 [28]. A 0.49 cm bore silica inlet tube was held coaxially in the open top of an alumina crucible (average internal dia 1.63 cm) and at a distance of 2 to 3 mm above the surface of the contained liquid iron. Temperature of the surface of liquid iron was measured by means of a pyrometer. Telescopic observation of the surface was possible through the optical system of the pyrometer. Induction melting and stirring of the iron was done by means of a 10 kW high frequency generator operating at 450 kHz. The high flow rate of gas was controlled by capillary flow meters with mercury filled "blow off" tubes. Calibration of these flow meters was done with the help of a wet test meter placed at the exit of the apparatus. Rapid turn over between argon and a given gas mixture was possible by the arrangement of stopcocks (Figure 2.3 [28]). In most of the experiments, carbon saturation of the iron was maintained by means of a submerged graphite disc which was cemented to the bottom of the crucible. In other experiments, the iron was taken to a given concentration of carbon by dissolution of a weighted quantity of graphite. The loss of carbon during an experiment was determined by measuring the weight loss.

The usual sample (iron) mass was 10 gm. The analysis of the four irons which were used in this study is shown in Table 2.2 [28].

The preweighed crucible and contents were slowly brought to temperature under flowing Ar or Ar-1 pct H_2.The inlet tube was adjusted to position and then the reacting gas was passed over the sample. Several attempts were made to preheat the gases by means of a spirally wound heater on the inlet tube. At these high gas flow rates (needed for the independence of the rate of weight loss on the flow rate), a pre-heat to about 600 °C led to sufficient jet momentum to cause ejection of the iron from the crucible. Lower preheat temperatures were found to have no effect on the result in the independent regime, and hence the preheater was dispensed with. Occasionally, iron was ejected during meltdown or while passing the reaction gas at the start of experiment; these experiments were rejected. Observation of the surface during an experiment showed no evolution of bubbles and no evidence of the separation of second phase. No fuming of the iron was observed and the several blank experiments which were carried out at 1600 °C with 20 1 min^{-1} of Ar-1 pct H_2 gave weight losses of only 0.001 to 0.002 gm min^{-1}

a (ii) Results

The reported value by them for rate constant at gas-metal interface was 3.3 $\times 10^{-2}$-6×10^{-3} (k_{g-m}, Mol cm^{-2} min^{-1} atm^{-1}) at 1400 °C.

(b) Cramb and Belton [29] used an isotope exchange technique by employing $C^{14}O_2$ as reactant and measured the rate of dissociation of CO_2 on liquid iron between 1540 and 1740 °C and at CO/CO_2 ratios of 6.67 to 100. The experiments were carried out over a sufficiently long period of time to ensure that chemical equilibrium existed between the gas phase and the specimen.

b (i) Experimental technique used by Cramb and Belton

The experimental arrangement was similar to that used by Sain and Belton decarburisation studies (Figure 2.3 [28]). The reaction gas mixture was delivered on the surface of inductively heated iron held in an alumina crucible (average ID 1.63 cm), through a co-axially placed alumina tube of about 8 mm ID, positioned approximately 5 mm above the surface of the metal. The crucible assembly was enclosed in a water-cooled silica chamber of approximately 600 ml internal volume and fitted with a suitable O-ring seal end cap for holding the inlet tube. Temperature measurement and observation of the surface of the liquid iron were done by means of a two-color pyrometer sighted through an optical flat inlet tube.

Labelled CO_2 was introduced into the gas stream after the initial 30 min period, the overall CO_2/CO ratio was maintained at a constant level. Samples for counting were taken from the ingoing CO_2 after a few minutes and from the exit gas after a further 10-15 min to confirm that steady state had been achieved. Blank experiments were carried out for several combinations of temperatures, flow rate, and CO_2/CO ratio by floating a closely fitting alumina disc on the surface of the liquid iron. No difference could be detected between the counts for the resulting CO_2, indicating that negligible exchange could be assumed to occur on the wall of the crucible during normal experiments and carry-over of $^{14}CO_2$ through the gas circuit could be neglected.

b (ii) Results

The forward rate constant for the dissociation of CO_2 on pure iron at 1700 °C was calculated from

$$k_{g-m} = \exp\left(-\frac{11700}{T} - 0.48\right)\bigg/\left[1 + \frac{P_{CO_2}}{P_{CO}}\exp\left(\frac{6700}{T} + 1.08\right)\right] \qquad (2.6)$$

k_{g-m} (mol cm^{-2}s^{-1}atm^{-1}) = 3.9 ×10^{-4} at 1550 °C

The rate constant was 2.34×10^{-2} ($k_{g\text{-}m}$, Mol cm^{-2} min^{-1} atm^{-1}) at 1550 °C and was similar to the data reported by Sain and Belton for decarburisation thereby confirming that dissociative chemisorption of CO_2 as the rate-controlling step.
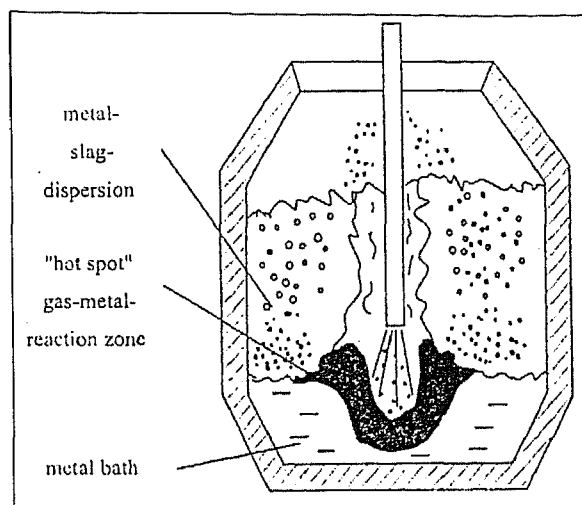
Figure 2.2: The LD - converter process showing different reaction zones [46]
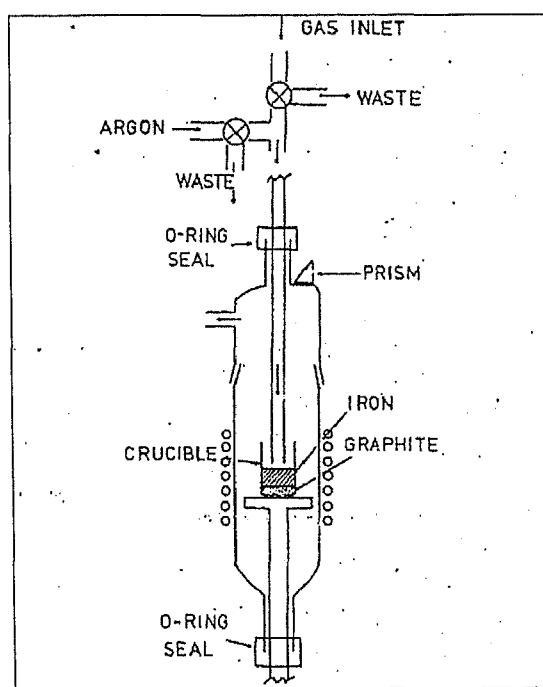
Figure 2.3: Experimental set up of Sain and Belton [28]

Table 2.2: Composition of iron samples, in mass pct (Sain and Belton) [28]

	Type A	Type B	Type C	Type D
C	0.0003	0.01-0.03	0.035	0.011
N	nd	nd	0.00045	nd
O	nd	nd	0.0017	nd
Mn	0.0002	0.001	0.001	0.001
P	ndc	nd	0.001	0.002
S	*ndc	0.0015	0.0020	0.0029
Si	0.001	0.001	0.008	0.007
Ni	ndc	0.1	0.006	0.03
Cr	ndc	0.001	0.003	0.002
V	ndc	0.01	0.001	0.004
W	ndc	0.01	0.001	nd
Mo	ndc	0.001	0.001	0.001
Co	ndc	0.01	0.003	nd
Cu	0.0001	0.001	0.001	nd
Al	0.0001	0.003	0.001	nd
Pb	ndc	0.001	0.01	nd
Sn	ndc	0.001	0.006	nd
Mg	0.0002	nd	nd	nd
Ag	0.0001	nd	nd	nd

nd = not determined ; ndc=not detected ; *ndc=less than 0.0005 mass pct

(c) **Molloseau and Fruehan's** [30] and Min and Fruehan used slag containing 10-30 mass % FeO. The droplet remained intact during the reaction with the slag (i.e. no emulsification). Thus rate was controlled by dissociation of CO_2 on the metal. Schematic diagram representing the reaction of a Fe-C droplet with FeO in the slag [37] is shown in Figure 2.1 [30].

c (i) Experimental technique used by Molloseau and Fruehan

- system: slag-metal
- slag type: $CaO-SiO_2-MgO$ and 3-35 mass pct FeO
- no stirring of bath
- temperature range : 1643-1763 K

The rate of reduction of FeO was determined by using a constant volume pressure increase technique (CVPI) in which 1 mole of CO gas produced is equivalent to 1 mole of FeO reduced. Approximately 60 g of a synthetic slag containing the appropriate amount of FeO was charged into high purity MgO crucible. The crucible was placed into the reaction chamber of a molybdenum disilicide resistance furnace and was heated to the experimental temperature in a purified argon atmosphere. Once the slag reached temperature, the furnace was sealed, and an approximately 1 g Fe-C-S alloy pellet of the appropriate composition was released from a rotary compartment into a tapered mullite tube centred over the slag bath. Once the pellet melted, it was released as a metal droplet from the tapered end of the tube, falling into the slag bath where it began to react. The pressure increase due to evolution of CO gas was measured by the pressure transducer in terms of milli volt and was converted to total moles of FeO reacted with time. After the reaction appeared to cease (indicated by a constant pressure transducer reading), another pellet was released and measurements were taken. Three metal pellets were released into the slag during an experiment. After reaction of the last pellet ceased, the furnace was cooled to room temperature in an argon atmosphere, and the crucible containing the metal –slag mixture were then analysed for C and FeO, respectively. X-ray fluoroscopy was used to observe the behaviour of the metal droplet while it reacted with slag. X-ray video recording began as soon as the Fe-C-S pellet (2.91 mass pct C and 0.011 mass pct S) was

released into the tapered mullite tube centred over the slag bath. Recording continued until reaction of the droplet with slag appeared to cease. At that time, another pellet was released and recording began once again.

c (ii) Results

Typical results for the measurement of the rate of reduction of FeO in the slag by carbon in the metal for 10,20, and 30 mass pct FeO and temperature ranging from 1643 to 1763 are presented in Figure 2.5 - 2.7 [30]. For 10 mass pct FeO, the initial rate varied greatly with temperature. At 1713 K, the initial rate was calculated (using linear regression) to be 3.0×10^{-5} moles/s and increased by an order of magnitude to approximately 2.0×10^{-4} moles/s and 3.0×10^{-4} moles/s at 1738 and 1763 K, respectively. Similarly for 20 mass pct and 30 mass pct FeO results obtained are shown in Table 2.3 [30]

Figure 2.8 [30] shows the total moles of CO evolved as a function of time for 3 to 30 mass pct FeO at 1713 K in order to demonstrate the large dependence of the rate on FeO content. As evident from this plot, below 10 mass pct FeO, only one distinctive rate was observed and was estimated to be 3.0×10^{-6} moles/s, which is two orders of magnitude slower than the initial rate measured at 20 and 30 mass pct FeO.
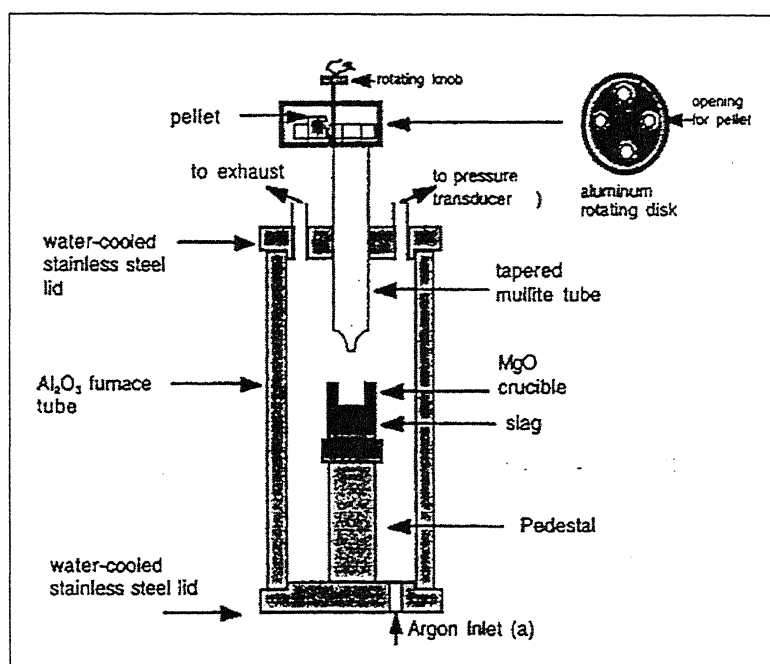
Figure 2.4: Experimental set up of Molloseau and Fruehan [30]
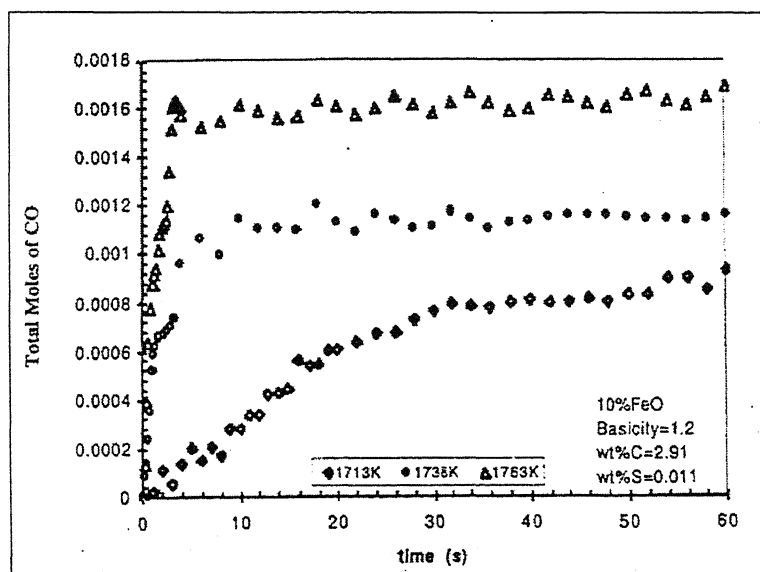
Figure 2.5: Variation of the total moles of CO evolved with time for 10 mass pct
FeO at 1643 to 1763 K (mass of the metal =1 g) [30]
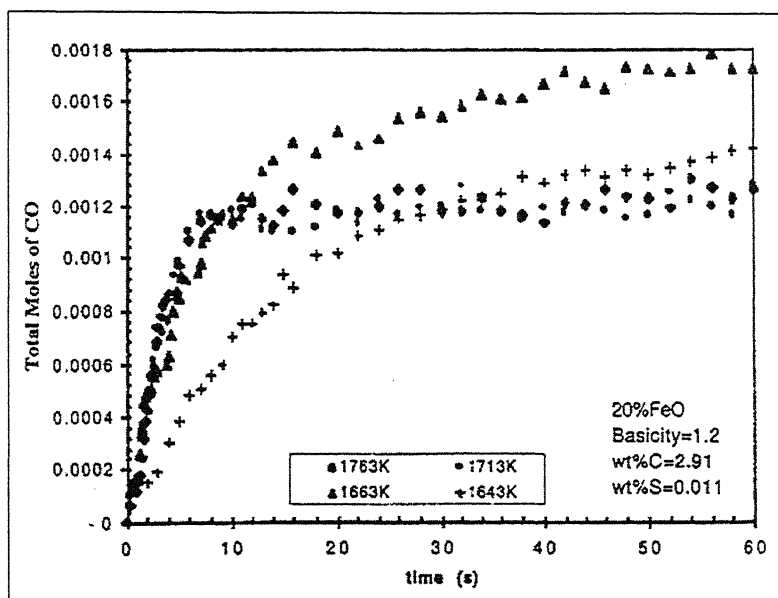
Figure 2.6: Variation of the total moles of CO evolved with time for 20 mass pct FeO at 1643 to 1763 K (mass of the metal =1 g) [30]
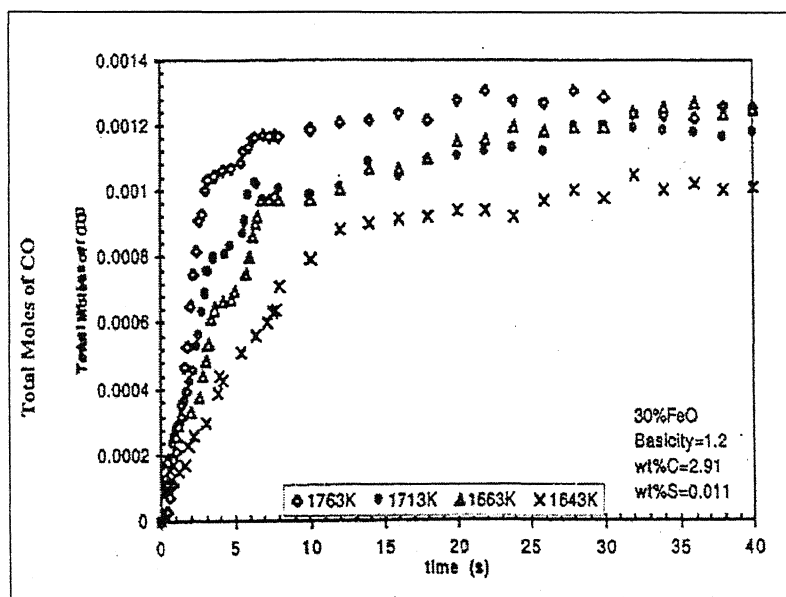
Figure 2.7: Variation of the total moles of CO evolved with time for 30 mass pct FeO at 1643 to 1763 K (mass of the metal =1 g) [30]
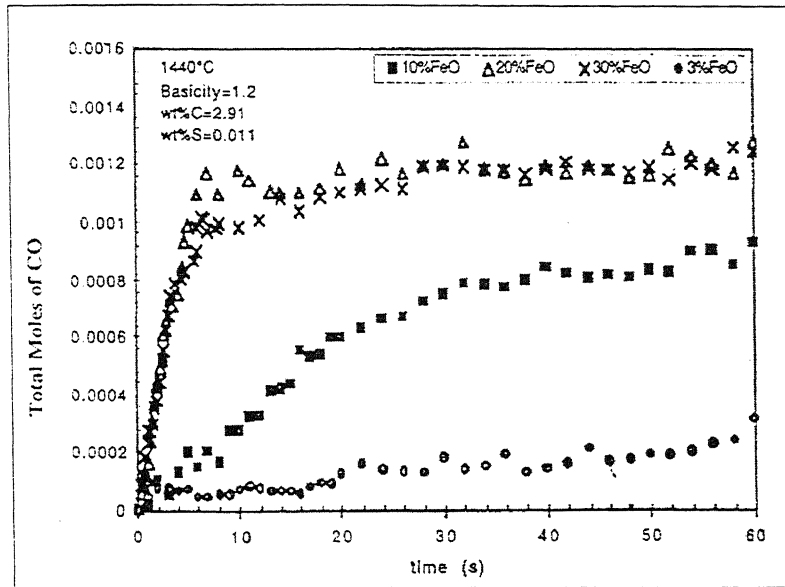
Figure 2.8 : Variation of the total moles of CO evolved with time for 3 to 30 mass pct FeO at 1713 K (mass of the metal =1.0 to 1.1 g) [30]

(d) **Sommerville et al [31]** carried out experiment for slag containing iron oxide less than 2.5 mass pct

d (i) Experimental technique used by Sommerville et al [31]

- system: slag –metal
- slag composition: 38% CaO-20%Al_2O_3-42%SiO_2 with low concentration of FeO in master slag
- no stirring of bath

For each experiment a small percentage of the iron oxide was introduced into 30g of the master slag. The mixture was homogenized, compacted to a pellet and placed inside the mild steel crucible, above the high-carbon iron, so that it was resting on the molybdenum ring. Once the top had been welded on to the crucible, it was connected to the apparatus for the measurement of gas evolution. The exact temperature was noted after a few minutes. Temperature adjustment of the reacting materials appeared to take place very quickly, and the reaction started immediately so that the zero time for each run was accurately known. Reaction progress was carefully followed by regular observation of the pressure change in the system until the reaction had virtually ceased; the pressure readings were converted to volume of gas evolved at NTP by using the previously determined P-V characteristics of the system, and the reaction was plotted as curves of volume of carbon monoxide vs. time. Unlike the case of metal containing sulphur, there were no complicating reactions and the volume of carbon monoxide evolved was a direct stoichiometric measure of the rate of reduction of iron oxide. Also, since 1 cm^3 CO $\equiv$ 0.0032g FeO $\equiv$ 0.011 % FeO in 30g slag, this method permitted higher accuracy than chemical analysis of slag samples for iron oxide.

d (ii) Results

The rate controlling step was chemical reaction at the gas-metal interface, for which the rate constant was estimated as 2.0 × 10^{-2} (mole $cm^{-2}min^{-1}$ atm^{-1}) at 1380 °C. At higher values of iron oxide content it was considered that the chemical reaction at the slag-gas interface took over as the rate-controlling step.
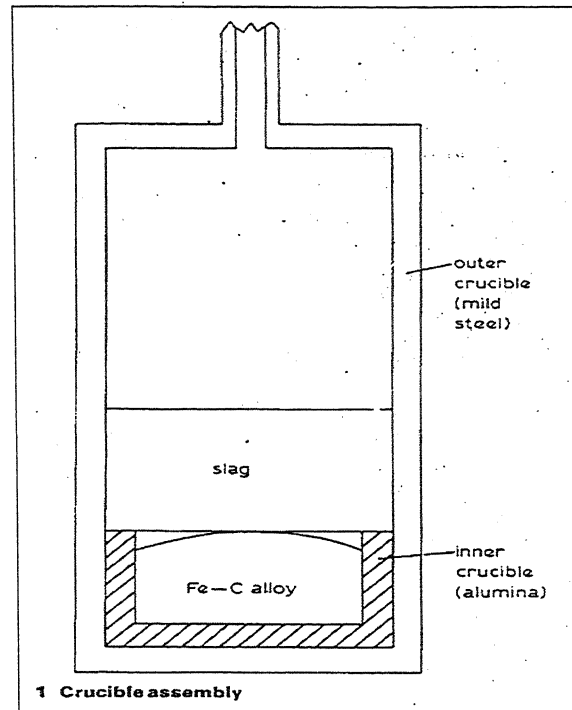
Figure 2.9: Schematic diagram of the experimental set up of Sommerville et al [31]

2.2.2 Gas-slag reaction as the rate controlling step

Several studies have been carried out in which the reaction of CO-CO_2 in gas stream with liquid slag was designed to be the rate controlling step.

(a) Li et al [32] measured the rates of interaction CO-CO_2 in gas phase with FeO in liquid slag.

$$(FeO) \quad + \quad \{CO\} \quad = \quad [Fe] \quad + \{CO_2\} \tag{2.7}$$

$$\{CO_2\} \quad + \quad [C] \quad = 2 \{CO\} \tag{2.8}$$
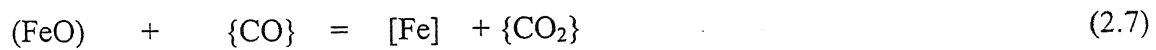
a (i) Experimental technique used by Li et al [32]

- Li et al studied the rate of the interfacial chemical reaction by eliminating the effect of liquid phase mass transfer and gas phase mass transfer by the use of high flow rate of gas through the slag

- slag-gas system

59

- slag composition: analytical grade $BaCO_3$, $CaCO_3$, Al_2O_3, TiO_2 and SiO_2 were used to prepare the binary slag.

The experimental system is shown in Figure 2.10 [32].Ten (10) gram of the slag sample was put in the platinum crucible and heated to the required temperature under argon atmosphere. The slag was then brought to equilibrium with gas mixture of CO-CO_2 before being reduced by an Ar-CO mixture. After a short period of reduction, during which sufficient data were collected, the slag was brought back to equilibrium with specific CO-CO_2 mixture. The practice made it possible to establish the relationship between the rate and the partial pressure of CO under identical conditions. At the end of an experiment, while the slag was in equilibrium with the gas mixture of CO-CO_2 of specific CO_2/CO ratio, the sample was quenched for subsequent chemical analysis. Three processes, namely, mass transfer in the gaseous phase (GPMT), interfacial chemical reaction, and liquid phase mass transfer (LPMT), are involved in a gas-slag reaction system. To study the rate of the interfacial chemical reaction, a high gas flow rate of CO-CO_2 mixture was passed through the slag to minimize the effect of GPMT and LPMT. Flow was not high to cause significant change in the interfacial area and temperature. To find the chemical rate constant, the dependence of the measured rate on the gas flow rate was determined by a series of experiments with gas flow rates varying from 0.5 to 4.0 standard litres per minute (SLM). Liquid iron oxide was pre-equilibrated with gases in which the CO_2/CO ratio was fixed at either 10 or 1.The-reducing gas was a mixture of 2.5 vol pct CO and 97.5 vol pct Ar. The effect of mass transfer in the liquid phase on the measured rate was examined by varying the partial pressure of CO or CO_2 in the reacting gas.

a (ii) Results

It was concluded that the dissociation or formation of CO_2 molecules at gas-slag interface was the prime rate controlling mechanism. Li et al [53] also measured the chemical diffusion coefficient of oxygen in liquid iron oxide at temperatures ranging from 1673 K to 1888 K and in calcium ferrite (Fe/Ca =2.57) in the temperature range of 1573 K to 1873 K using gravimetric method. Through this they found that the value of chemical

diffusivity was two order of magnitude higher than the earlier studies and thus demonstrated that the rate-controlling step could be the interfacial reaction rather than liquid phase mass transfer (LPMT).

The results of the reduction and oxidation rate measurements (melts in equilibrium with gases of CO_2/CO ratio of 10 and 3.2) are shown in Figure 2.11 and Figure 2.12 [32].With P_{CO} (or P_{CO2})<0.05 atm,a first order rate with respect to partial pressure of CO and CO_2, was followed indicating interfacial chemical reaction control. Only the rates obtained with partial pressures of CO or CO_2 below 0.05 atm were used to calculate the apparent first-order rate constant, k_{red} or k_{oxi} .

For reduction,

$$k_{red} = 4.08 \times 10^{-5} \left(\frac{p_{CO_2}}{p_{CO}} \right)^{0.18} \quad \text{(Mol cm}^{-2} \text{ s}^{-1} \text{ atm}^{-1}\text{)} \tag{2.6}$$

For oxidation,

$$k_{oxi} = 3.86 \times 10^{-5} \left(\frac{p_{CO_2}}{p_{CO}} \right)^{-0.80} \quad \text{(Mol cm}^{-2} \text{ s}^{-1} \text{ atm}^{-1}\text{)} \tag{2.7}$$

Similar experiments were conducted at a temperature of 1673 K over a constricted range of P_{CO2}/P_{CO} ratio. The results are given in Figure 2.13 [32], where the datum corresponding to the lowest P_{CO2}/P_{CO} ratio was taken from the result of an experiment carried out using a metallic iron crucible. The value of rate constant k_{g-s} was 1.84 $\times 10^{-5}$ (Mol cm^{-2} s^{-1} atm^{-1}) at 1673 K and 3.08 $\times 10^{-5}$ (Mol cm^{-2} s^{-1} atm^{-1}) at 1773 K for the reduction of iron oxide to metallic iron, as obtained from the present study, is higher than 1.13 $\times 10^{-5}$ (Mol cm^{-2} s^{-1} atm^{-1}) reported by Nagasaka et al [54] using a similar experimental set up. Since the interfacial chemical reaction step is always accompanied by mass transport steps in the gas and liquid phases, the higher rates reported in this study are believed to be more reliable,i.e.,closer to the "true" chemical reaction rate.
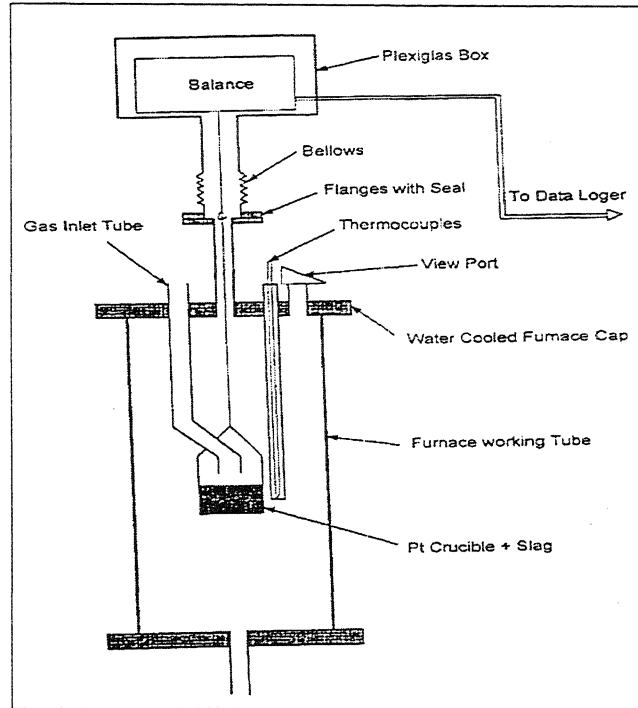
Figure 2.10: Schematic diagram of the Experimental set up Li et al [32]
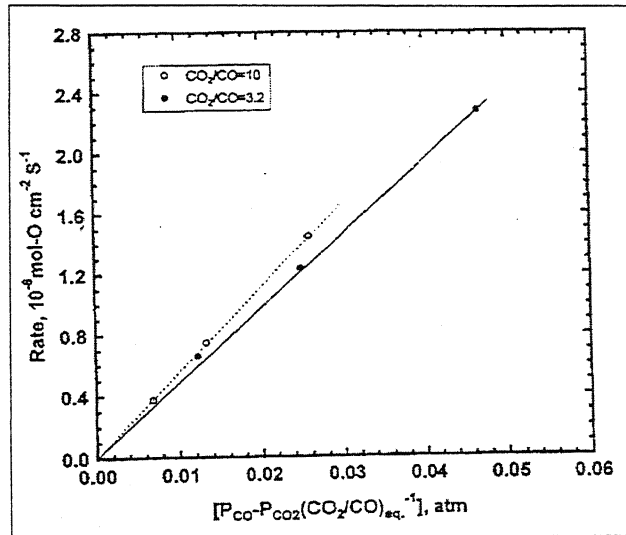
Figure 2.11: Dependence of the reduction rate of iron oxide on the effective
partial pressure of CO in the gas mixture for liquid iron oxide
at 1773 K. The melts were pre-equilibrated with CO_2-CO gas
mixture of $CO_2/CO =10$ (open circle) and 3.2 (solid circle) [32]
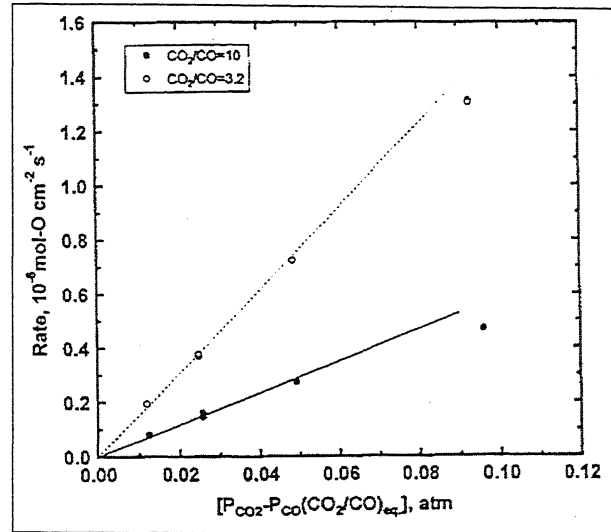
Figure 2.12: Dependence of the reduction rate of iron oxide on the effective partial pressure of CO_2 in the gas mixture for liquid iron oxide at 1773 K. The melts were Pre-equilibrated with CO_2-CO gas mixture of CO_2/CO =10 (open circle) and 3.2 (Solid circle)[32]
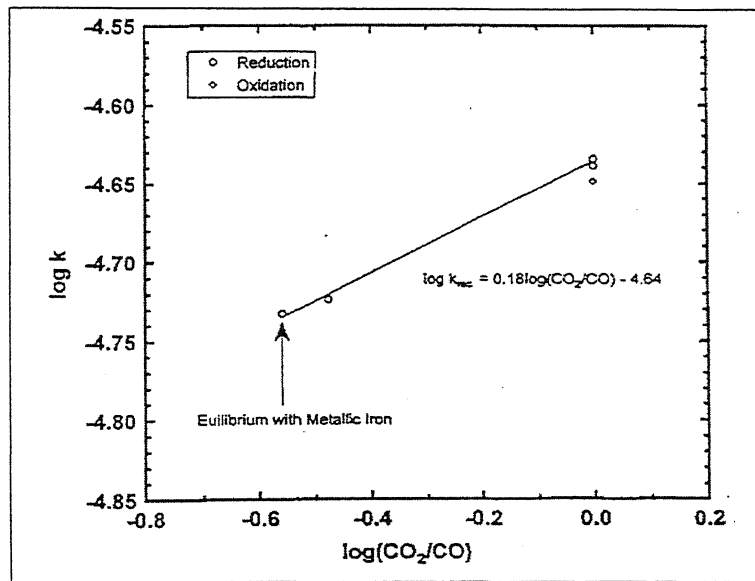
Figure 2.13: Apparent first-order rate constant, k, in mol $cm^{-2}s^{-1}$ atm^{-1}, for reduction of liquid iron oxide at 1673 K as a function of the equilibrium CO_2/CO ratio [32]

63

(b) Graenzdoerffer et al [33] studied the rate of reduction of iron oxide by CO from the synthetic slag in the system $CaO-MgO-SiO_2-FeO-FeO_{1.5}$ with 5-90 mass pct Fe_2O_3, by measuring the rate of generation of CO_2.Experiments were done at 1873 K with slag basicity between 1.0 and 1.6.

b (i) Experimental technique used by Graenzdoerffer et al [33]

- system: gas-slag
- slag system: $CaO-MgO-SiO_2-FeO-FeO_{1.5}$ with 5-90 mass pct Fe_2O_3
- temperature: 1873 K
- basicity: 1.0-1.6

The experimental apparatus is shown if Figure 2.14 [33]. Master slags were made from reagent grade chemicals, which were mixed and then fused at approximately 1950 K for one hour in graphite crucibles. After quenching the molten slag on a copper plate, the slag was ground, placed in alumina boats and decarburised at 1273 K for 12 hours. Slag samples of the desired compositions for the reduction experiments were then prepared by mixing one of the master slag and reagents grade Fe_2O_3. Once in the apparatus and at temperature, the state of oxidation of the sample was fixed. This was accomplished by holding the sample for an hour either at a fixed CO_2/CO ratio or under purified argon with molten iron in the bottom of the crucible. After fixing the state of oxidation, the system was purged with purified argon for five minutes. Finally, reducing gas of the desired composition was switched on and the reduction experiment begun. Four different master slags were used to make samples for the reducing studies. The calculated and analysed composition of these slag are shown in Table 2.4 [33].

The initial Fe_2O_3 content of the samples ranged from 5 to 90 pct by mass. The range of CO/CO_2 ratios used to fix the state of oxidation was 5 to 40 and partial pressure of CO varied between 0.006 and 1 atm. All of the experiments were done at 1873 ± 2 K.

At the initiation of reduction experiment, a constant and measurable 1.4 sec delay occurred before the gas analyser detected the presence of CO_2. A 2 to 3 sec period

64

followed this 'transportation lag' during which time the rate of generation of CO_2 rose rapidly. At low partial pressure of CO in the reducing gas, the rate of generation of CO_2 then became approximately constant. The rate of generation of CO_2 at partial pressure of CO equal to or greater than 0.05 atm was characterized by a maximum followed by a gradual decline to a constant value.

b (ii) Results

Typical results for a slag made from the master slag number 1, initially containing 70 pct by mass Fe_2O_3, and equilibrated at a CO/CO_2 ratio of 5 are shown in Figure 2.15a [33].The result for master slag number 1 equilibrated at CO/CO_2 ratio of 5 but with varying initial amounts of Fe_2O_3 are presented in Figure 2.15b [33] at a partial pressure of CO in the reducing gas of 0.0098 atm. The rate of generation of CO_2 for master slag number 1 with an initial 20 percent Fe_2O_3 and with varying states of oxidation is shown in Figure 2.15c [33]. Finally, the effect of the master slag composition on the rate of generation of CO_2 (for slag which initially contained 70 percent by mass Fe_2O_3, and was equilibrated at a CO/CO_2 ratio of 5 and reduced with a CO partial pressure of 0.0098 atm) is shown in Figure 2.15d [33].

It can be seen from Figure 2.15 [33] that the rate of generation of CO_2 increased with the partial pressure of CO in the reducing gas. In addition, the rate increased with increasing initial Fe_2O_3 content (as the state of oxidation increased). Similar trend was found for the other three master slag systems. The rate of generation of CO_2 was clearly dependent on the initial iron oxide concentration, state of oxidation, and the master slag used to prepare the slag sample. In addition, the rate was dependent on the partial pressure of CO in the reducing gas and time.

Analysis of the result was based on the assumption that the reaction, which occurs, is

$$FeO + CO \rightarrow Fe + CO_2$$
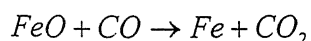
Where the standard state for FeO is assumed to be pure stoichiometric liquid FeO. The rate of generation of CO_2 thus equals the rate of generation of Fe and the rate of reduction of FeO.

For a first order irreversible reaction, the rate per unit area, R/A, equals

$$R/A = k_{s-g}\, a_{FeO}\, P_{CO} \tag{2.9}$$

For a first order reversible reaction, the rate per unit area, R/A, will equal

$$R/A = k_{s-g}\, (\, a_{FeO}\, P_{CO} - a_{Fe} P_{CO2}/K) \tag{2.10}$$

Where K is the equilibrium constant for the above reaction, a_{FeO}, a_{Fe}, P_{CO} and P_{CO2} are the activities of FeO and Fe relative to pure stoichiometric liquid FeO and pure liquid Fe, and the partial pressure of CO and CO_2, respectively. This rate law was found to fit all of the results for experiments performed with P_{CO} less than or equal to 0.05 atm,

The resulting rate constant k_{s-g} was 4.2×10^{-5} (mol cm^{-2} s^{-1} atm^{-1}) at 1873 K.
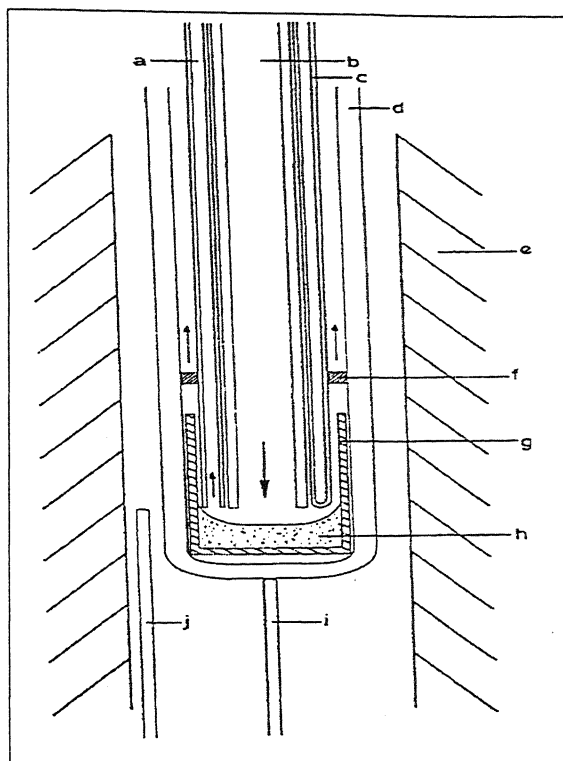
Figure 2.14: Schematic representation of experimental set up of Graenzdoerffer et al
[33] (a) Alumina gas sampling tube (b)Alumina gas inlet tube (c)
Thermocouple (d) Alumina reaction tube (e) Tantalum furnace (f) Alumina
spacer (g) MgO crucible (h)Slag sample (i and j) Thermocouple

Table 2.4 : Master Slag Compositions [33]

Slag Number	mass pct CaO	mass pct MgO	mass pct SiO$_2$
1	44.0 (44.6)*	17.5 (15.3)	38.4 (39.8)
2	16.0 (17.4)	34.0 (31.3)	50.0 (51.2)
3	26.5 (28.5)	30.0 (27.3)	43.3 (45.0)
4	51.2 (50.2)	0.0	48.8 (50.1)
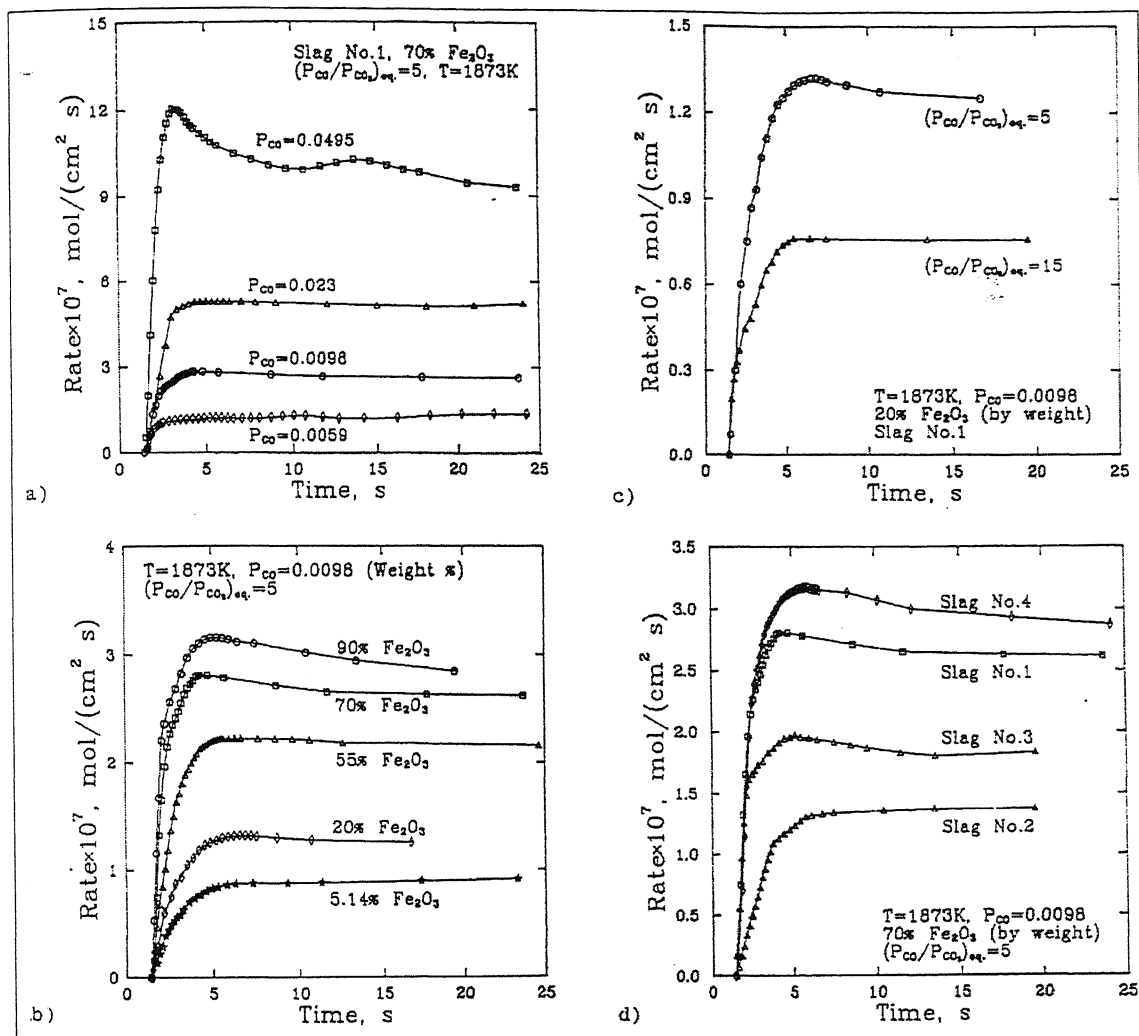
Figure 2.15: The rate of generation of CO_2 as a function of (a) CO partial pressure in the reducing gas(b) Initial Fe_2O_3 concentration (c) Initial state of oxidations, and (d) Master slag composition [33]
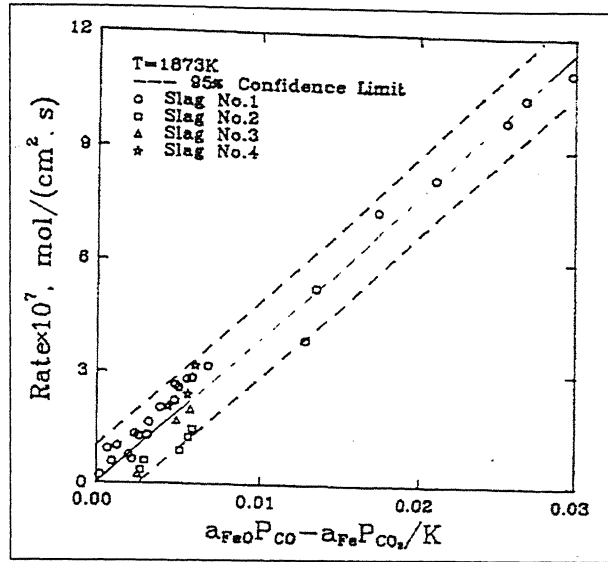
Figure 2.16: First order reversible reaction rate equation for CO partial pressure less than or equal to 0.05 atm [33]

2.2.3 Mass transport of FeO in slag as a rate controlling step

Mass transfer of FeO as a rate controlling step has been proposed specially for slags containing 5-35 mass % FeO depending upon slag composition and temperature as discussed in section 2.3.

(a) C.L Molloseau and R.J. Fruehan [30] studied the reaction behaviour of Fe-C-S droplets in $CaO-SiO_2-MgO-FeO$ slag (3-35 % FeO at 1643-1763K) and reported that mass transfer of FeO as Fe^{2+} and O^{2-} ions in the slag was rate controlling mechanism for the rate of reduction of FeO in the slag by carbon in iron droplets (2.9 mass % C, 0.01 mass % S).The behaviour of the metal droplets in the slag, as observed by X-ray fluoroscopy, changed significantly with FeO content in the slag below 10 mass pct FeO, the droplet remained intact while reacting with the slag, however above this FeO concentration, the droplet become emulsified within the slag. The large increase in surface area of metal droplet due emulsification caused the rate of reaction to be one or two order magnitude faster than for the droplets that did not become emulsified. It was suggested that when the droplet is emulsified, the surface area and reaction kinetics are

69

greatly increased, and the mass transfer of FeO as Fe2+ or O2- ions in the slag to the emulsified droplet controlled the rate.

2.2.4 Gas phase mass transfer as the rate controlling step

In many studies, gas-phase mass transfer has been proposed as the rate determining mechanism in the range of high carbon contents. The decarburisation at high carbon contents is accompanied with high mass flux across the gas-metal interface. That is, when the reacting gas is blown onto the melt, the resultant CO gas may alter the compositions and flow velocity in the gas phase.

(a) Hiroyuki et al. [34] investigated the decarburisation of liquid Fe-C alloy in CO-CO_2 gas mixtures and concluded that at high carbon content the rate of decarburisation is controlled predominantly by the diffusion rate in the gas phase.

a (i) Experimental technique used by Hiroyuki et al. [34]
- system: gas-metal
- inductively stirred bath
- temperature: 1600 °C

The starting experimental material was electrolytic iron with the chemical compositions shown in Table 2.5 [34].Approximately 400g of electrolytic iron was melted in an argon atmosphere. After the iron was melted, the melt was deoxidised by Ar-H_2 gas mixture. Carbon content in the melt was then adjusted by adding graphite and blowing CO-CO_2 gas mixture onto the melt. Initial concentration of carbon was about 1%. The reacting gases were metered with capillary flow meter and introduced into the reaction chamber through an alumina tube with 4, 6, or 10 mm in ID, the end of which was located at 5 mm above the surface of the melt. Samples were taken out by suction with silica tube and quenched into water.

a (ii) Results

The rate of decarburisation in the industrial steel making process is mainly determined by the rate of oxygen supply. Actually the maximum of oxygen utilisation efficiency reaches almost 100 %. In contrast with this the highest value of the oxygen utilisation efficiency found in the Hiroyuki et al work was 75 %.Under the experimental conditions employed, since the jet momentum of gas blowing was so low, the gas-metal interface was not disturbed and counter diffusion by CO_2 and CO occurred in the gas phase boundary layer. The amount of resultant CO gas increased with increasing the supply of oxidant gas, and therefore it was difficult to eliminate the resistance of gas-phase mass transfer even at high gas flow rates.

Under the actual steel making conditions, the reacting oxygen gas, which is blown onto the melt with an extremely high jet momentum, may be trapped as FeO emulsion by liquid iron. The FeO emulsion will be successively dispersed into the bulk liquid and consumed by the reaction with carbon. Under these conditions mass transfer resistance due to the resultant CO gas may not be important.
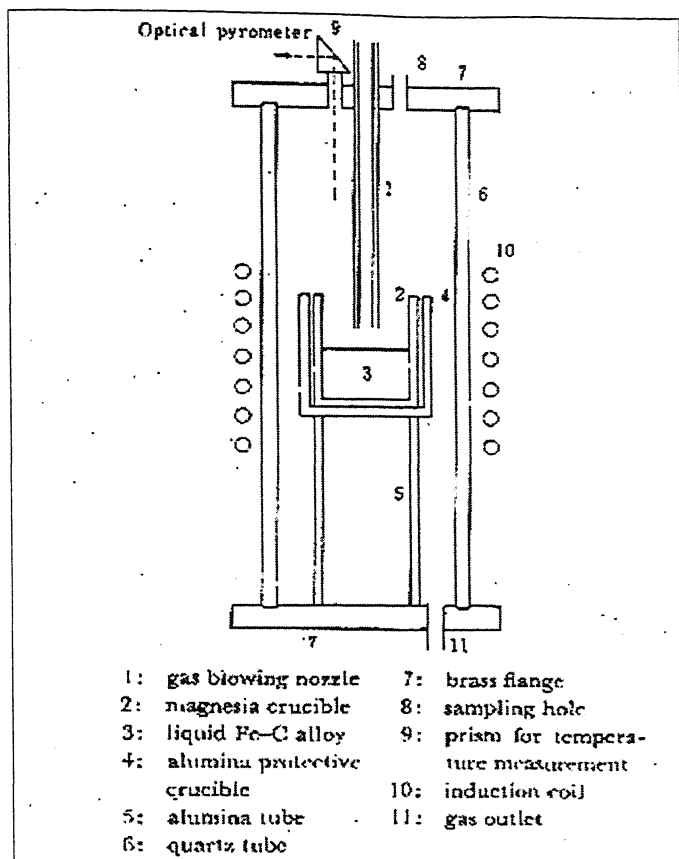
Figure 2.17: Experimental apparatus of Hiroyuki et al [34]

Table 2.5 : Compositions of electrolytic iron (Hiroyuki et al.) [34]

Element	C	S	P	Si	Mn	Cu
Percentage	0.004	0.004	0.003	0.004	0.004	0.004

2.3 Kinetic model for reduction of FeO in BOF slag

In oxygen steelmaking, the slag may contain 5-35 % mass pct FeO and also co-exist simultaneously with iron-carbon melt and the metal droplets dispersed in slag. The general kinetic model described in this section is essentially the same as proposed elsewhere [27]. As described in section 2, the overall reaction of FeO with carbon [C], in the melt is a three phase reaction involving slag, ( ), liquid metal, { }, and gas,$(CO)_g$:

$$(FeO) \quad + \quad [C] \quad = \quad \{Fe\} \quad + \quad (CO)_g \qquad (2.11)$$
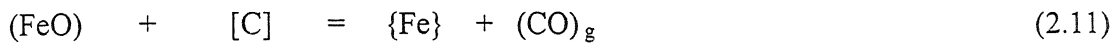
Since three phases can meet simultaneously across a line, reaction (1) proceeds in two separate steps:

At the gas-slag interface

$$(FeO) \quad + \quad (CO)_g \quad = \quad \{Fe\} \quad + \quad (CO_2)_g \qquad (2.12)$$
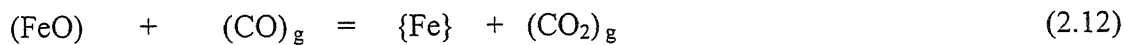
And at the gas-metal interface

$$(CO_2)_g \quad + \quad [C] \rightarrow 2\,(CO)_g \qquad (2.13)$$

As the slag containing FeO comes in contact with metal containing dissolved carbon, a $CO\text{-}CO_2$ gas film forms at the interface separating the slag and metal (Figure 2.1).

Various steps of reduction of FeO by carbon dissolved in iron can be written as:

1. Transport of carbon in the iron melt to the gas-metal interface
2. Chemical reaction at the gas –metal interface

   $$(CO_2)_g \quad + \quad [C] \rightarrow 2\,(CO)_g$$

3. Transport of gas from the gas-metal interface to gas-slag interface and vice versa
4. Transport of iron oxide in the slag to the gas-slag interface

5. Chemical reaction at the gas –slag interface

$$(FeO) \quad + \quad (CO)_g \quad = \quad \{Fe\} \quad + \quad (CO_2)_g$$
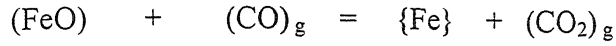
Under the conditions of BOF, step1 (carbon transport in melt) can be disregarded as rate limiting because no change in the reaction rate is observed when the mass content of the melt varies from 0.2 % (up to the saturation value 1). The gas phase mass transfer step (step 3) probably is not rate limiting due to intrinsic turbulence of the BOF process. The CO/CO_2 gas bubble formed on the metal droplet continues and grows quickly as a thin film at the interface of gas and metal. However, at low concentration of iron oxide in slag the mass transfer of FeO in slag can become one of the rate controlling steps (i.e. step 4). Only at higher concentrations of FeO in slag, when oxide ions are presents in slag in sufficient quantity to facilate ionic conduction, the mass transfer of FeO in slag can be ignored as a rate controlling step and then gas-slag chemical reaction (step 5) can become a rate controlling step. In both the cases (i.e. at low and high FeO concentrations) gas-metal chemical reaction (step 2) could act as one of the active rate controlling steps. The gas-metal reaction can be subdivided into dissociative chemisorption of CO_2 and chemical reaction of adsorbed oxygen with dissolved carbon:

$$(CO_2)_g \rightarrow (CO)_g + [O]_{ad} \qquad (2.13a)$$

$$[O]_{ad} + [C] \rightarrow (CO)_g \qquad (2.13b)$$

Dissociative chemisorption of CO_2, equation (2.13a) has been shown to be a slow process at iron and steel making temperature (due to a very small value of CO_2/CO ratio at high carbon content of melt).Owing to scarcity of CO_2 at gas-metal interface the reaction (2.13a) can slow down to such an extent that it becomes a rate controlling reaction. At intermediate FeO concentration, all three steps (steps 2, 4 and 5) can control the overall reaction given by equation (2.11).

2.3.1 General kinetic model

The overall rate equation for the reduction of FeO in slag-gas-metal system (considering steps 2, 4 and 5 as rate controlling) can be derived as follows.

The rate equation for reaction (2.12) can be written as:

$$-\frac{d(n_{CO})}{dt}\bigg|_{gas-slag} = A.k_{g-s}\left[a^i_{FeO}P_{CO} - \frac{a_{Fe}P_{CO_2}}{K}\right] \tag{2.14}$$

The rate equation for reaction (2.13a) is given by:

$$-\frac{d(n_{CO_2})}{dt}\bigg|_{gas-metal} = A.k_{g-m}.P_{CO_2} \tag{2.15}$$

It should be noted that reaction (2.13a) is considered to be an irreversible reaction because as soon as CO_2 dissociates into CO and O_{ad}, the latter reacts with dissolved with carbon and regeneration of CO takes place.

The mass transfer of rate of FeO in slag is given by:

$$-\frac{d(n_{CO})}{dt}\bigg|_{from-bulk} = A.k_{FeO}\left[C^b_{FeO} - C^i_{FeO}\right] \tag{2.16}$$

From reaction (2.12):

$$-\frac{d(n_{CO})}{dt}\bigg|_{gas-slag} = \frac{d(n_{CO_2})}{dt}\bigg|_{gas-slag} \tag{2.17}$$

And under steady state conditions,

$$-\frac{d(n_{CO_2})}{dt}\bigg|_{gas-slag} = \frac{d(n_{CO2})}{dt}\bigg|_{gas-metal} \qquad (2.18)$$

Thus from equation (2.17) and (2.18)

$$-\frac{d(n_{CO})}{dt}\bigg|_{gas-slag} = -\frac{d(n_{CO2})}{dt}\bigg|_{gas-metal} \qquad (2.19)$$

And from equation (2.14), (2.15) and (2.19)

$$A.k_{g-s}\left[a^i_{FeO}\ P_{CO} - \frac{a_{Fe}\ P_{CO_2}}{K}\right] = A.k_{g-m}.P_{CO_2} \qquad (2.20)$$

Therefore,

$$P_{CO_2} = \frac{a^i_{FeO}\ k_{g-s}\ P_{CO}}{\left[k_{g-m} + \dfrac{k_{g-s}}{K}\right]} \qquad (2.21)$$

Substituting P_{CO_2} value in equation (2.14):

$$-\frac{d(n_{CO})}{dt}\bigg|_{gas-slag} = a^i_{FeO}\ p_{CO}\ A\left[\frac{1}{\dfrac{1}{k_{g-s}} + \dfrac{1}{k_{g-m}.K}}\right] \qquad (2.22)$$

76

Now from reaction (2.12):

$$-\frac{d(n_{CO})}{dt}\bigg|_{gas-slag} = -\frac{d(n_{FeO})}{dt}\bigg|_{gas-slag}$$

2.23)

And from mass transport of FeO in slag from bulk to gas-slag interface

$$-\frac{d(n_{FeO})}{dt}\bigg|_{gas-slag} = -\frac{d(n_{FeO})}{dt}\bigg|_{from-bulk}$$

(2.24)

Thus from equation (2.23) and (2.24)

$$-\frac{d(n_{FeO})}{dt}\bigg|_{from-bulk} = -\frac{d(n_{CO})}{dt}\bigg|_{gas-slag}$$

(2.25)

From equation (2.6), (2.22) and (2.25)

$$A.k_{FeO}\left[C_{FeO}^{b} - C_{FeO}^{i}\right] = a_{FeO}^{i}\, p_{CO}\, A\left[\frac{1}{\dfrac{1}{k_{g-s}} + \dfrac{1}{k_{g-m}.K}}\right]$$

(2.26)

Since,

$$C_{FeO}^{i} = \frac{a_{FeO}^{i} n_{tot}}{V \gamma_{FeO}}$$

Or,

$$a^i_{FeO} = \frac{k_{FeO} \gamma_{FeO} V C^b_{FeO} (k_{g-s} + K k_{g-m})}{k_{FeO} n_{tot} (k_{g-s} + K k_{g-m}) + P_{CO} K k_{g-s} k_{g-m} \gamma_{FeO} V} \qquad (2.27)$$

Substituting a^i_{FeO} into equation (2.22) and from equation (2.25):

$$-\frac{d(n_{FeO})}{dt}\bigg|_{from-bulk} = A C^b_{FeO} \left[\frac{1}{\dfrac{1}{a.k_{g-s}} + \dfrac{1}{a.K.k_{g-m}} + \dfrac{1}{k_{FeO}}} \right] \qquad (2.28)$$

Where

$$a = \frac{P_{CO} \gamma_{FeO} V}{n_{tot}}$$

On integrating equation (2.28) the final expression for rate equation is given by equation (2.29):

$$-\ln\left[\frac{FeO_t}{FeO_o}\right] = \frac{A.t}{V} \left[\frac{1}{\dfrac{1}{a.k_{g-s}} + \dfrac{1}{a.K.k_{g-m}} + \dfrac{1}{k_{FeO}}} \right] \qquad (2.29)$$

The model developed is a general model for the reduction of iron oxide when the rate-controlling step is the chemical reaction occurring at gas-slag and gas-metal interface and the mass transport of FeO in slag.

Option 1: When only mass transfer of FeO in slag is rate controlling then

$$-\ln\left[\frac{FeO_t}{FeO_o}\right] = \frac{A.t}{V} \left[\frac{1}{\dfrac{1}{k_{FeO}}} \right] \qquad (2.30)$$

78

Option 2: When chemical reaction occurring at gas slag interface is rate controlling then;

$$-\ln\left[\frac{FeO_t}{FeO_o}\right] = \frac{A.t}{V}\left[\frac{1}{\dfrac{1}{a.k_{g-s}}}\right] \tag{2.31}$$

Option 3: When chemical reaction occurring at gas metal interface is rate controlling then;

$$-\ln\left[\frac{FeO_t}{FeO_o}\right] = \frac{A.t}{V}\left[\frac{1}{\dfrac{1}{a.K.k_{g-m}}}\right] \tag{2.32}$$

2.4 Industrial data

The plant data for FeO reduction in 300 ton BOF is same as that used for lime dissolution model and summarized in Table 1.3. The data were collected during the middle period of the blow (between 3.75 min. to 13.95 min of blow period Figure 1.13).Each set of values in Table 1.3 represents an average for approximately 20 heats made under similar conditions of hot metal composition and temperature, scrap amount, oxygen blow rate, lance height, blowing regime, addition sequence and amount of flux and ore added, etc.

2.5 Procedure adopted for the calculation of rate constants and mass transfer coefficient

The procedure involves the following steps of calculation:

- Calculation of liquidus composition
- Calculation of change in the number of moles of FeO during a time step
- Estimation of slag, slag-gas and slag-gas-solid viscosity
- Calculation of residence time of droplet, foam height and total area of droplets
- Calculation of activity coefficient of FeO in slag
- Calculation of mass transfer coefficient

The details of procedure for each of the steps are as follows:

(a) Calculation of liquidus composition and solid fraction of the bulk slag

For a given temperature and overall composition of slag, solid fraction is calculated from ternary diagram (Figure 1.12) by applying Lever rule. Suppose the overall (bulk) slag composition is 37 mass pct CaO, 33.5 mass pct FeO and 28.7 mass pct SiO_2 at 1429 °C and lies at point B. From the point A of dicalcium silicate ($2CaO \cdot SiO_2$), a straight line is drawn passing through composition point B, which cuts the liquidus line at, given temperature (1429 °C) at point C.

Composition of slag at point C is - 35.6 mass % CaO, 36.4 mass % FeO and 28.0 mass % SiO_2 at 1429 °C

Now solid fraction can be calculated from Lever rule

Solid fraction (ε) = BC /AC = 0.08

The liquidus composition for entire slag path Figure 1.13 is calculated and summarised in Table 2.6.

Table 2.6: Liquidus composition obtained by program

Time	Slag Temp	Solid fraction	(CaO)b	(FeO)b	(SiO2)b
Min			Mass %	Mass %	Mass %
3.75	1429	0.08	35.6	36.4	28.0
4.35	1460	0.06	37.4	33.9	28.7
4.8	1481	0.08	38.0	33.7	28.3
5.4	1491	0.12	38.5	33.1	28.4
5.85	1499	0.13	39.7	30.9	29.5
6.45	1496	0.21	39.5	31.1	29.4
6.9	1491	0.35	37.7	35.0	27.3
7.5	1486	0.47	34.5	40.8	24.7
8.1	1481	0.53	33.6	42.6	23.8
8.55	1481	0.65	27.3	56.2	16.5
9.15	1481	0.73	22.8	68.8	8.5
9.6	1486	0.73	26.2	67.6	6.2
10.2	1499	0.64	39.4	54.3	6.4
10.65	1502	0.61	42.4	51.1	6.5
11.25	1522	0.56	43.6	49.2	7.2
11.85	1538	0.52	43.7	48.5	7.8
12.3	1558	0.46	45.8	45.8	8.4
12.9	1584	0.42	45.5	45.1	9.4
13.35	1620	0.32	46.9	42.2	10.9
13.95	1656	0.26	46.3	41.2	12.5

(b) Calculation of change in the number of moles of FeO (Δn_{FeO}) between two consecutive points

As determined in section 2.5 (a) at t = 3.75 min, mass pct FeO in liquid slag is 36.4 % and slag mass is (17353 kg). The change in moles of FeO in liquid slag can be calculated as

$$n_{3.75} = \frac{36.4 \times 17353 \times 1000}{72 \times 100} \, moles$$

Similarly for t = 4.35 min

$$n_{4.35} = \frac{33.9 \times 17647 \times 1000}{72 \times 100} \, moles$$

Hence the change in the number of moles of FeO is

$$\Delta n_{FeO} = n_{3.75} - n_{4.35} = 4479.57 \, moles$$

(c) Estimation of slag, slag-gas and slag-gas-solid continuum viscosity

The viscosity can be calculated by using tow models published in literature, namely, the model by Urbain et al [62] and the model by Forsbacka et al [63]

C (1) Calculation of slag viscosity, μ_s using the model by Urbain et al [62]

(i) Calculation of slag viscosity, μ_s

Expression for the viscous flow is

$$\mu = A.T.\exp\left(\frac{1000.B}{T}\right) \tag{2.33}$$

Where, the pre exponential parameter A is a function of m, E_w, v and ΔS_v; m is mass of structural unit, v is the volume of structural unit, E_w is the energy of the potential well and the parameter B is function of E_w, ΔH_v, where ΔH_v is partial molar enthalpy

$$A = A_0 \cdot \exp\left(-\frac{\Delta S_v}{R}\right) \tag{2.33a}$$

$$A_0 = R.(2M / E)^{\frac{1}{2}}.(1 / V)^{\frac{2}{3}}.(1 / N)^{\frac{1}{3}} \tag{2.33b}$$

$$B = (E + \Delta H_v) / R \tag{2.33c}$$

Where

$$\Delta G_v(T) = \Delta H_v - T\Delta S_V \tag{2.33d}$$

At T = T$_c$, we have $\Delta S_v = \Delta H_v / T_c$ \hfill (2.33e)

Now $\ln A = \ln A_0 + \dfrac{E}{RT_c} - \dfrac{1000.B}{T_c}$ \hfill (2.33f)

Where A_0, E , T_c are constant for a given liquid, A simple formulation is

$$-\ln A = m.B + n \tag{2.33g}$$

Where m and n are deduced from the experimental parameters A and B [62].The mean values of m and n are:

$m=0.29$ and $n=11.57$ for ionic melt

$m=0.207$ and $n=10.288$ for network liquid such as SiO_2 ,B_2O_3,GeO_2

$m=0.269$ and $n=11.67$ for CaO-SiO_2-FeO system

Now, mass of slag (kg) Wslag: 17353 kg ; temperature (Kelvin) T = 1702 K ; mass % CaO = 35.6; mass % FeO = 36.4; mass % SiO_2 = 28.0

The mole fraction of each oxides can be calculated as follows

$$X_{CaO} = \frac{\dfrac{35.6}{56}}{\dfrac{35.6}{56} + \dfrac{36.4}{72} + \dfrac{28.0}{60}} = 0.39$$

$$X_{FeO} = \frac{\dfrac{36.4}{72}}{\dfrac{35.6}{56} + \dfrac{36.4}{72} + \dfrac{28.0}{60}} = 0.31$$

$$X_{SiO_2} = \frac{\dfrac{28.0}{60}}{\dfrac{35.6}{56} + \dfrac{36.4}{72} + \dfrac{28.0}{60}} = 0.29$$

Glass formers TO2 = X_{SiO2} = 0.29

Modifiers MO = X_{CaO} + X_{FeO} = 0.70

Amphoterics A_2O_3 = 0.0

$\alpha = MO/(MO + A_2O_3) = 1.0$

X= $TO2/(TO2+MO + A_2O_3)$ = 0.29

Published values of a0, a1...b0, b1...c0, c1.etc are as follows

i	ai	bi			ci		
		Mg	Ca	Mn	Mg	Ca	Mn
0	13.2	15.9	41.5	20	-18.6	-45.0	-25.6
1	30.5	-54.1	-117.2	26	33	130.0	186.2
2	-40.5	138	232.1	-110.3	112	298.6	186.2
3	60.8	-99	-156.4	64.3	97.6	213.6	-104.6

$B_{i\_CaO} = ai + bi \times \alpha + ci \times \alpha^2$

$B_{0\_CaO} = 13.2 + 41.5 - 45 = 9.7$

$B_{1\_CaO} = 30.5 - 117.2 + 130 = 43.3$

$B_{2\_CaO} = -40.5 + 232.1 - 298.6 = -107.0$

$B_{3\_CaO} = 60.8 - 156.4 + 213.6 = 118$

$B_{CaO} = B_{0\_CaO} + B_{1\_CaO} \times X + B_{2\_CaO} \times X^2 + B_{3\_CaO} \times X^3$

$B_{CaO} = 9.7 + 43.3 \times (0.29) + (-107.0) \times (0.29)^2 +$

$\qquad 118 \times (0.29)^3 = 16.14$

$X_{MgO} = 0.0$

$X_{MnO} = 0.0$

$B_{globle} = 16.14$

$A_{globle} = \exp(-n- (m \times B_{globle}))$

For CaO-FeO-SiO_2 system, n =11.67 and m= 0.27

$A_{globle} = \exp(-11.67- (0.27 \times 16.14)) = 1.09 \times 10^{-7}$

$\mu_s = 0.1 \times T \times A_{globle} \times \exp(1000 \times B_{globle}/T)$

$\quad = 0.1 \times 1702 \times 1.09 \times 10^{-7} \exp(1000 \times 16.14/1702)$

$\quad = 0.25$ (kg/m.s)

(ii) Calculation of slag-gas (continuum) viscosity, μ_{sg} (kg/m.s)

$$\mu_{sg} = \mu_s \left(1 + \frac{1.25}{(1 - \phi_g)} \right)^2 \qquad (2.34)$$

$\mu_s = 0.25$ (kg/m.s) as calculated above

Initial value of gas fraction, $\phi_g = 0.4$ (assumed)

By putting these values, we get,

$\mu_{sg} = 2.37$ (kg/m.s)

(iii) Calculation of slag-gas-solid (continuum) viscosity, μ_{sgs} (kg/m.s)

$$\mu_{sgs} = \mu_{sg} (1 + 2.5\varepsilon + 10.05\varepsilon^2 + 0.00273 \exp(16.6\varepsilon)) \qquad (2.35)$$

On substituting the following,

Solid fraction as calculated above, $\varepsilon = 0.07752$

$\mu_{sg} = 2.37$ (kg/m.s) as calculated above

We get,

μ_{sgs} = 2.76 (kg/m s)

Similarly for all the slag compositions the viscosity is calculated and summarized in Table 2.7

The viscosity values solid fraction in slag is also plotted as function of time in Figure. 2.18. It is clear that solid fraction of slag which is formed due to the precipitation of di-calcium silicate rises up to approximately 52 pct in the first 8 min. The slag and slag-gas viscosity continuously decreases throughout the entire blow period due to increase in the temperature of the system whereas the slag-gas-solid slag viscosity rises in first 10 min due to foaming nature of slag and then falls down continuously when foamy slag begin to collapse.

C(2) Calculation slag viscosity using Iida model [63]

c (i) Calculation of slag viscosity, μ_s

This model is based on the Arrhenius-type equation, where network structure of the slag is taken into account by using the so-called modified basicity index $Bi^{(j)}$

$$\mu = A\mu_o \exp\left(\frac{E}{Bi^{(j)}}\right) \tag{2.36}$$

$$A = 1.03\text{-}2.08 \times 10^{-3}\,T + 1.05 \times 10^{-6}\,T^2 = 0.53 \text{ (at T=1702K)} \tag{2.37}$$

$$E = 28.46\text{-}2.09 \times 10^{-2}\,T + 4.0 \times 10^{-6}\,T^2 = 4.50 \text{ (at T=1702K)} \tag{2.38}$$

$$\mu_o = \sum \mu_{oi}\,X_i \tag{2.39}$$

$$\mu_o = \mu_{oCaO}\,X_{CaO} + \mu_{oFeO}\,X_{FeO} + \mu_{oSiO_2}\,X_{SiO_2} \tag{2.40}$$

For the first slag composition at t = 3.75 min, T=1429 °C (1702 K)

86

$\mu_{o\,CaO}$, $\mu_{o\,FeO}$ and $\mu_{o\,SiO2}$ can be calculated .

$\mu_{oSiO_2}(mpas) = 3.56$

$\mu_o(mpas) = 10.83$

Calculation of modified basicity index Bi $^{(j)}$ at first slag composition i.e. t=3.75 min (1702K)

$$Bi^{(j)} = \frac{\alpha_{CaO}W_{CaO} + \alpha_{FeO}W_{FeO}}{\alpha_{SiO_2}W_{SiO_2}} \qquad (2.41)$$

$\alpha_{CaO} = 1.53$

$\alpha_{SiO_2} = 1.48$

$\alpha_{FeO} = 0.96$

W_{CaO} = 6297.95 kg [36.29 % of 17353 kg (slag wt at t= 3.75 min)]

W_{SiO2} = 4980.31 kg [28.60% of 17353 kg (slag wt at t= 3.75 min)]

W_{FeO} = 5813.26 kg [35.10 % of 17353 kg (slag wt at t= 3.75 min)]

$Bi^{(j)} = 2.06$

Using Iida model μ_s

$\mu_s = 0.05\ (kg\ /\ m.s)$

(ii) Calculation of slag-gas (continuum) viscosity, μ_{sg} (kg/m.s)

$$\mu_{sg} = \mu_s\left(1 + \frac{1.25}{(1 - \phi_g)}\right)^2 \qquad (2.42)$$

μ_s = 0.05 (kg/m.s) as calculated above

Initial value of gas fraction, ϕ_g = 0.4

By putting these values, we get,

μ_{sg} = 0.49 (kg/m.s)

(iii) Calculation of slag-gas-solid (continuum) viscosity, μ_{sgs} (kg/m.s)

87

$$\mu_{sgs} = \mu_{sg}(1 + 2.5\varepsilon + 10.05\varepsilon^2 + 0.00273\exp(16.6\varepsilon)) \tag{2.43}$$

On putting,

Solid fraction as calculated above, $\varepsilon = 0.08$

$\mu_{sg} = 0.49$ (kg/m.s) as calculated above

We get,

$\mu_{sgs} = 0.58$ (kg/m.s)

Similarly for all the slag composition viscosity is calculated and the results are summarized in Table 2.8.

Figure 2.19 shows the variation of solid fraction, slag, slag-gas and slag-gas-solid viscosity with time using Iida model. Fig. 2.20 and 2.21 compare the values obtained by the two models. The nature of the plot for viscosity calculation is same except for slight variation in the magnitude. This implies that both Urbain and Iida predict the rise in viscosity of slag-gas-solid continuum at the beginning of the blow with sudden fall after 11 min whereas slag and slag-gas viscosity fall down continuously with the blowing time. The discontinuity during 8-10.5 minutes in Fig. 2.21-2.22 is due to high solid fraction values and hence high viscosity in this time period.

Table 2.7: Calculated values of slag, slag-gas and slag-gas-solid viscosity using Urbain model

Time	Solid fraction	μ_s	$\mu_{s.g}$	$\mu_{s.g.s}$
min		kg/m.s	kg/m.s	kg/m.s
3.75	0.08	0.25	2.37	2.76
4.35	0.06	0.22	2.07	2.30
4.80	0.08	0.19	1.85	2.20
5.40	0.12	0.19	1.77	2.35
5.85	0.13	0.18	1.75	2.41
6.45	0.21	0.19	1.78	3.20
6.90	0.35	0.18	1.71	6.05
7.50	0.47	0.17	1.61	17.57
8.10	0.53	0.17	1.60	34.12
8.55	0.65	0.12	1.19	173.24
9.15	0.73	0.07	0.70	342.43
9.60	0.73	0.06	0.55	284.47
10.20	0.64	0.06	0.53	66.78
10.65	0.61	0.06	0.52	36.72
11.25	0.56	0.05	0.52	19.10
11.85	0.52	0.05	0.52	10.33
12.30	0.46	0.05	0.51	4.92
12.90	0.42	0.05	0.51	3.04
13.35	0.32	0.05	0.50	1.50
13.95	0.26	0.05	0.49	1.06

Table 2.8: Calculated values of slag, slag-gas and slag-gas-solid viscosity using Iida model

Time	Solid fraction	μ_s	μ_{sg}	$\mu_{s.g.s}$
min		Kg/m.s	Kg/m.s	Kg/m.s
3.75	0.08	0.05	0.49	0.58
4.35	0.06	0.05	0.45	0.50
4.80	0.08	0.05	0.44	0.52
5.40	0.12	0.05	0.44	0.59
5.85	0.13	0.05	0.46	0.63
6.45	0.21	0.05	0.50	0.91
6.90	0.35	0.06	0.55	1.94
7.50	0.47	0.06	0.61	6.67
8.10	0.53	0.07	0.68	14.47
8.55	0.65	0.09	0.83	121.18
9.15	0.73	0.11	1.04	508.69
9.60	0.73	0.08	0.80	412.64
10.20	0.64	0.04	0.38	48.74
10.65	0.61	0.03	0.33	22.91
11.25	0.56	0.03	0.27	9.93
11.85	0.52	0.03	0.24	4.78
12.30	0.46	0.02	0.21	2.06
12.90	0.42	0.02	0.19	1.12
13.35	0.32	0.02	0.16	0.49
13.95	0.26	0.02	0.15	0.32

Time vs Viscosity
Urbain model

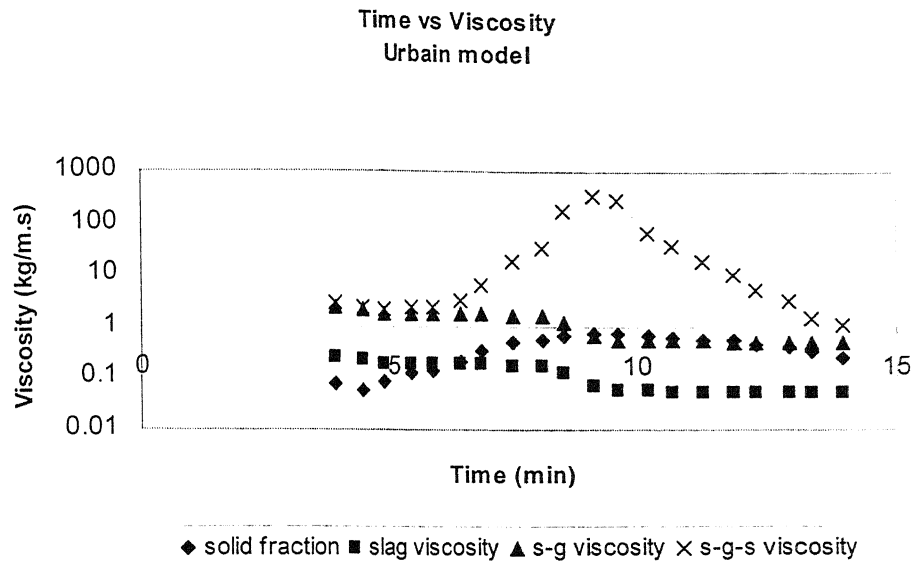Figure 2.18: Variation of solid fraction in slag, slag viscosity, slag-gas viscosity and slag-gas-solid viscosity with time using Urbain model
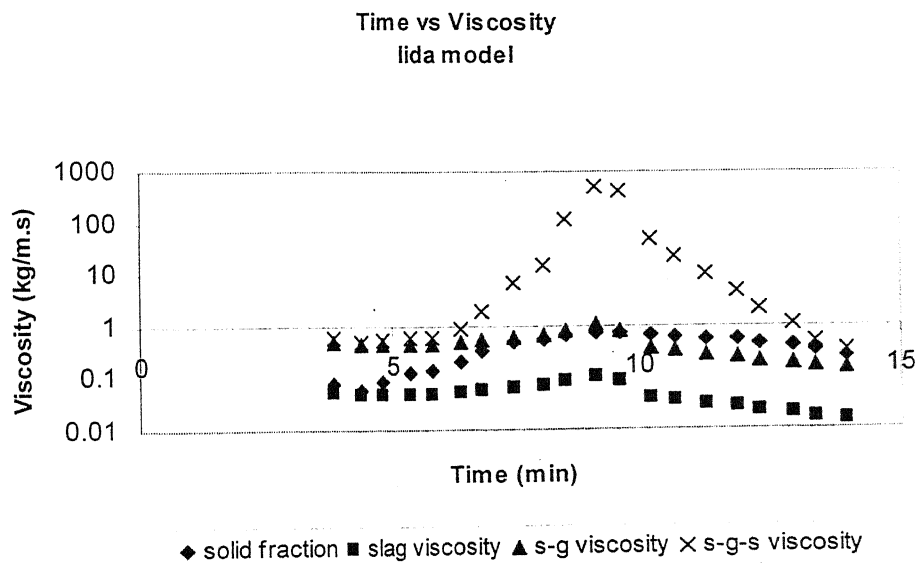

Time vs Viscosity
Iida model

Figure 2.19: Variation of solid fraction, slag, slag-gas and slag-gas-solid viscosity with time using Iida model

Tim e vs Slag viscosity

1

0   2   4   6   8

Fig

1

0   2   4   6
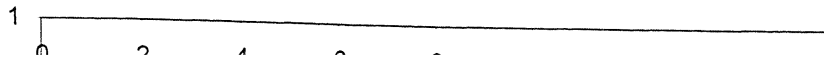
(d) Calculation of total droplet area and related parameters

Typical process parameter values are:

- Oxygen flow rate, F_{O2} = 900 Nm³/min
- Lance Height, X = 2.5 m
- Number of nozzle = 6
- Throat diameter of each nozzle, d_t = 0.0406 m
- Supply pressure, P_o = 11 atm
- Coefficient of friction, η = 0.97
- Pressure inside the vessel, P_x = 1.2 atm
- Surface tension of the metal, σ_m = 1.7 N/m
- Density of liquid metal, ρ_m = 7000 kg/m³
- Volume of gas entrapped in foam, ϕ_g = 0.4
- Angle of nozzle, θ = 14°
- Ambient pressure, P_a = 1.0 atm
- Initial value of A_{sm} = 1.0

(i) Calculation of slag density, ρ_S (kg/m³)

$$\rho_S = 2460 + 18 \times mass\% FeO \tag{2.44}$$

mass % FeO = 36.36

ρ_S = 3114.56 (kg/m³)

(ii) Calculation of slag-gas density, $\rho_{s\text{-}g}$ (kg/m³)

$$\rho_{sg} = \rho_s (1 - \phi_g) \tag{2.45}$$

Initial value of gas fraction, ϕ_g = 0.4

ρ_S = 3063 (kg/m³) as calculated above

On putting above value, we get,

$\rho_{sg} = 1868.74$ (kg/m^3)

(iii) Calculation of oxygen gas density, $\rho_{g,x}$ (kg/m^3)

$PV=NRT$ (2.46)

$\rho_{g,x} = P \times M_{O2} / RT$ (2.47)

Molecular weight of oxygen, $M_{O2} = 32$ g

Pressure inside the vessel, $P_x = 1.2$ atm

$T = 1702$ K

$\rho_{g,x} = 1.2 \times 1.01 \times 10^5 \times 32 \times 10^{-3} / (8.31 \times 1702)$ (kg/m^3)

$= 0.27$ (kg/m^3)

(iv) Calculation of jet centre line velocity at metal surface, $U_{o,x}$ (m/s)

$$\frac{P_{d,x}}{P_o} = 230 \left(\frac{X}{d_t} \right)^{-2.4}$$ (2.48)

Where

$$P_{d,x} = \frac{1}{2} \rho_{g,x} U_{o,x}^2$$ (2.49)

Supply pressure $P_o = 11 \text{atm} = 11 \times 1.01 \times 10^5$ (pa)

Lance Height, $X = 2.5$ m

Throat diameter of the nozzle, $d_t = 0.0406$ m

Oxygen gas density as calculated above $\rho_{g,x} = 0.27$ (kg/m^3)

By putting above value in the equation below:

94

$$U_{o,x} = \left[\frac{460 * P_o}{\rho_{g,x}} \left(\frac{X}{d_t} \right)^{-2.4} \right]^{1/2}$$

(2.50)

We get,

Centre line velocity of jet at the metal surface,

$U_{o,x}$ = 307.60 m/s

(v) Calculation of Weber number, We

$$We = \frac{\rho_{g,x} U_{o,x}^2}{(\rho_m \cdot g \cdot \sigma_m)^{1/2}}$$

(2.51)

Oxygen gas density as calculated above $\rho_{g,x}$ = 0.27 (kg/m^3)

$U_{o,x}$ = 307.60 m/s

Density of liquid metal, ρ_m = 7000 kg/m^3

Surface tension of the liquid metal, σ_m = 1.7 N/m

Acceleration due to gravity, g = 9.8 N/m^2

By putting the values in above equation, we get

Weber number, We = 76.16

(vi) Calculation of iron conversion rate, M_g (kg/s)

By using the following equation, we get approximate value of iron conversion

$$\frac{M_g}{F_{O_2}} = 9.862 - 0.8816 We + 0.02368 We^2 - 1.415 \times 10^{-4} We^3 + 1.572 \times 10^{-7} We^4 + 5.402 \times 10^{-10} We^5$$

(2.52)

Weber number, We = 76.16 (as calculated above)

Flow rate of oxygen, F_{O2} = 900 Nm^3/min

By putting values in above equation, we get,

Iron conversion rate, M_g (kg/s) = 363.63

(vii) Calculation of foam height, h (m)

$$h = \frac{Ws}{\left(\rho_S A(1 - \phi_g)\right)}$$ (2.53)

mass of slag, $Ws = 17353$ kg

Area of the bath, $A = 32$ m^2

Initial value of gas fraction, $\phi_g = 0.4$

$\rho_S = 3114.56$ (kg/m^3)

$h = 0.29$ m

(viii) Calculation of limiting droplet diameter d$_{lim}$ (m)

$$d_{lim} = 5.513 * 10^{-3} \left[10^6 \left(\frac{d_t}{X}\right)^2 (P_a) \left\{ 1.27 \left(\frac{P_o}{P_a} - 1\right) \right\} \cos \theta \right]^{1.206}$$ (in mm)   (2.54)

Throat diameter of the nozzle, $d_t = 0.0406$ m

Lance Height, $X = 2.5$ m

Ambient pressure, $P_a = 1.0$ atm

Supply pressure, $P_o = 11.0$ atm

Angle of nozzle, θ (rad) $= 3.14 \times 14 / 180 = 0.24$ rad

By putting above value we get,

$d_{lim} = 97.21 mm = 0.097 m$

$d_{avg} = 0.2 d_{lim} = 0.019 m$

(ix) Calculation of metal droplet velocity, V$_d$ (m/s)

$$V_d = \frac{1}{18} \frac{\left(\rho_m - \rho_{sg}\right) g d_{avg}^2}{\mu_{sgs}} \Delta_{sm}$$ (2.55)

Initial guess value of $\Delta_{sm} = 1.0$

$\rho_{sg} = 1837.8$ (kg/m^3)

$d_{avg} = 0.2d_{lim} = 0.019m$

$\mu_{sgs} = 2.52$ (kg/m.s)

$g = 9.8$ m/s^2

$\rho_m = 7000$ kg/m^3

$V_d = 0.38$ m / s

(x) Calculation of metal droplet residence time, t_r (s)

$$t_r = \frac{h}{V_d}$$ (2.56)

Foam Height, h = 0.29 m

$V_d = 0.38$ m / s

$t_r = 0.75$ s

(xi). Calculation of total surface area of metal droplets, A (m^2)

$$A = \frac{6 M_g t_r}{\rho_m d_{avg}}$$ (2.57)

Iron conversion rate, M_g (kg/s)= 363.63

$t_r = 0.75$ s

$\rho_m = 7000$ kg/m^3

$d_{avg} = 0.2d_{lim} = 0.019m$

On putting the above value, we get

$A = 12.16$ m^2

(xii) Calculation of slag volume, V (m³)

$$V_s = \frac{\dot{W}_s}{\rho_s}$$
(2.58)

mass of slag, $Ws = 17353$ kg

$\rho_S = 3114.56$ (kg/m³)

On putting the above value, we get

$V_s = 5.57$ m³

(xiii) Calculation of volume fraction of metal phase in gas-metal-slag emulsion, ϕ_m
(dimensionless)

$$\phi_m = \frac{M_g \left(\dfrac{t_r}{\rho_m}\right)(1 - \phi_g)}{M_g \left(\dfrac{t_r}{\rho_m}\right) + \left(\dfrac{W_s}{\rho_s}\right)}$$
(2.59)

Iron conversion rate, M_g (kg/s)= 363.63

Initial value of gas fraction, $\phi_g = 0.4$

$t_r = 0.75 \ s$

$\rho_m = 7000$ kg/m³

$\rho_S = 3114.56$ (kg/m³)

mass of slag, $Ws = 17353$ kg

On putting the above value, we get

$\phi_m = 0.0042$

(xiv) Calculation of new Δ_{sm} at second slag composition (using previous ϕ_m)

$$\Delta_{sm} = \frac{3\mu_{sgs}\left(1-\phi_m^{1/3}\right)\left(1-\phi_m^{3/5}\right)+\left[3-\frac{9}{2}\left(\phi_m^{1/3}-\phi_m^{3/5}\right)-3\phi_m^2\right]\mu_m}{2\mu_{sgs}\left(1-\phi_m^{5/3}\right)+\left(3+2\phi_m^{5/3}\right)\mu_m} \tag{2.60}$$

$\phi_m = 0.0042$

$\mu_{sgs} = 2.76$ (kg/m.s)

$\mu_m = 0.00568$ (kg/m.s)

On putting the above value, we get new Δ_{sm}

$\Delta_{sm} = 1.25$

(xv) Calculation of metal droplet velocity at second slag composition (using new Δ_{sm}), V_d (m/s)

$$V_d = \frac{1}{18}\frac{\left(\rho_m - \rho_{sg}\right)gd_{avg}^2}{\mu_{sgs}}\Delta_{sm} \tag{2.61}$$

$\Delta_{sm} = 1.25$

$\rho_{sg} = 1842.45$ (kg/m^3)

$d_{avg} = 0.2d_{lim} = 0.019444m$

$\mu_{sgs} = 2.29$ (kg/m.s)

$g = 9.8$ m/s^2

$\rho_m = 7000$ kg/m^3

$V_d = 0.57\ m/s$

(xvi) Calculation of metal droplet residence time at second slag composition, t_r (s)

$$t_r = \frac{h}{V_d} \tag{2.62}$$

Foam Height, h = 0.29 m

$V_d = 0.57 \; m \, / \, s$

On putting the above value, we get

$t_r = 0.51 \; s$

(xvii) Calculation of total surface area of metal droplets at second slag composition, A (m²)

$$A = \frac{6 \, M_g \, t_r}{\rho_m \, d_{avg}} \tag{2.63}$$

Iron conversion rate, M_g (kg/s) = 363.63

$t_r = 0.51 \; s$

ρ_m =7000 kg/m³

$d_{avg} = 0.2 d_{lim} = 0.019 m$

On putting the above value, we get

$A = 8.29 \; m^2$

(xviii) Calculation of slag volume at second slag composition, V (m³)

$$V_s = \frac{W_s}{\rho_s} \tag{2.64}$$

mass of slag, W_s = 17647 kg

ρ_s = 3070.76 (kg/m³)

On putting the above value, we get

V_s =5.74 m³

(xix) **Calculation of volume fraction of metal phase in gas-metal-slag emulsion at second slag composition, ϕ_m (dimensionless)**

$$\phi_m = \frac{M_g \left(\dfrac{t_r}{\rho_m} \right)\left(1 - \phi_g\right)}{M_g \left(\dfrac{t_r}{\rho_m} \right) + \left(\dfrac{W_s}{\rho_s} \right)} \qquad (2.65)$$

Iron conversion rate, M_g (kg/s)= 363.63

$t_r = 0.51\ s$

mass of slag, $Ws = 17647$ kg

Gas fraction, $\phi_g = 0.4$

$\rho_m = 7000$ kg/m^3

$\rho_S = 3070.76$ (kg/m^3)

On putting the above value, we get

$\phi_m = 0.0027$

Thus using this ϕ_m, we can calculate A_{sm} for the next slag composition and so on. By knowing A_{sm} we can find out V_d for the corresponding slag compositions and thus residence time t_r and total surface area of metal droplets A at each slag composition. Calculated values of different parameters are summarized in Table 2.9 and plotted in Figure 2.22-2.25. The discontinuity during 8-10.5 minutes in Fig. 2.22-2.25 is due to high solid fraction values and hence high viscosity in this time period.

Table 2.9: Calculated foam height, droplet velocity, residence time and total droplet surface area (assuming $\phi_g = 0.4$)

| Time (min)	Foam height (m)	Droplet velocity (m/s)	Residence time (s)	Droplet surface area (m^2)
3.75	0.29	0.38	0.76	12.16
4.35	0.30	0.58	0.52	8.29
4.8	0.30	0.62	0.48	7.74
5.4	0.31	0.58	0.52	8.41
5.85	0.31	0.57	0.54	8.73
6.45	0.31	0.43	0.72	11.60
6.9	0.30	0.22	1.38	22.15
7.5	0.29	0.07	4.08	65.41
8.1	0.29	0.03	8.82	141.32
8.55	0.27	0.01	48.07	770.58
9.15	0.25	0.00	138.34	2217.66
9.6	0.25	0.00	170.62	2735.09
10.2	0.27	0.01	44.21	708.71
10.65	0.28	0.02	15.41	247.07
11.25	0.28	0.05	6.19	99.26
11.85	0.29	0.10	2.92	46.81
12.3	0.31	0.24	1.31	20.95
12.9	0.32	0.41	0.77	12.36
13.35	0.34	0.87	0.39	6.20
13.95	0.35	1.29	0.28	4.41
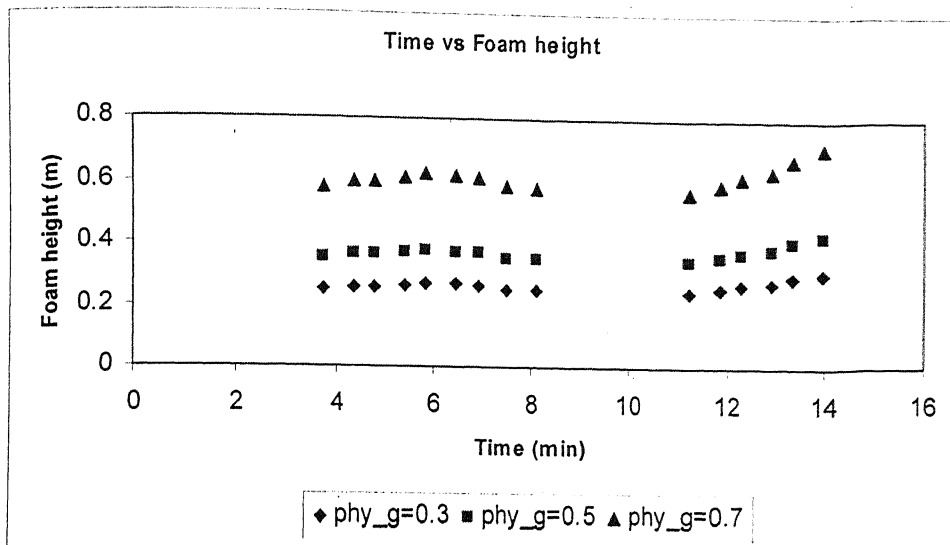
Figure 2.22: Variation of foam height with time
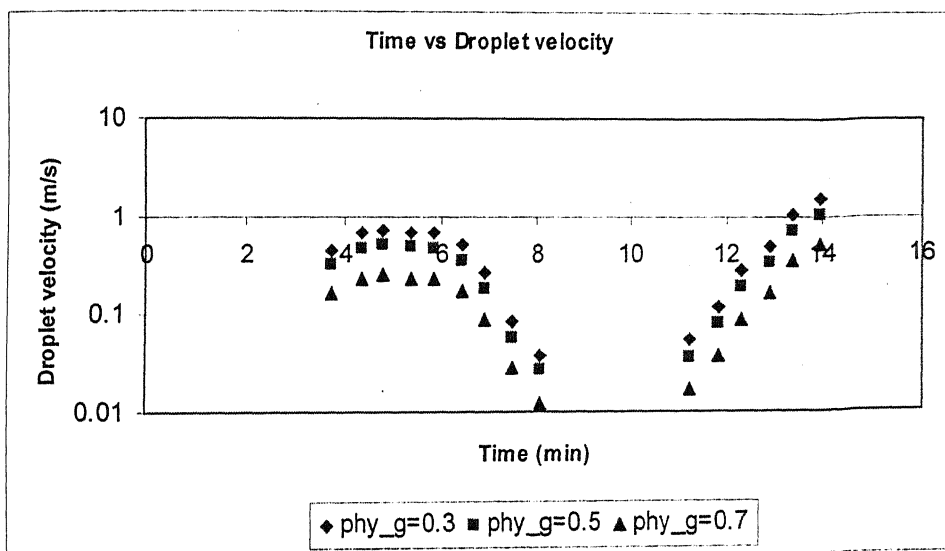

Figure 2.23: Variation of metal droplet velocity with time
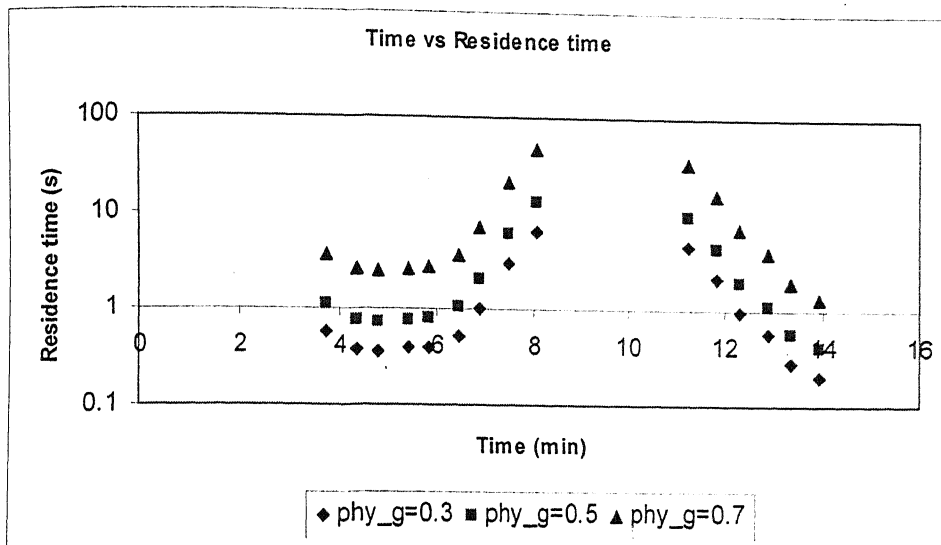
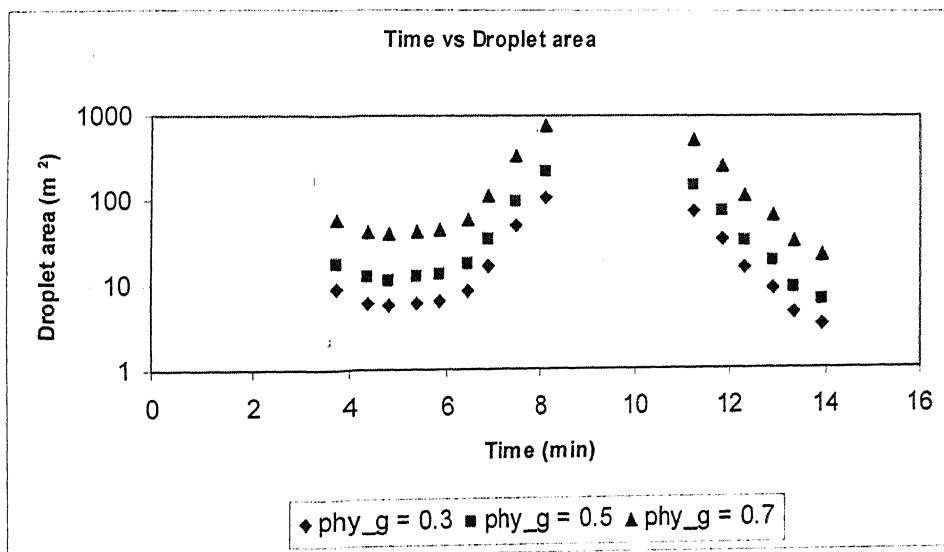Figure 2.24: Variation of droplet residence time with time

Figure 2.25: Variation of metal droplet total surface area with time

(e) Calculation of γ_{FeO} using regular solution model

According to the regular solution model the activity coefficient of component, i, in a multi-component regular solution is expressed by following equation [63]:

$$\bar{G}_i^E = \Delta \bar{H}_i = RT \ln \gamma_i \tag{2.66}$$

$$RT \ln \gamma_i = \sum a_{ij} X_j^2 + \sum \sum (a_{ij} + a_{ik} - a_{jk}) X_j X_k \tag{2.67}$$

Where $\bar{G}_i^E$ is the excess partial molar free energy, $\Delta \bar{H}_i$ is the relative partial molar enthalpy, X_i and X_k are the respective fractions of the cation species j and k and a_{ij} is the interaction energy between cations i.e ,(i cations)-O-(j cations). The use of interaction energy parameters (a_{ij}) for CaO-FeO-SiO_2 slag is given in Table 2.10. From above equation the value of γ_{FeO} for the CaO-FeO-SiO_2 slag can be calculated from:

Table 2.10: Interaction energy parameters (a_{ij}) for CaO-FeO-SiO_2 slag

i \ j	Fe^{2+}	Ca^{2+}	Si^{2+}
Fe^{2+}	-	-31380	-41840
Ca^{2+}	-31380	-	-133890
Si^{2+}	-41840	-133890	-

$$RT \ln \gamma_i = -41840 X_{SiO_2}^2 - 31380 X_{CaO}^2 + 60670 X_{CaO} X_{SiO_2} \tag{2.68}$$

In the above equation the reference state of stoichiometric FeO is taken as regular solution (R.S.); the standard state is pure liquid iron oxide in equilibrium with metallic

iron. The standard free energy change involved in the change of reference state is given by [63]:

$Fe_tO + (1-t) Fe(s \text{ or } l) = FeO$ (R.S)
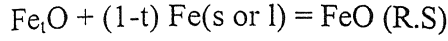
$$\Delta G^o = -8540.0 + 7.14T (J) \tag{2.69}$$

So by knowing the regular solution activity, a_{FeO} (R.S), the Raoultian activity can be calculated from:

$$RT \ln a_{Fe_tO(l)} = RT \ln a_{FeO(R.S)} - 8540.0 + 7.142T (J) \tag{2.70}$$

Thus from equation d and e expression for $\gamma_{Fe_tO(l)}$ can be obtained as:

$$RT \ln \gamma_{Fe_tO(l)} = -41840 X^2_{SiO_2} - 31380 X^2_{CaO} + 60670 X_{CaO} X_{SiO_2} - 8540.0 + 7.142T (J) \tag{2.71}$$

$\ln \gamma_{Fe_tO(l)} = -41840(0.290599)^2 - 31380(0.395313)^2 + 60670(0.290599 \times 0.395313)$
$- 8540.0 + 7.142(1702)/(8.314 \times 1702)$

$\gamma_{Fe_tO(l)} = 1.6394$

(i)Calculation of parameter a

$$a = \frac{p_{CO} \gamma_{FeO} V}{n_{tot}} \tag{2.72}$$

$P_{CO} = 1$ bar

Total no of moles in slag is

$n_{tot} = n_{CaO} + n_{FeO} + n_{SiO2} = 279041.822$

$P_{CO} = 1.0$

V = volume of slag = $5.57156 \ m^3$

$$a = \frac{1 \times 1.67801 \times 5.746785}{285341.11} = 2.35 \ E\text{-}05$$

(f) Calculation of mass transfer coefficient, k_{FeO} (cm/s), and rate constant (mol cm^{-2} s^{-1}atm^{-1}) for given slag compositions

Option 1: when mass transfer of FeO in slag is rate controlling

$$-\ln\left[\frac{FeO_t}{FeO_o}\right] = \frac{A.t}{V}\left[\frac{1}{\frac{1}{K_{FeO}}}\right]$$

$$-\ln\left[\frac{FeO_t}{FeO_o}\right] = \frac{A.t}{V}\left[K_{FeO}\right]$$

$$K_{FeO} = \frac{V}{A.t}\left(-\ln\frac{FeO_t}{FeO_o}\right) = \frac{5.57}{12.16*4.35*60}\left(-\ln\frac{36.4}{33.9}\right) = 0.018 \text{ cm/s}$$

Option 2: when chemical reaction occurring at gas slag interface is rate controlling

$$-\ln\left[\frac{FeO_t}{FeO_o}\right] = \frac{A.t}{V}\left[\frac{1}{\frac{1}{a.k_{g-s}}}\right]$$

$$-\ln\left[\frac{FeO_t}{FeO_o}\right] = \frac{A.t}{V}\left[a.k_{g-s}\right]$$

Rate constant at slag-gas interface

$$k_{g-s} = \frac{V}{A.t}\left(-\ln\frac{FeO_t}{FeO_o}\right) = \frac{5.57}{8.29\times4.35\times60\times2.35\times10^{-5}}\left(-\ln\frac{33.9}{36.4}\right)$$

$$= 7.82\times10^{-4} \, mol.cm^{-2}.s^{-1}.atm^{-1}$$

Option 3: when chemical reaction occurring at gas metal interface is rate controlling

$$-\ln\left[\frac{FeO_t}{FeO_o}\right] = \frac{A.t}{V}\left[\frac{1}{\frac{1}{a.K.k_{g-m}}}\right]$$

$$-\ln\left[\frac{FeO_t}{FeO_o}\right] = \frac{A.t}{V}\left[a.K.k_{g-m}\right]$$

Rate constant at gas metal reaction

$$k_{g-m} = \frac{V}{A.t.a.K}\left(-\ln\frac{FeO_t}{FeO_o}\right) = \frac{5.746785}{8.29470 \times 4.35 \times 60 \times 2.35 \times 10^{-5} \times 0.27549}\left(-\ln\frac{33.9}{36.4}\right)$$

$$= 28.38 \times 10^{-4}\, mol.cm^{-2}.s^{-1}.atm^{-1}$$

Similarly rate constants and mass transfer coefficient can be calculated for other slag compositions and the results are summarized in Table 2.11.

Table 2.11: Calculated mass transfer coefficient and rate constant values

Time	k_{FeO} (cm/s) ($\times 10^{-4}$)	ks-g mol.cm^{-2}.s^{-1}.atm^{-1} ($\times 10^{-4}$)	kg-m mol.cm^{-2}.s^{-1}.atm^{-1} ($\times 10^{-4}$)
4.35	183.9	7.82	28.38
4.80	16.5	0.70	2.70
5.40	39.2	1.65	6.59
5.85	135.8	5.69	23.26
6.45	10.1	0.42	1.71
6.90	75.3	3.19	12.71
7.50	29.2	1.24	4.89
8.10	3.5	0.15	0.57
8.55	3.6	0.16	0.62
9.15	0.8	0.04	0.14
9.60	0.1	0.00	0.01
10.20	2.7	0.07	0.30
10.65	2.0	0.04	0.16
11.25	3.1	0.05	0.20
11.85	2.5	0.03	0.13
12.30	21.7	0.21	1.00
12.90	9.9	0.08	0.40
13.35	86.3	0.58	3.30
13.95	43.1	0.24	1.52

2.6. Results and Discussion

2.6.1 Comparison of results with the reported data

The rate constant value obtained for both chemical reaction occurring at slag-gas interface (7.8×10^{-4} to 2.42×10^{-5}, Mol cm^{-2} s^{-1} atm^{-1}) and at gas-metal interface (2.83×10^{-3} $- 1.52 \times 10^{-4}$, Mol cm^{-2} s^{-1} atm^{-1}) are an order of magnitude higher than the reported value by various investigators (Figure 2.26 and Figure 2.27). The mass transfer coefficient value is in the range of 0.0184 - 0.0043 cm/s which is comparable with the values reported in the literature (Figure 2.28). Thus it can concluded from the result that chemical reaction can be disregarded as rate controlling step and mass transport of FeO in slag is the dominant rate controlling mechanism for FeO reduction in BOF slags.
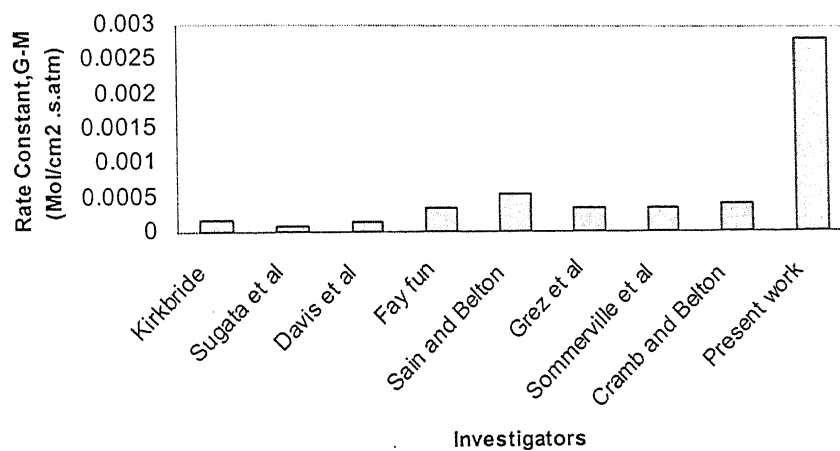

Figure 2.26: Comparison of rate constant values for the reaction at gas-metal interface
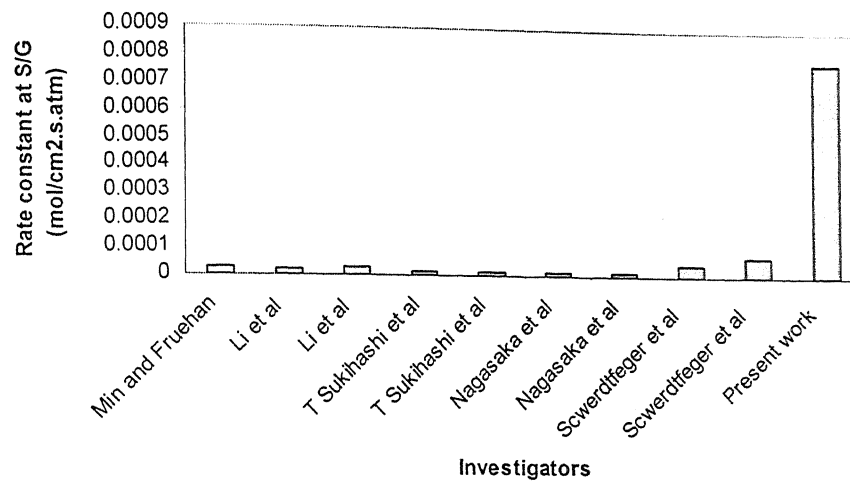
110

Figure 2.27: Comparison of rate constant values for the reaction at gas-slag interface
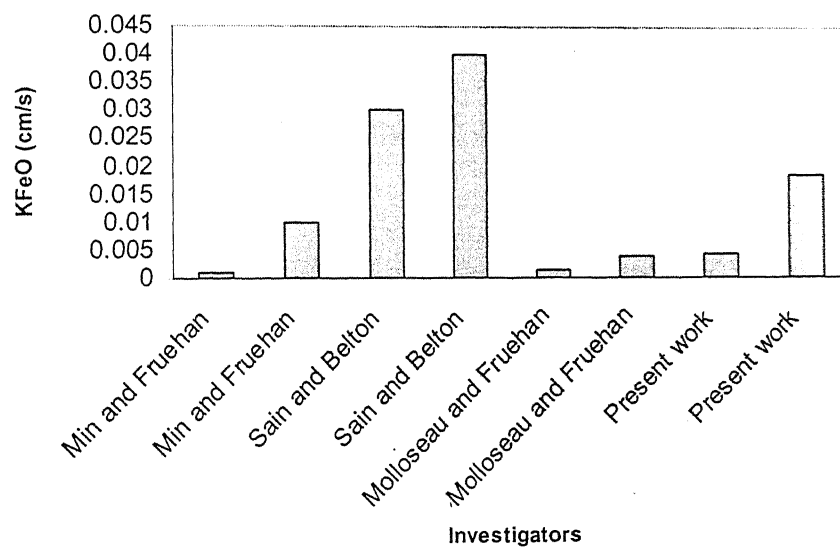

Figure 2.28: Comparison of mass transfer coefficient values of FeO, k_{FeO} (cm/s)

111

2.6.2 Variations of mass transfer coefficient with time

The residence time (Fig. 2.24) increases in first 10 min and is accompanied by the rise in total droplet surface area in Figure 2.25, but as soon as s-g-s viscosity comes down the there is sudden increase of droplet velocity and hence decrease in residence time. Figure 2.29 shows the variation of mass transfer coefficient of k_{FeO}, with time for three different gas void faction values, 0.3, 0.5 and 0.7, so to consider the range of slag foaming conditions in the vessel. It can be seen that mass transfer coefficient may undergo a great amount of fluctuation through out the blow period of 4 -14 min. Initially, the mass transfer coefficient in Figure 2.29 decreases with time because of increase slag-gas-solid continuum viscosity (Figure 2.19) but as soon as the solid part of the slag dissolves back (see the corresponding changes in solid fraction plotted in Figure 2.19) then there is again slight increase in the mass transfer coefficient of FeO. These results show that slag-gas-solid viscosity plays a dominant role and contributes most to the fluctuation of mass transfer coefficient.
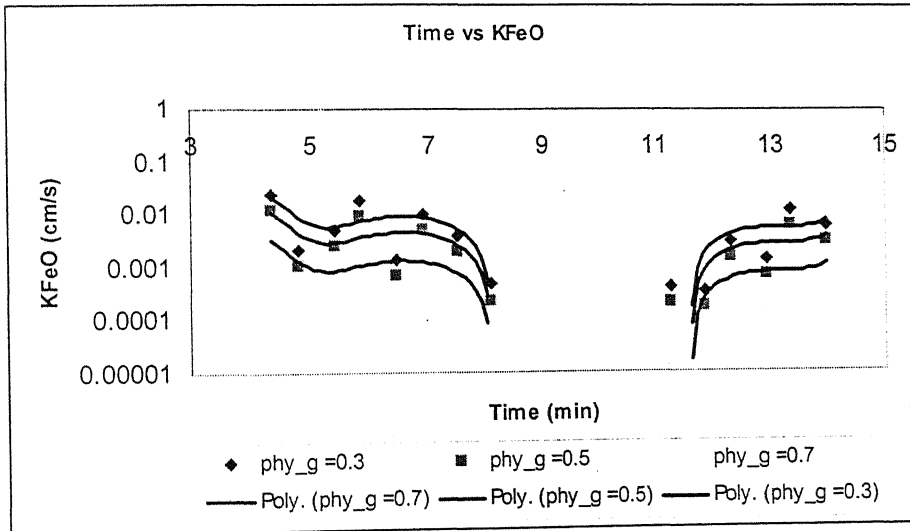
Figure 2.29: Variation of k_{FeO} with time; three different gas void faction values are assumed, 0.3, 0.5 and 0.7

2.6.3 Comparison of mass transfer coefficient of FeO and CaO

The k_{FeO} and k_{CaO} vales obtained in his work are plotted together, for the sake of comparison, in Figure 2.30. It can be seen that mass transfer coefficient of CaO (k_{CaO}) is less than the mass transfer coefficient value of FeO (k_{FeO}). It implies that mass transfer coefficient of CaO will control the process of lime dissolution and not mass transfer of FeO. It can also be observed from the figure that mass transfer coefficient of FeO (k_{FeO}) shows a larger amount of fluctuation than the mass transfer coefficient of CaO (k_{CaO}). It is observed in practice that lime dissolves more or less at a steady rate where as the the reduction rate of FeO can fluctuate considerably.
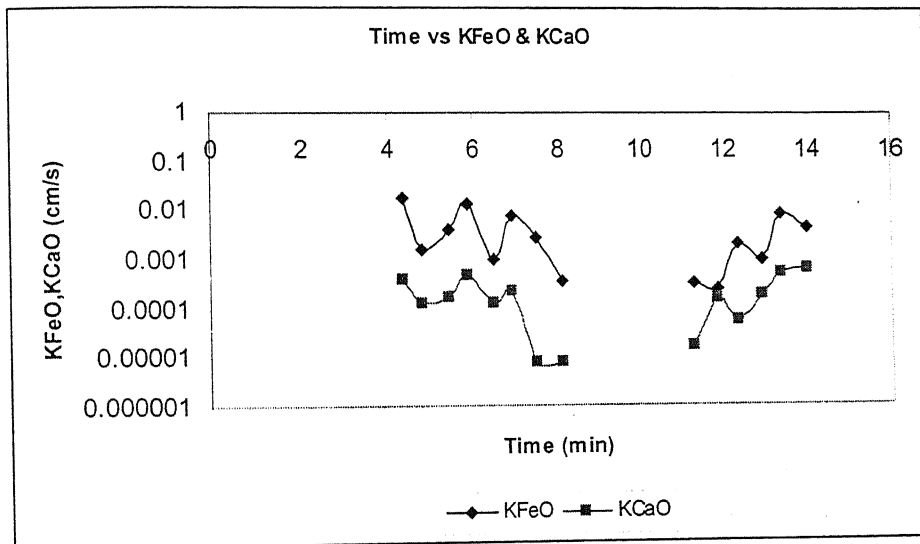
Figure 2.30: Variation of mass transfer coeff. of FeO and CaO with time

2.7 Conclusions

A kinetic model is developed for the reduction of FeO in slag in 300 ton BOF. Jet parameters are considered to calculate the amount of metal droplets thrown into the slag. Residence of time of metal droplets is calculated on the basis of slag composition, temperature, gas void fraction, and solid fraction of lime in slag. The results show that:

- Mass transfer of FeO in slag is rate controlling.
- The mass transfer coefficient changes during the blow primarily due to changes in slag viscosity.
- The average value of mass transfer coefficient is 3.5×10^{-3} cm/s and compares with some laboratory investigations.
- The value of mass transfer coefficient of FeO is higher than that of mass transfer of CaO in slag. It shows that for the case of lime dissolution the rate controlling step is mass transfer of CaO and not the mass transfer of FeO, as reported in literature.

2.8 Scope for further work

- The kinetic models developed in this work can be tested on line to predict the slag foaming and formation in an actual 300 ton BOF.
- Sonic probes can be used to predict the foam height and then related it to slag conditions in BOF.
- Optimum size of lime to charged in BOF and timing of addition of lime can be determined with the help of the model.

References

[1]   R.Boom, B.Deo, W. Van der Knoop, F. Mensonides and G. Van Unen, 3rd Int. Conf. on Molten Slags and Fluxes, 1988, Univ.of Strathclyde, 27-29 June (1988), pub. by The Institute of Metals, pp. 273-76.

[2]   L.Hachtel, W.Fix and G. Tromel, Arch. Eisenhuttenwesen, 40 (1972), pp. 361-69.

[3]   F.Oeters and R.Scheel, Arch. Eisenhuttenwesen, 45 (1974), pp. 575-58.

[4]   M.Matsushima, S.Yadoomaru, K.Mori and Y. Kawai, Trans. ISIJ,17 (1977), pp. 442-49.

[5]   H. Kimura, T. Yanagase, F. Naguchi and Y. Ueda, J. Inst. Metals, 38 (1974), pp.226

[6]   C.A Natalie, J.W Evans *"Influence of lime properties on the rate of dissolution in FeO-CaO-SiO$_2$ slag"*, Ironmaking and Steelmaking, Vol. 6, No. 3 (1979) pp.101-09.

[7]   P.Williams, M.Sunderland and G.Briggs *"Interaction between dolomitic lime and iron silicate melts"*, Ironmaking and Steelmaking, Vol.9, (1982), pp.150-62

[8]   G.J.W.Kor, L.J.Martonik and R.A.Miller *"Evaluation of lime for the BOF process and effect of degree of calcinations on its dissolution rate in slags"*,Fifth international iron and steel congress process technology proceedings,Vol.6, Washington, DC (1986), pp. 679-89

[9]   Boom, Beiser,van der Knoop Hoogovens *"Studies of lime and flux properties related to slag formation in Oxygen Steel Making"* pp.1041-60

[10]   M. Verhoog , *"La vitesse de dissolution de la chaux et de la dolomie dans la scorie report C.N.R.M. DS"*, (1968), pp. 47-69

[11].   G. König, H. Rellermeyer and K.H. Obst , *"Vorgänge bei der Auflösung von Hart- und Weichbrandkalk in Schlacken aus dem Sauerstoffaufblas Konverter"*, Stahl und Eisen ,Vol.87, Heft 18 (1967)

[12]   F. Bardenheuer, H vom Ende, P-G. Oberhäuser

Kalkauflösung, Schlackenführung und Haltbarkeit des Dolomitfutters beim Verblasen von phosphorarmem Roheisen im Sauerstoffaufblas Konverter.

Stahl und Eisen, Vol.88, Heft 23 (1968), pp.1285-90

[13]   König

Qualitätskontrolle von Stahlwerkskalk

Stahl und Eisen,Vol.89, Nr. 22, (1969), pp.1231-35

[14]   Schiele

Kalk (Herstellung-Eigenschaften-Verwendung)

ISBN 3-514-00115-4 (1972)

[15]   F Naguchi et al,World Min Metall. Tech., 1970, chap.43, pp.685

[16]   Anderson, *"The quality and production of lime for basic oxygen Steelmaking"*

Journal of the Iron and Steel Institute, (1970), pp.329-35

[17]   L.A.Leonard "Influence of Lime Quality on Oxygen Steelmaking",

JISI,Vol.208, (1970), pp.324-28

[18]   Frank *"Die Bestimmung der Reaktionsfahigkiet von kalken mittels der Nassloschkurve"*

Zement-Kalk-Gips Nr. 4 1970, (1970), pp.172-76

[19]   Paretosh Mishra,Brahma Deo and R.P. Chhabra, *"Dynamic model of slag foaming in oxygen steelmaking converters"* , ISIJ International,Vol 38(1998), No.11, pp.1225-32

[20]   Slag Atlas, Verlagstahleisen MBH, Dusselforf, 1981, pp.117

[21]   S. Ban-Ya, ISIJ Int.,Vol.33,(1993), pp. 2-11

[23]   K-H. Obst and J. Stradtmann, Archiv fur das Eisenhuttenwesen,Vol.40,No.8, (1969), pp.615-17

[24]   K.Ito, T. Hamano and K. Matsuzaki, *"Reaction kinetics of FeO containing molten slags"*, 5th Japan Germany Seminar, pp.12-17

[25]   J.Green, Ph.D. Thesis, Sheffield Polytechnic. 1975, UK

[26]   Y.E.Lee and D.R.Gaskel, Metall. Trans., Vol.5, pp. 853

[27]   Amitava Paul, Brahma Deo and Narayan Sathyamurthy, *"Kinetic model for reduction of iron oxide in molten slags by iron-carbon melt"*,Steel Research,65 (1994), No 10, pp.414-20

116

[28] D.R Sain and G.R. Belton, "*Interfacial reaction kinetics in the decarburisation of liquid iron by carbon dioxide*", Metall. Trans.B, Vol.7B,June (1976), pp.235-44

[29] A.W.Cramb and G.R.Belton , "*Studies of the interfacial kinetics of the reaction of CO_2 with liquid iron by the $^{14}CO_2$-CO isotope exchange reaction*", Metall.Trans.B, Vol.12B, June (1981), pp.699-704

[30] C.L. Molloseau and R.J. Fruehan "*The reaction behaviour of Fe-C-S droplets in CaO-SiO_2-MgO-FeO slag*", Metall. Trans.B, Vol. 33B, June (2002), pp. 335-44

[31] I.D.Sommerville, P.Greiveson, and J Taylor "*Kinetics of reduction of iron oxide in slag by carbon in Iron: Part 1 Effect of oxide concentration*", Ironmaking and Steelmaking, (1980), No1, pp.25-32

[32] Y. Li, I.P. Ratchev, J.A.Lucas, G.M.Evans, and the late G.R. Belton "*Rate of interfacial reaction between liquid iron oxide and CO-CO_2*", Metall. Trans.B,Vol.31B, October(2000), pp.1049-57

[33] G.Graenzdoerffer, W.M. Kim and H. Alan Fine "*Kinetics of the reduction of Fe_xO from molten slag*", Process Technology Conference Proceedings, (1988), pp.137-43

[34] Hiroyuki Nomura and kazumi Mori "*Kinetics of decarburisation of liquid iron with high concentration of carbon*",Trans. ISIJ, Vol.13,(1973), pp.265-73

[35] T. Gare and G.S.F Hazeldean "*Basic oxygen steelmaking: decarburization of binary Fe-C droplets and ternary Fe-C-X droplets in ferruginous slags*", Ironmaking and Steelmaking,(1981), No.4, pp.169-81

[36] E.W. Mulholland, G.S.F Hazeldean , and M.W. Davies: J. Iron Steel Inst., (1973), Vol.9, pp. 632-39

[37] D.J Min and R.J Fruehan, Metall.Trans.B, (1992), Vol.23B, pp.29-37.

[38] B.Sarma, A.W. Cramb, and R.J Fruehan: Metall.Trans.B, (1996), Vol. 27 B, pp. 717-30

[39] Y Ogawa and N. Takumitsu, Proc. 6th Inst. Iron and Steel Congr., Nagoya, Japan, Irons and Steel Inst.Jpn.,Tokyo, (1990), pp.147-52

[40] T. Fuwa, Trans.Jpn Inst.Met.,(1988), Vol. 29, pp.353-64

[41] M.W. Davies, G.S.F. Hazeldean, and P.N. Smith, in Physical Chemistry of Process Metallurgy: the Richardson Conf., J.H.E. Jeffes and R. J. Tait, eds.

117

The Institute of Mining and Metallurgy, London (1973), pp.95-107

[42]   K. Ishiiand Y. Kashiawaya, 3rd Int. conf. on molten slags and fluxes, Glasgow, United Kingdom,The Institute of Metals, London, (1989), pp.142-45

[43]   S. Hara and K.Ogino: Tetsu-to Hagane, 1990, Vol.76, pp.360-67

[44]   G.R. Belton, "*Kinetics of gas/slag reactions*", 3rd international conference on molten slags and fluxes, Glasgow, (1988), pp.96-106

[45]   Fumitaka Tsukihashi, Kimio Kato,Ken-ichi Otsuka, "*Reduction of molten iron oxide in CO gas conveyed system*", Tetsu-to-Hagane,68 (1982),pp.750

[46]   Anke Traebert, Michael Modigell,Peter Monheim and Klaus Hack, "*Development of a modeling technique for non equilibrium metallurgical processes*", Scandivian Journal of Metallurgy, (1999), Vol.28, pp.285-90

[47]   P.Chattopadhyay, R.C Gupta, and H.S. Ray, "*Kinetics of iron oxide reduction in molten slag*", A.K.Jouhari,R.K. Galgali, Scandivian Journal of Metallurgy, (2001),Vol.30,pp.14-20

[48]   Y.Li and I.P Ratchev,"*Rate of interfacial reaction between molten CaO-SiO₂- Al₂O₃-FeₓO and CO-CO₂*", Metall. Trans.B,(2002),Vol.33 B, pp. 651-59

[49]   Geoffrey.R.Belton,"*How fast can we go? The status of our knowledge on the rates of gas-liquid metal reactions*", 10th PTD conference proceedings,(1992), pp.3-20

[50]   R.J Fruehan, D Goldstein,B Sarma,S.R. Story,P.C. Glaws and H.U. Pasewicz, "*Recent advances in the fundamentals of the kinetics of steelmaking reactions*" Metall.Trans.B, (2000), Vol. 31B, pp 891-98

[51]   Brahma Deo,Arun Karamcheti,Amitava Paul,Pankaj Singh and R.P. Chhabra, "*Characterization of slag-metal droplet-gas emulsion in oxygen Steelmaking converters*", ISIJ International,Vol.36,(1996),No.6,pp.658-66

[52]   Marcelo Breda Mourao, "*Kinetics and mechanism of reaction between iron oxides and iron-carbon melts*", Steel Research,Vol.71, (2000), No.1+2, pp. 3-8

[53]   Y.Li, J.A Lucas,R.J Fruehan, and G.R. Belton "*The chemical diffusivity of oxygen in liquid iron oxide and a calcium ferrite*", Metall.Trans.B,(2002), Vol.31B,pp.1059-68

[54]   T. Nagasaka, Y.Iguchi, and S. Banya, 5th Int. Iron and Steel Congr., Process Technology Proc., ISS, Washington, DC, (1986),Vol.6, pp.669-78

118

[55]   K. Schwerdtfeger and K. Klein, Ironmaking and Steelmaking, (1977),Vol.4, pp.45-50

[56]   D.R.Lloyd, D.R.Young, L.A.Baker, Ironmaking and Steelmaking,(1975), No.1, pp. 49-55

[57]   W.O Philbrook and L.D. Kirkbride: ibid., 1956,206,351-56

[58]   M. Sugata, T. Sugiyama, and S. Kando: Trans. ISIJ, (1974),14, pp.88-95

[59]   M.W. Davies, G.S.F. Hazledean, and P.N. Smith: *"Physical chemistry of process metallurgy, The Richardson conference"*,(eds. J.H.E. Jeffes and R.J. Tait), London, The Institute of Mining and Metallurgy,(1974),pp.95-107

[60]   Fay Fun, Metall. Trans., (1970), Vol.1, pp.2537-41

[61]   K.J. Grez, J.M. Burgess, and N.A. Molloy, 2nd Australasian conf. on "Heat and Mass Transfer", Sydney, (1977)

[62]   George Urbain, *"Viscosity estimation of slags"*, Steel Research 58, (1987), No.3, pp.111-16

[63]   Lasse Forsbacka, Lauri Holoppa,Takamichi,Yoshifumi Kita and Yunie Toda, *"Experimental study of viscosities of selected CaO-MgO-Al2O3-SiO2 slag and application of the Iida model"*, Scandinavian Journal of Metallurgy,32,(2003),pp.273-280

Date Slip

This book is to be returned on the
date last stamped.

....	....
....	....
....	....
....	....
....	....
....	....
....	....
....	....
....	....
....	....
....	....
... .	....